SERIAL NO. **SSC-30**

FINAL REPORT

(Project SR-96)

on

CORRELATION OF LABORATORY TESTS WITH FULL SCALE SHIP PLATE FRACTURE TESTS

by

E. P. Klier
UNIVERSITY OF MARYLAND

and

M. Gensamer
COLUMBIA UNIVERSITY

Transmitted through

NATIONAL RESEARCH COUNCIL'S
COMMITTEE ON SHIP STEEL

Advisory to

SHIP STRUCTURE COMMITTEE

Division of Engineering and Industrial Research
National Academy of Sciences - National Research Council
Washington, D. C.

January 30, 1953

SERIAL NO. **SSC-30**
BuShips Project NS-011-042

SHIP STRUCTURE COMMITTEE

MEMBER AGENCIES:

BUREAU OF SHIPS, DEPT. OF NAVY
MILITARY SEA TRANSPORTATION SERVICE, DEPT. OF NAVY
UNITED STATES COAST GUARD, TREASURY DEPT.
MARITIME ADMINISTRATION, DEPT. OF COMMERCE
AMERICAN BUREAU OF SHIPPING

ADDRESS CORRESPONDENCE TO:

SECRETARY
SHIP STRUCTURE COMMITTEE
U. S. COAST GUARD HEADQUARTERS
WASHINGTON 25, D. C.

January 30, 1953

Dear Sir:

As part of its research program related to the improvement of hull structures of ships, the Ship Structure Committee has sponsored an investigation on the "Correlation of Laboratory Tests with Full-Scale Ship Plate Fracture Tests" at Pennsylvania State College. Herewith is a copy of the Final Report, SSC-30, of the investigation, entitled "Correlation of Laboratory Tests with Full-Scale Ship Plate Fracture Tests", by E. P. Klier and M. Gensamer.

The project has been conducted with the advisory assistance of the Committee on Ship Steel of the National Academy of Sciences-National Research Council.

Any questions, comments, criticism or other matters pertaining to the Report should be addressed to the Secretary, Ship Structure Committee.

This Report is being distributed to those individuals and agencies associated with and interested in the work of the Ship Structure Committee.

Yours sincerely,

K. K. Cowart

K. K. COWART
Rear Admiral, U. S. Coast Guard
Chairman, Ship Structure Committee

FINAL REPORT
(Project SR-96)

on

CORRELATION OF LABORATORY TESTS WITH FULL SCALE SHIP PLATE FRACTURE TESTS

by

E. P. Klier
University of Maryland

and

M. Gensamer
Columbia University

under

Department of the Navy
Bureau of Ships
Contract NObs-31217
with the

Pennsylvania State College

BuShips Project NS-011-042

for

SHIP STRUCTURE COMMITTEE

TABLE OF CONTENTS

Page

Introduction 1

Materials Research Program 1

David W. Taylor Model Basin 2

The University of California, Project SR-92 2

The University of Illinois, Project SR-93 2

The New York Naval Shipyard, Project SR-104 2

Swarthmore College, Project SR-98 2

The Pennsylvania State College, Project SR-96 2

University of California, Project SR-92 3

David W. Taylor Model Basin, Project SR-105 3

New York Naval Ship Yard, Project SR-104 3

Ductile-Brittle Transition Phenomena 3

Uniaxial Stress-Loading - The Tensile Test 4

Biaxial Stress Loading 7

Triaxial Stress 10

Criteria of the Ductile-Brittle Transition 11

Bend Specimen 12

Tension Tear Specimens 12

Notched Tension Specimens 12

TABLE OF CONTENTS (Continued)

Page

Metallurgical Structure and The Ductile-Brittle Transition 12

Fatigue and The Ductile-Brittle Transition 13

Velocity of Loading and the Ductile-Brittle Transition 14

Size Effect and the Ductile-Brittle Transition 15

The Testing Program 16

Experimental Results 20

Project Steels

The Ductile-Brittle Transition - Project Steels 21

Tensile Strength and Size Effect - Project Steels 24

Additional Tests

Fractured Liberty Ship Plate Tests 26

Tests of Other Steels 28

The Studies of Kahn and Imbembo 29

Discussion 32

The Ductile-Brittle Transition 33

Loading Condition in Structures 36

Ship Steel Selection 38

Acknowledgments 40

Bibliography 41

LIST OF TABLES

A. Chemical Analyses of the Steels.

B. Summary of Test Results - 20-in. Diameter Tubes.

C. Transition Temperatures of Project Steels as Determined by Various Notched Tests.

D. Chemical Analysis in % of Specimens From PIERRE S. DUPONT and PONAGANSET (1-in. Wide Full-Thickness Specimens).

E. Mechanical Properties of Steel from PIERRE S. DUPONT and PONAGANSET (1-in. Wide Full-Thickness Specimens).

F. Transition Temperature in ^{o}F of Steels as Determined by Various Tests.

G. Properties and Composition of High Yield Strength Structural Steels Used in the Investigation .

H. Approximate Transition Temperatures of High Yield Strength Structural Steels Determined by Means of Different Specimens.

I. Composition, Tensile and Tear-Test Properties of Ship Plate Steels, Medium, Semikilled, 48-S-5, Normal Managanese (Mn/C<3) and Medium Semi-killed ABS-B Manganese 0.60-0.90 (Mn/C < 3)

J. Composition, Tensile and Tear Test Properties of Ship Plate Steels, Medium, Rimmed, Medium Rimmed and Fully Killed and High-tensile Vanity-type 48-S-5.

LIST OF FIGURES

1. The transitions in energy absorption and fracture appearance in the Charpy keyhole impact specimen. Steel D_r.

2. The per cent reduction in area versus temperature of testing Steel E.

3. Effect of temperature on tensile properties of Steel "C" in the "as rolled" condition.

4. Hypothetical flow and fracture curves depicting conditions leading to ductility and fracture transitions.

5. The strain hardening exponent (n) versus temperature for Steel E and Steel H.

6. Spherical test specimen.

7. Variation of nominal biaxial properties with temperature.

8. Slow bend test results.

9. Torsion specimen.

10. Distribution of elastic stress at the base of the notch in a notch-bend test bar.

11. Charpy keyhole notch specimen.

12. Charpy V-notch specimens.

13. The change in transition temperature versus notch root radius-Charpy V-notch specimens.

14. Diagram showing types of transition curves obtained on notched specimens.

15. Influence of normalizing on Lehigh Bend Test transition as indicated by fracture appearance. Silicon-killed steel, 0.25%C, 0.66%Mn, 0.19%Si.

16. Influence of pre-strain on the transition temperature of notched and un-notched mild steel impact specimens.

17. Effect of fatigue on notched impact strength.

LIST OF FIGURES (Continued)

18. The transition temperature versus impacting velocity for selecting project steels in tension impact. Adapted from Bruckner and Newmark, (24).

19. A suggested extrapolation of the curves of Figure 18.

20. Suggested variation of transition temperature in the Charpy v-notch impact test with impacting velocity. The two experimental points were determined respectively in slow bending and impact bending.

21. Influence of specimen width on absorbed energy at constant temperature.

22. Form of Taylor Model Basin tensile test specimens.

23. Details of slot - Taylor Model Basin specimen.

24. Effect of ratio of length of slot to width of plate on energy absorbed. Results are for Steel E specimens notched with a jeweler's saw.

25. Effect of temperature on energy absorbed for specimens of Steel E.

26. Sketch of wide plate specimens and type of stress-raiser.

27. 72-inch specimen in 3,000,000-lb. testing machine.

28. Specimen cooling mechanism.

29. Revised design of the full scale hatch corner model.

30. Hatch corner tests. Specimen 4: Overall view from above.

31. Hatch corner tests. Specimen 4: Overall view from below.

32. Sections of apparatus for tests of 20" diameter tubes at low temperatures.

33. Restrained welded specimen used for tests of high yield strength structural steels.

34. Restrained welded specimen in testing machine showing pulling tabs and manganin wire extensometer.

35. Laboratory test specimens employed for correlation with large plate test results.

LIST OF FIGURES (Continued)

36. Keyhole Notch Summary - Project Steels

37. V-Notch Summary - Project Steels

38. Energy absorption, fracture appearance, and lateral contraction vs. testing temperature for v-notch milled and v-notch pressed (both Schnadt modification) charpy impact specimens. Mild steel.

39. Charpy v-notch impact transition temperature in °F at 25 and 50% maximum energy absorption for specimens prestrained in compression.

40. Charpy keyhole tests of Steel N following different heat treatments.

41-45. The influence of plate thickness and variations from plate of constant thickness on notched bar test results, all steel from one heat. Project Steel C.

46. Steel Br - Summary of test data

47. Steel C.

48. Steel A.

49. Steel Bn.

50. Steel Dr.

51. Steel Dn.

52. Steel E.

53. Steel H.

54. Steel N.

55. Wide Plate Test Results.

56. Hatch Corner Tests. Maximum nominal stress and energy absorption (all tests at 70°F.)

57. PIERRE S. DUPONT - Plan view of the upper deck showing the plate removed for testing and the adjacent crack.

LIST OF FIGURES (Continued)

58. PIERRE S. DUPONT - Sample from deck plate C-10 showing location of test specimens.

59. PONAGANSET - Elevation of the starboard side-shell showing the location of test specimens in the topside strake.

60. PONAGANSET - Plan view of main deck showing the location of test specimens.

61. Twelve-inch wide specimens. Results of tests of samples removed from fractured ships. 3/4 or 13/16-inch thick plate.

62-a. Energy to maximum load vs. temperature relation for restrained welded specimens of high yield strength structural steels, results of tests of specimens made from mild steel with E-6020 electrode are shown for comparison.

62-b. Energy to failure vs. temperature relation for restrained welded specimens of high yield strength structural steels. Results of tests of specimens made from mild steel with E-6020 electrode are shown for comparison.

63. Transition temperatures for H. Y. S. S. Steels amd mild steel B as determined by 12" centrally notched specimens.

64. Tear-test transition temperatures of medium and high-tensile ship plate steels, 1/2 and 5/8-inch thicknesses.

65. Tear-test transition temperatures of medium and high-tensile ship plate steels, 7/8, 1, 1-1/4 and 1-1/2 inch thicknesses.

66. Tear-test transition temperatures of medium and high-tensile ship plate steels, 1/2, 5/8, 3/4, 7/8, and 1-1/4-inch thicknesses.

67. Tear-test transition temperatures of medium ship plate steels 1/2, 5/8, 3/4, 1 and 1-1/2-inch thicknesses, as rolled condition.

68. Tear-test transition temperatures of medium steel ship plate, 3/4-inch thickness.

69. Stresses in upper deck of liberty ship.

70. Twelve inch wide flat plate tests.

INTRODUCTION

The role of materials in the ship fracture problem is obvious. If such materials were not susceptible to brittle failure, the problem would cease to exist. With the objective of a final evaluation of weldable steels as to their suitability for merchant vessel construction, a wide experimental program was initiated by the Board of Investigation to Inquire into the Design and Methods of Construction of Welded Steel Merchant Vessels[1]* and continued by the Ship Structure Committee[2,3]. It was the objective of the research program conducted at the Pennsylvania State College under Bureau of Ships Contract NObs-31217 to correlate the work conducted for the Board and the Ship Structure Committee. This final report attempts, therefore, the correlation of the results of the entire "material" research program as conducted between 1944 and approximately the end of 1950. This program, in abbreviated outline, is given below.

MATERIALS RESEARCH PROGRAM

The specifications for the Liberty ship called for a medium steel. Such steel can be furnished in rimming, semi-killed, and fully killed grades. In order to supply a series of steels which would have appreciably different fracture characteristics in the projected tests, the steels listed in Table A were supplied by different mills. These steels have been generally designated as

---

*For numbers in parenthesis see Bibliography

"project" steels. These steels were studied extensively under the cooperative research programs conducted at the University of California, the David W. Taylor Model Basin, the University of Illinois, the New York Naval Shipyard, the Pennsylvania State College, and Swarthmore College.

The research programs conducted at the respective laboratories were designated as follows:

David W. Taylor Model Basin: (a) Flat plate tests.

The University of California, Project SR-92: (a) Flat plate tests, (b) large tube tests, (c) similitude tests, (d) bend tests, (e) full-scale hatch corner tests.

The University of Illinois, Project SR-93: (a) Flat plate tests, (b) impact tests.

The New York Naval Shipyard, Project SR-104: (a) Standard impact tests, (b) Navy tear tests.

Swarthmore College, Project SR-98: (a) 12-inch plate tests, (b) aspect ratio tests.

The Pennsylvania State College, Project SR-96: (a) Impact tests, (b) slow bend tests, (c) edge-notched bar tension test, (d) low-temperature tension tests, (e) strain-gradient measurements.

In addition to the above tests conducted all or in part on the project steels, tests were run on certain additional mild and high strength steels. The augmented testing program included the

indicated tests run at the following laboratories:

University of California, Project SR-92: (a) Restrained welded specimen tests on high strength steels, (b) edge-notched bar tension tests (c) 12-inch plate tests.

David W. Taylor Model Basin, Project SR-105: (a) 12-inch plate tests on mild steels taken from fractured Liberty ships, (b) edge-notched bar tension tests.

New York Naval Shipyard, Project SR-104: (a) Tear tests on selected mild and high strength steels.

The results of the tests conducted on the above program will be discussed at length in the following, but before these data are examined it may prove profitable to consider certain generalizations which may be made with reference to the ductile-brittle transition and which must be considered in the ultimate evaluation of the ship fracture problem.

DUCTILE-BRITTLE TRANSITION PHENOMENA

The ductile-brittle transition as it is encountered in mild steel, has in the past generally been associated with the impact test. In the impact test it is customary to give the results in terms of the work required to break a specified test bar. This work to failure has been found to vary with temperature for a suitable test specimen as in Figure 1[4]. Thus at relatively high temperature much work is required to fracture the specimen, while at relatively lower temperature little work is required to fracture

the specimen. The high temperature condition is known as the ductile or tough condition, while the low temperature condition is known as the brittle condition, with the intermediate range being designated as the transitional range, or the ductile-brittle transition.

Of the many factors which modify the ductile-brittle transition in mild steel, unquestionably the most important is the stress system. It is not possible considering present knowledge to discuss fully the phenomena associated with the ductile-brittle transition, as the stress system is arbitrarily varied; but certain reasonably integrated data are now available for consideration on this point. In the sections immediately below, the behavior of steels tested under certain uniaxial, biaxial, and triaxial stress systems* will be considered.

Following this, the criteria of the ductile-brittle transition will be noted, and generalizations concerning metallurgical structure, fatigue, velocity of loading and size effect, as pertinent, will be introduced.

Uniaxial Stress Loading -- The Tensile Test: If a mild steel is tested in tension in an appropriate temperature range, a transition to brittle behavior will be observed as is indicated in Figure 2. This transitional behavior is comparable to that observed in the impact test on notched bars, but the test bar used here is a standard test bar and does not contain an artificial notch. Thus it may be concluded that an external notch is not required to induce

*The terms "uniaxial, biaxial, and triaxial" are somewhat loosely applied and at best apply with good approximation only during the initial steps of loading.

brittleness in such steels, and the brittleness observed must be considered an intrinsic property of these materials tested in tension.

In the further analysis of tensile test data, it is informative to compare the yield strengths and the fracture strengths as is done in Figure 3. It is evident that the transition from ductile to brittle behavior takes place at a temperature at which the yield and fracture strengths are in near coincidence. This does not per se preclude ductile behavior, but this phenomenon has been used explaining brittle behavior. Thus, Le Chatelier[5] has argued that the coincidence of the yield and fracture strengths would serve to localize plastic distortion with a consequent reduction in energy absorption. On the other hand, Ludwik[6], in a consideration of comparable data, has proposed that two strength factors exist, namely, flow and fracture strengths, and, in general, the flow strength is less than the fracture strength. When the flow strength attains a value equal to that of the fracture strength, failure ensues. In both of these analyses of the ductile-brittle transition, the nature of the fracture process is not explained. There is no differentiation, therefore, of two classes of fracture phenomena as indicated by the terms shear (fibrous) and normal (cleavage) type failures. This latter differentiation should be made, as from a practical point of view it may be important.

The introduction of the concepts of two fracture types on the fracture, flow-strength, temperature diagram was first undertaken

by Davidenkov[7] and has subsequently been variously modified as for example in Figure 4[8]. This type of diagram is phenomenological in character and does not aid in a basic understanding of the fracture process. It is, however, an informative construction and because of this has proven to be of considerable value.

It is interesting to consider the change in fracture appearance as a means of differentiating ductile from brittle failure. Fracture type data are plotted in Figure 1 for comparison with the energy absorption data, and it is seen that the two transitional phenomena do not agree. This is a point well worth emphasizing, for as will become evident below, the non-agreement in the transitions in energy absorption and fracture appearance is the rule for small specimens; and it is only for very limited conditions that agreement in these two transitions is achieved.

The treatment of tensile test data by the method of Ludwik, while initially holding promise for a solution of the problems associated with the intrusion of brittleness in mild steels under certain conditions of testing and use, have under further inspection proved to be unsatisfactory. This does not mean, however, that tensile test data may not ultimately prove of much importance in the analysis of the fracture behavior of steels.

Thus, it may be that the fracture characteristics of a steel are intimately connected with the ability of that steel to propagate strain[9]. The propagation of strain is envisaged as

depending on two quantities, namely, a work hardening exponent and a velocity coefficient which is similar to a viscosity coefficient. These two quantities are not easy to separate and cannot be separated in the standard tensile test. By testing at a series of temperatures in the vicinity of that of liquid air, however, it can be shown that the strain hardening exponent n defined by the equation $\sigma = \sigma_0 \delta^n$, varies with the temperature.*

Extreme values for the project steels studied are presented in Figure 5. These data at present cannot be used directly to predict the fracture characteristics of mild steel, but it is significant that the steel showing the minimum value of n at low temperature has the highest transition temperature in the notched bar tests.

Biaxial Stress Loading: Three sets of data will be considered here comprising the results of sphere[10], tube[11], and torsion tests[12]. For the sphere, to a close approximation, the stress system is balanced biaxial tension; for the tubes it is biaxial tension with a variable ratio of the principal stresses; for the torsion test, the principal stresses are a tensile stress and an equal compression stress.

The spherical test specimen diagrammed in Figure 6 was made of a steel comparable to Project Steel A. The fracture characteristics of this specimen were studied at numerous temperatures,

*n here is a complex quantity comprising both a strain hardening exponent n_0 and a velocity coefficient η. These two quantities cannot be separated by means of the data collected here.

with the pertinent data being summarized in Figure 7. It is evident from this figure that for the temperature range covered there is indicated no transition in ductility, despite the fact that by fracture appearance this transition was observed at about 60°F. It should be noted that the presence of a flaw in the sphere (as perhaps arising from a faulty weld) was a positive embrittling factor.

For purposes of comparison, slow-bend test data for this steel are described in Figure 8, wherein it is revealed that the transition as indicated by fracture appearance for the two tests is in good agreement. This perhaps suggests that failure of the spheres took place only after the development of effective notches in the course of straining, with these notches bringing about failure.

The tube specimen which was tested in biaxial tension is shown in Figure 32. The test data are summarized in Table 3[11]. The temperatures of testing of the tubes are so far apart that it is not possible to state transition ranges, but the transition in fracture appearance lies at about 70°F., while the transition in ductility presumably lies at a somewhat lower temperature[11]. It is interesting to note, however, that for these tubes either welds or structural defects were primarily responsible for failure, and therefore these tube specimens in the main may be considered as having failed prematurely. In other words failure of the tubes was initiated by some localized stress raiser and only indirectly by the principal biaxial stress system.

The sphere and tube tests were conducted on specimens which may be considered as large compared to standard laboratory test specimens. Despite the size of the specimens, high ductility was observable, particularly in the sphere tests, and presumably indicated in the tube tests in the absence of crack initiators and at temperatures which must be considered as low for the steel being used. On the other hand, for both the sphere and tube tests the transition in fracture appearance occurred at relatively high temperatures, and these temperatures are sensibly those predicted by small scale notched specimen tests.

In comparison with the sphere and tube tests, the torsion tests conducted by Larson[12] may be considered as small scale tests, and the element of size effect enters in the consideration of transition phenomena. The test bar used by Larson is indicated in Figure 9 and was made from steels C and E. The test data reported are not sufficient to describe fully the transition phenomena, but the transition in energy absorption definitely lies below -190°C. while the transition in fracture appearance definitely lies above -190°C, but below -70°F. It will be noted that for these steels the transition in ductility in the tension test lies above -190°C. The above results may be summarized briefly by stating that the loading of a specimen in biaxial tension will not in general lead to brittle failure unless the temperature is excessively low. In a specimen plastic flow is initiated which ultimately leads to the

development of an effective notch. Once this condition is reached for a large specimen, failure may result by the cleavage mechanism, if the temperature of the specimen is at or below the transition temperature indicated by a notched specimen such as, for example, the slow bend test specimen.

From the torsion test data it may be emphasized that the cleavage fracture and the temperature range in which it is found for a given steel is by no means relatable to a basic reference temperature which has a simple physical significance. Presumably in the compression test these steels would have no ductile-brittle transition.

Triaxial Stress Loading: Perhaps the simplest way in which a triaxial stress system can be developed is by the introduction of a notch in a bend test member. In general the more acute the notch, the more marked is the triaxiality of the resultant stress system, but for an edge-notched bend bar this stress system has in general the characteristics indicated in Figure 10[13]. This stress system is complex and cannot be used directly to interpret notch-bend-bar test results, but it has been observed that, in general, the more acute is the notch in the test bar, the higher is the temperature at which the transition from ductile to brittle behavior occurs, Figures 11 and 12[14].

It will be noted, however, that again as before there may be diagreement in the transition temperatures revealed by energy

absorption and fracture appearance, cf. Figure 11. For the V-notch specimen, however, it is indicated, cf. Figure 12, that under certain conditions of testing full agreement in the two criteria of ductile-brittle transition does obtain.

The test data which are reviewed in this report will have been largely obtained for notched specimens; therefore, specimens in which triaxial stress systems obtain. The magnitude of these stress systems will be largely unknown, and for this reason it may appear surprising that correlation of a consistent nature is at all possible. In anticipation of this objection, it is noted that both on theoretical and experimental grounds, there are indications that the triaxiality of the stress system arising from notch action has a limiting value[15,16]. The theoretical aspect of this problem has been thoroughly discussed by Neuber[13], while the results of Zeno and Low[17] and Bagsar[18] support the theoretical argument. Thus both Zeno and Low, and Bagsar studied the effect of notch acuity on the temperature of the ductile-brittle transition and found that it could be elevated to only a limited extent by increasing notch acuity. Bagsar's data are reproduced in Figure 13.

Criteria of the Ductile-Brittle Transition: In the above discussion two criteria of the ductile-brittle transtion have been examined. Numerous other criteria of this transition have been used but seemingly all are more or less intimately associated with either the transition in energy absorption or the transition in fracture

appearance. These criteria have been examined by Stout and McGeady for bend specimens and for the Navy tear test[19]. The criteria for determining the ductile-brittle transition may be summarized as follows:

Bend Specimen: fracture appearance, lateral contraction, bend angle, energy absorption to failure, maximum nominal load;

Tension Tear Specimens: fracture appearance, lateral contraction, energy absorbed to initiate crack, energy absorbed to propagate crack, nominal tensile strength, nominal yield strength;

Notched Tension Specimens: fracture appearance, lateral contraction, elongation, energy absorbed to failure, energy absorbed to maximum load, and nominal tensile strength.

Of the above criteria, the most easily interpreted are energy absorption and fracture appearance. That certain of the other criteria may on occasion be misleading is indicated by consideration of the idealized diagram, Figure 14, taken from Osborn, et al.[20]. The significance of these criteria has been discussed by Vanderbeck and Gensamer[8].

Metallurgical Structure and the Ductile-Brittle Transition: The steels which are of interest in the construction of merchant vessels must be of welding grades, and, therefore, steels which can undergo only limited metallurgical structural changes. In general, modifications of metallurgical structure which are possibly beyond the as-rolled structure result from normalizing or cold straining operations, the latter of which usually leads to strain aging.

Normalizing, when it clearly brings about a reduction in ferrite grain size, may profoundly lower the ductile-brittle transition[21] but when normalizing is effected without appreciable change in grain size, this lowering of the transition temperature may not be fully realized. As indicated by Lehigh Slow Bend test data, Figure 15, the optimum lowering of the transition temperature obtains for a normalizing temperature of about 1650°F. At normalizing temperatures appreciably above and below 1650°F., this treatment may not be efficacious.

Cold straining, in general, is considered as undesirable and leads to an elevation of the ductile-brittle transition as revealed by standard impact test data, but that the effects of cold straining may be complex is indicated in Figure 16[22]. For the notched impact bars the transition temperature was found to rise regularly with increasing strain. For the unnotched impact bars, however, the transition temperature passed through a maximum at about 10% elongation.

Fatigue and The Ductile-Brittle Transition: Pertinent data on the effects of fatigue on the ductile-brittle transition are summarized in Figure 17[23]. It is clearly evident from this figure that as fatigue damage increases, the ductile-brittle temperature is adversely modified and is elevated by about the same order of magnitude as results from strain-aging.

Velocity of Loading and the Ductile-Brittle Transition: The stress conditions in notched specimens are frequently complex beyond the powers of convenient mathematical analysis. For this reason alone loading effects cannot be considered in terms of true strain rates. However, it is known that for a given specimen the rate of loading may alter appreciably the temperature of the ductile-brittle transition. The manner in which this alteration is brought about is not at present clear and the limited data available are in some measure ambiguous. This is illustrated by a consideration of Figure 18[24]. Here are plotted transitions in energy absorption and fracture appearance for several of the project steels tested in tension impact at several impacting velocities.*

It will be noted that the curvatures of the respective lines for energy absorption and fracture appearance are inverted and in this sense are inconsistent. That the curvature of the fracture appearance lines are the more nearly correct may be surmised from an attempted extrapolation of the energy absorption curves to higher impacting velocities. If this is done consistent with the data given in Figure 18, first steel A and ultimately steels D_r and D_n will be evaluated as of less merit than either steel C or steel E. Since this conclusion does not seem warranted, on the basis of other test data obtained on these steels, it is surmised that the energy absorption curve undergoes a change of curvature perhaps as indicated in Figure 19. The shape of the transition temperature-velocity curve may be attributed to the experimental testing

*These velocities are converted from energy values and are considered as approximate only.

conditions and probably is not of fundamental importance. It is important to note, however, that the transition temperature is sensitive to the velocity of loading; and in a test where the transitions in energy absorption and fracture appearance coincide, it would appear that the ductile-brittle transition should increase monotonically with velocity of loading to develop a curve as drawn in Figure 20[14]. This latter curve reveals that an increase in the loading rate from that encountered under static loading conditions (head movement 3 inches per min.) to that encountered in impact testing (head movement 18 feet per sec.) produces a displacement of the transition temperature of +70°F. It will be noted that loading rates appreciably less than those encountered in impact loading may still result in an elevation of the transition temperature curve.

Size Effect and the Ductile-Brittle Transition: The term "size effect" as used in a discussion of the mechanics of the loading and deformation of different sized test bars presupposes the use of similar test bars. The term cannot be extended with this rigorous restriction to a consideration of the ductile-brittle transition, because of intrinsic defection from the requirements of similarity, experienced in the testing of the larger test bars. The modification of the ductile-brittle transition by "size effect" must be discussed with this reservation in mind.

Extensive research which is summarized by Fettweis[25] has shown conclusively that the ductile-brittle transition for similar specimens is higher, the larger the specimen. This for a given steel in an appropriate temperature range leads to a ductile-brittle transition with increasing size as is indicated in Figure 21. This phenomenon is critical in the problem of merchant vessel failures, in that because of it small-scale laboratory tests have not been available for use in predicting the fracture characteristics of structures. However, this difficulty can seemingly be overcome in the bend specimen by the use of a suitably formed sharp notch. Thus with a pressed notch of 0.0015 inch root radius transitions in lateral contraction and fracture appearance for a Schnadt-type slow-bend bar were in full agreement and constant as specimens dimensions were varied from 0.394 by 0.394 by 2.1 inches to 1.187 by 1.172 by 2.1 inches[14].

The engineering properties of metals are also modified by size effect. These properties have been extensively studied but are modified to only a limited degree by the ductile-brittle transition and so will be reviewed in a later section.

THE TESTING PROGRAM

In the analysis of the ship fracture problem, early appraisal of knowledge on the subject of the ductile-brittle transition indicated that "size effect" was largely responsible for these

failures. The testing program, therefore, was organized to include large-scale tests along with small-scale tests, the latter designed to attain correlation with the large-scale laboratory tests.

Toward the development of a large-scale laboratory test, exploratory work on flat plate specimens was completed at the David W. Taylor Model Basin[26]. The largest size specimen tested was 12 by 3/4 inches with an internal notch, Figure 22. Pertinent details of the internal notch are given in Figure 23. Specimens with suitable notch geometry were tested in both 6- and 12-inch widths at appropriate temperatures. Pertinent results are summarized in Figures 24 and 25.

From Figure 24, it is evident that a minimum length notch must be used in this type of specimen to insure consistent results for comparison purposes, and this length has been standarized as one fourth of plate width.

In keeping with the discussion on size effect it was expected that the plate tests would give transition temperatures which would be relatively lower than those for a ship structure. By an adjustment of notch acuity this condition could be minimized. The results obtained in the study of notch terminus radius are given in Figure 25, where it will be noted that jeweler's saw cut was the most severe of the notches studied. This notch terminus was used throughout in subsequent flat plate testing.

Of the large-scale tests the most completely explored were the internally notched flat plate tests in the 12-, 24-, 48- and 72-inch widths[11,27]. Several additional specimens 108 inches in width were tested. A drawing of the test specimen is given in Figure 26, and a picture of the 72-inch plate specimen in the tensile test machine is given in Figure 27.

The data of the original flat plate test program indicated that the results obtained with the 12" plate specimens are equivalent to those obtained with the 72-inch plate specimens, and the subsequent flat plate testing at Swarthmore College[28] has been limited to the 12-inch wide specimen in which $L = \frac{W}{4}$, see Figure 26. This specimen in place in the testing machine and ready for testing is shown in Figure 28. The Swarthmore data which are considered in this report were obtained with this specimen. This fact is noted to eliminate confusion with the later modification of this test specimen for the Swarthmore aspect-ratio test program. Data from this program will not be considered in this report.

It was recognized that the data which were obtained in the various tests could not be applied directly to the problem of ship failures without further testing, preferably on a ship structure, but under controlled conditions. Full-scale ship tests meeting the above restrictions are conceivable but hardly feasible, so the full scale hatch corner test was devised[29]. The objectives of the hatch corner testing program included: (a) the determination of the ductile-brittle transitional behavior of selected project steels fabricated

into hatch corners of the basic design, and (b) the redesign or modification of the basic Liberty ship hatch corner detail. This first program was essential to the integration of the flat plate testing program with structural behavior.

The test specimen based on the basic hatch corner design is given in Figure 29. The method of testing behavior in testing are in some measure indicated from a consideration of Figures 30 and 31.

The basic hatch corner specimen was tested in numerous modifications and several additional new designs were also tested. Details of these design alterations must be sought in the original report[29].

Because of its size, it is not possible to test a full width of ship's deck in way of the hatch opening. The specimen selected, see Figures 29, 30 and 31, was as large as could be accommodated in the testing machine of greatest capacity then available.

The problem of brittle ship failures was recognized as arising from the action of stress raisers such as structural discontinuities, accidental notches, etc. The large-scale test program as outlined above took cognizance of this fact, and all specimens possessed effective stress raisers. The magnitudes of these multiaxial stresses, however, were not known; and it appeared desirable to explore the field of multiaxial stress in structures. To this end large tube tests were designed such that the temperature of testing could be varied over wide controlled limits, while the longitudinal and hoop stresses in the shell could be varied regularly through prescribed values to fracture[30]. This test specimen is shown in

Figure 32. (The data obtained with this type specimen have already been discussed.)

The completed program of tests on large-scale specimens indicated that the mild steels tested all experienced brittle failures at temperatures above about 20°F. Since temperatures of this order and lower are regularly encountered in service, it appeared desirable that the ductile-brittle transition phenomena in certain high-yield strength structural steels be examined. Since these steels were to be examined for possible merchant vessel use, the full-scale model hatch corner test specimen would be a logical specimen to test, but because of the high strength properties of the steel used, the capacity of the tensile machine would be exceeded by this specimen. For this reason the restrained welded specimen given in Figure 33 was designed[31]. This specimen ready for testing is presented in Figure 34. Comparable tests for the 12-inch flat plate specimen, previously described, were also run.

The specimens described above are, in all instances, large specimens and are too large for routine laboratory testing. It was necessary, therefore, that experimentation be undertaken to explore the possibilities of the correlation of small-scale laboratory test results with those obtained in the large-scale tests. In the course of this experimentation the specimens given in Figure 35 were variously used.

EXPERIMENTAL RESULTS

I. Project Steels.

The data obtained for the project steels will be considered

following which the further data obtained on the augmented program will be examined. The ductile-brittle transition data are considered first.

The Ductile-Brittle Transition -- Project Steels: Over a period of many years the ductile-brittle transition has been extensively studied in the impact test. For this reason one of the first steps in the examination of the project steels consisted in the determination of the impact transition curves for standard test conditions. Data so obtained for the standard keyhole and V-notch Charpy test bar are presented in Figures 36 and 37.

The impact transition curves are drawn as smooth curves which vary regularly through a range of temperature from the maximum value of energy absorption, or ductile condition, to the minimum value of energy absorption or brittle state. Comparison of transition temperature ranges becomes possible from such curves, but occasional irregularities in individual curves preclude this method of comparison from being generally applicable. Further, the comparison of energy absorption--temperature curves is not a desirable method of evaluating the fracture characteristics of steels, as this is an unwieldly procedure. It has been general practice, therefore, to select some energy absorption value as a reference value for evaluating impact transition temperatures. Thus a commonly used method specifies that temperature, as the transition temperature, at which the energy absorption for a standard keyhole Charpy

specimen equals 20 ft. lbs. Other methods have required that 1/4 maximum, 1/2 maximum or maximum energy absorption can be specified as the reference criterion.

The impact transition temperatures as specified above may prove fully acceptable for control purposes, but it is probable that with the exception of the maximum energy absorption value, these arbitrarily specified transition temperatures are not suitable for a fundamental study of the fracture problem. Thus it has been argued that the gradual decrease of energy absorption through the transition range, for the V-notch Charpy bar, is an effect resulting from the fracture behavior of the metal on the compression side of the test bar[32]. If this were true, the elimination of the compression side of the test bar, as is effectively done in the Schnadt-type bar, should eliminate the characteristic broad transition range indicated, for example, in Figure 37 (as shown by the slope of the curve in the transition range). The data in Figure 38 reveal that an elimination of this broad transition range does obtain when the compression zone of the impact bar is removed[14]. The impact test transition temperatures for the project steels, by the indicated criteria are summarized in Table C.

It has been indicated earlier that certain of the steels which are being considered here are especially sensitive to strain rate. In the impact test an unknown factor due to strain rate sensitivity precludes the adjustment of the impact data to predict static notch-bar test results. The impact test, however, can be used with this

reservation in mind, to examine steel quality, thus for example, to indicate the effects of strain-aging, grain size, plate thickness, etc., on the fracture behavior of a given steel. Groups of data which may be compared on this basis are presented in Figures 39 to 45. These data show that the ductile-brittle transition is markedly elevated by increase in grain size (plate thickness constant) and by increase in plate thickness (grain size approximately constant). Variations from plate to plate within the heat tested are not large as shown in Figures 41, 42 and 43.

It is needless to discuss the steps taken in the development of suitable correlation tests, by means of which the ductile-brittle transition in the large plate tests could be predicted. Such tests have been developed in several directions as may be gathered from a consideration of the data presented in Figures 46 to 54. These figures summarize all pertinent data relevant to the temperature of the ductile-brittle transition in the project steels (see Table A). Some few test results have not been included because of the incompleteness of the data.

From Figures 46 and 47 it will be seen that virtually complete agreement in the transition temperature data obtains for the large-- and small-scale tests that have been reported. By analogy this statement can reasonably be extended to embrace all the project steels as Figures 48 to 54 show. There is little question, therefore, that the ductile-brittle transition temperatures, for such steels loaded under static conditions in structures, can be predicted

with a relatively high degree of accuracy. As will follow from a consideration of the results reported from the 3-inch edge-notched tension test, it is necessary to specify the criteria of the ductile-brittle transition for restricted tests, with, in general, fracture appearance being the most suitable criterion for correlating the results of the small-scale tests with the large-scale test results.

Tensile Strength and Size Effects -- Project Steels: A structure is designed to carry a prescribed load, and in the interests of economy this load should be as great as possible and yet safe from failure. Experience has shown that in meeting these combined needs the nominal tensile strength is not a suitable criterion of the strength of a structure but must be modified by a safety factor.

Since safety factors are regularly used in structural design, it should not, perhaps, be unsuspected to find that in the flat plate tests a marked drop-off in tensile strength accompanies and increase in plate size, as shown in Figure 55. The drop-off steels (of 55,000 to 65,000 lb./sq.in. tensile strength) frequently amounts to about 1/3 of the tensile strength so that the tensile strength value for 48-inch internally notched plate lies between 35,000 and 45,000 lb./sq. in. Hatch corner test data, however, show that the reduction in tensile strength indicated for the flat plates is not the maximum to be observed, for nominal tensile strengths as low as 25,000 lb./sq. in. observed, for nominal tensile

strengths as low as 25,000 lb/sq.in. have been reported for the hatch corner tests. In other words a reduction in tensile strength by 50% can arise in a structure.

The reduction in the tensile strength in the hatch corner tests is in large measure a design problem, as is indicated in Figure 56. Redesigning is frequently relatively simple; but while marked improvement in strength can be achieved in this manner, this can be done only by the virtual elimination of all important local stress raisers. Accompanying this increase in tensile strength there is a more or less general increase in ductility which is very desirable.

In the examination of Figure 56 it is noted that wide variations in energy absorption values have been obtained. This may be construed as a lowering of the transition range for the steel, a conclusion, however, that should be avoided. The model hatch corners were all made of steel C which in the large plate tests has a transition temperature of +100°F. The test data which are compared in Figure 56 were all obtained at 70°F., and all fractures were by cleavage. Specimen 35 failed by cleavage which was initiated at an accidental arc strike incidental to the welding of the structure. A discussion of matters pertinent to this behavior will be undertaken below.

II. Additional Tests.

The testing program which has been reviewed in the previous section can be expanded in two obvious directions, the first of

which consists in an attempted correlation of the properties revealed in the above tests with the properties of the same materials in a ship structure. The second consists in the exploration of the possibility of improved structural materials. Limited experimentation in these two directions has been completed and is considered below.

Fractured Liberty Ship Plate Tests: It was generally accepted during the formative stages of the research program under consideration that the brittle problem in Liberty Ships was directly a size-effect problem. Thus for the small-scale tests a low transition range might be expected, and this transition range would be displaced to increasingly higher temperatures as the size of the test bar was increased. Figuratively then a full-size ship should characterize a more or less definite transition range for a specified steel, and this would lie at a higher temperature than that for a small-scale test bar. By this predicate, a ship could be considered as safe from brittle failure as long as the operating temperature was above that of the transition range, but it would become highly susceptible to brittle fracture once the temperature fell below that of the transition range. By this principle of behavior it becomes reasonably convenient to attempt suitable correlation between the many laboratory test results and full-scale ship behavior.

Thus, for example, of the several ships which broke in two, a restricted few failed under well-documented conditions of temperature and loading and were accessible for experimental purposes.

From these ships, therefore, plate pertinent to the initiation, propagation and termination of the crack could be removed for laboratory testing, particularly in the interests of a precise determination of the ductile-brittle transition in the small-scale tests. Since the correlation attempted in this manner assumes that the temperature at which the ship broke will reveal the temperature of the ductile-brittle transition for the ship, the small laboratory tests should allow the determination of any needed correction factor for ship plate evaluation by means of the small-scale tests. Test data pertinent to this correlation for the 12-inch flat plate specimen have been reported for two ships, the "Pierre S. Dupont" and the "Ponaganset"(33).

The "Pierre S. Dupont" suffered brittle fracture during a severe winter storm at sea on February 10, 1948, with the air/water temperatures reported as 27°/42°F., respectively. Details of the location of the plate available for testing and the specimen lay-out are given in Figures 57 and 58. The T-2 Tank Ship "Ponaganset" broke in two on December 9, 1947, while moored and under a hogging load, with the air/water temperatures being reported as 34°/41°F., respectively. Details of the plate location for specimens from the "Ponaganset" are given in Figures 59 and 60. In both the ships studied the cracks were initiated at about air temperature which allows fixing the apparent transition ranges at about 30°F. for the "Pierre S. Dupont" and at about 35°F. for the "Ponaganset".

The chemical analyses of the plates removed from these two ships are given in Table D and the mechanical properties are given in Table E. The results of the 12 inch flat plate tests are given graphically in Figure 61, while the various transition temperature data are accumulated in Table F. The data for the 12-inch flat plate tests on the fractured ship plate indicate the transition temperatures for the plates tested lie between 40°F. and 110°F. These data indicate that these plates through which the crack propagated had transition temperatures above the apparent transition temperatures of the ships and hence extended fractures should have been possible.

Tests of Other Steels: The high yield strength steels which were studied at the University of California could not be fabricated into full-scale hatch corner test specimens because of load restrictions on the available testing machine. A reduced sized specimens called the restrained welded specimen was tested instead. For comparison purposes steels Br and C were tested using this specimen, and the data obtained have already been presented. The restrained welded specimen gives nearly the same transition temperatures for the two steels as does the full-scale hatch corner test. The results obtained for the high yield strength structural steels using this specimen will, therefore, be considered as equivalent to the full-scale hatch corner tests run on the project steels.

The chemical compositions, thermal treatment, and mechanical properties of the high yield strength structural steels studied are presented in Table G. The transition range data are summarized in Figures 62 and 63, and transition temperatures are accumulated in Table H.

In brief, these data reveal that much reduced transition range is possible with selected HYS steels but that a low transition temperature is not assured by the use of such steels. Further, it is evident that the good correlation that obtained among the respective tests for the project steels is not typical, as transition temperatures given by the 12-inch flat plate HYSS specimen are as much as 50°F. removed from those given by the restrained welded specimen.

The nominal tensile strength values of the restrained welded specimen of the HYS steels studied here may drop to as low as 35 to 40% of standard room temperature coupon test values, but the average nominal strength of the specimens tested was approximately 65% of the standard test bar tensile strength.

The Studies of Kahn and Imbembo: The survey of the ductile-brittle transition phenomena in the Navy tear test by Kahn and Imbembo[34] has been especially revealihg because of the large number of different types of steels which have been studied with this test. Since the transition phenomena associated with this test have already been described for the project steels, it will

be sufficient to consider here only the transition temperature data which have been accumulated. Details of the chemical composition and thermal treatment of the steels studied are presented in Tables I and J, and the transition temperature data are presented in Figures 64 to 68.

From the tabulated data it is seen that the work included the testing of:

a. Semi-killed medium steels
   1. Normal manganese contents
   2. Higher manganese contents
b. Fully killed medium steels
c. Vanity-type high-tensile steels
d. Medium steels of several thicknesses
e. Steels finished by non-conventional mill practices.

Many of the steels were also tested after stress-relieving and normalizing treatments.

The following generalizations, which have been stated previously, are emphasized in a consideration of these data:

a. The transition temperature for a given steel is lower, the lesser is the finished plate thickness, cf., Figure 64.
b. The transition temperature for a given steel is lower, the smaller is the ferrite grain size, and the reduction in transition temperature by the reduction in grain size may be of large magnitude.

c. Normalizing when accompanied by a reduction in the ferrite grain size may reduce the transition temperature by as much as 150°F., but when a reduction in grain size does not accompany the normalizing treatment, the reduction in transition temperature may not be present. In this latter case when a reduction in transition temperature is noted, it is normally of small magnitude.

In addition to the above generalizations, it may also be concluded that:

a. For the as-rolled condition, there is a probable slight reduction in the transition temperature as the deoxidation practice varies to produce from a rimming to fully killed class of comparable steels. This reduction is more marked for aluminum treated steels.

b. An adjustment of the (Mn/C) ratio to higher values does not ensure a reduction in transition temperature for the as-rolled plate. For such steels, however, a normalizing treatment may produce a reduction of the transition temperature by as much as 40°F., cf., Figure 65. This reduction seemingly is brought about by a reduction in ferrite grain size.

c. The lighter plate for the high (Mn/C) ratio steels consistently shows the smaller ferrite grain size, and this grain size is not materially reduced by normalizing. The

grain size in heavier plate in the normalized condition approaches that representative of the light plate, and similarly the transition temperatures for the heavier plate approach those of the light plate.

d. In the steels studied the McQuaid-Ehn grain size was of minor importance in determining the transition temperature.

e. Stress-relieving treatments were not observed to improve the fracture characteristics of the plate studied.

DISCUSSION

The experimental data which have been presented, indicate that much of the steel which has been used in Liberty and Victory ship construction may ordinarily be expected to fail with brittle fractures at the temperatures at which these ships regularly operate. That the ductile-brittle characteristics of these steels, then, do not of necessity determine the structural behavior of the steels must follow, since most Liberty and Victory ships continue to operate satisfactorily. From this it follows that either the correlation of laboratory tests with ship structural behavior is precluded by the operation of unknown quantities, or that the factors which modify the transition temperature of a steel are improperly combined in the tests to simulate the conditions of ship operation.

That the second alternative is the more probable follows from a consideration of Figure 69. Here are presented maximum nominal strength deck stress levels, determined for ships of a type considered

here under operating conditions, and it will be noted that these stress values are very much less, for all conditions of loading, than the comparable stress values measured in the hatch corner tests.

In examining the apparent incompatability of the laboratory test results with full-scale ship behavior it becomes desirable to examine more closely the significance of the ductile-brittle transition as determined in the small-scale tests, and to re-examine the conditions of loading in both the laboratory tests and in a ship structure. Of these the ductile-brittle transition will be considered first.

The Ductile-Brittle Transition: The appearance of brittle fractures in mild steel specimens has been shown to be possible in unnotched tensile bars tested at a suitable low temperature. None of the steels which have been studied are brittle in this way at ship operating temperatures. Such brittleness in ships must result, therefore, from the existence of effective notches in extreme tensile structural members. Such notches may arise from design or from defective workmanship, or from a variety of incidental factors such as arc strikes, the welding of clips to the deck, etc. It is further possible that effective notches may arise from the action of fatigue. It is evident, therefore, that the effective notches that exist in two ships of the same design may vary over a considerable latitude of intensities in corresponding areas. However, the design of a ship

may be such that the incidence of severe effective notches is high, a case that proved to be true in the basic Liberty ship design. When effective notches arise in this way, design changes may be introduced to bring about a structure which then becomes as resistant to brittle fracture as the structural materials will allow. An effective stress raiser may not be a design feature of the ship but may arise from operations involved in tying down cargo, the welding of clips to the deck, or from fatigue action. The significance of the ductile-brittle transition observed in the small-scale tests with respect to ship structural behavior must center then from the outset on a consideration of the intensities of notch action possible in a ship structure. Such knowledge will be informative in the design of small-scale tests to predict the transition temperature of a ship structure under essentially static loading conditions.

The most severe notch that can be in a ship structure will result from fatigue action. This is a notch which from earlier discussion may be considered as having attained a limiting stress raising capacity and should characterize a limiting maximum transition range. Under static conditions of loading the ship structure possessing a fatigue notch as the effective stress raiser would then have its highest transition temperature.

If the effective notch is not a fatigue crack, in general under static loading the metal in the notch may be expected to

reach the yield point and deform before the adjacent material. Even in a relatively mild notch, however, the stress in the notch may exceed the fracture stress of the metal before yielding takes place in the adjacent material. Once this happens, a crack will form which if propagated brittlely the structure will fail with a transition temperature characterized by this crack, thus with a transition temperature in agreement with that determined for the fatigue crack in the same structure.

When the effective notch in the ship structure is sufficiently mild so that plastic flow is possible in regions outside the notch before cracking takes place in the notch, extensive plastic distortion of the structure is possible to failure.

Under conditions of static loading it is useful to know the maximum temperature at which brittle fracture can occur and this is a temperature determined by the most acute notch available--the fatigue crack. This temperature is important for it would appear that all ship fractures originate in notches equal in intensity to fatigue cracks, and if this is so that latent transition temperature of the ship, when this ship is made of mild steel, must be high. Under static conditions of loading to failure this high transition temperature would be realized.

Under service conditions the ship would possess a still higher transition temperature due to the dynamic conditions of loading, but brittle failure thus to be expected is not normally realized.

That brittle failure does not take place must arise because of differences in loading under the laboratory and service conditions. These deviations in loading conditions will now be considered.

Loading Conditions in Structures: Nominal tensile stress values of 10,000 lb./sq. in. are not regularly experienced in the strength deck of ships in operation, whereas, the nominal stress in the hatch corner test specimen was measured at 25,000 lb/sq. in. at failure. In an examination of this question a consideration of the load-elongation diagram for a 12-inch plate specimen as given in Figure 70 is informative. On this diagram the load is specified at which the initial crack is formed. A consideration of the numerous stress-strain diagrams included in the indicated reference[28] reveals that this crack is regularly formed very early in the course of the test and at a load of about 5/7 the tensile strength determined in this test. The ratio of the load to initiate cracking to the maximum load increases somewhat when the specimen fails with low energy absorption, but in this case also the initial crack is normally present for some time prior to failure.

In a ship structure the conditions of loading are not such that a crack can be initiated and propagated slowly to fracture of the structure. On the contrary the loading cycle due to wind loading and wave action can be expected to be quite short with a consequent "impact" type of loading being experienced. With this type loading the structure may be overloaded for but a

relatively short time, following which the overload is released. The problem of fracture in the ship then is resolved into two components, namely, a loading factor and a time factor. The interplay of these two factors may be quite complex and may modify the strength properties of the ship steel in a way not now recognized. The response of the ship steel to such loading cycles will now be considered.

Since the loading rate experienced by the ship can be relatively high, the transition temperature considered typical of the ship constructed of a given steel must be elevated by a proportionate velocity factor over that experienced under static loading conditions. If the ship is operating at a temperature that lies in the range of brittle behavior, two conditions must now be fulfilled before cleavage failure will result. The ship must be overloaded; i.e., the stress in the effective notch must exceed the fracture strength of the steel, and secondly, this stress must be maintained sufficiently long to allow the crack to be initiated and propagated.

It is recognized that all cleavage fractures are generally preceeded by some, though slight, amounts of strain. It is also accepted that the crack is developed in the initial stages of its life at a slow rate but is propagated at a high rate. From this it is concluded that a short but important time interval must elapse before a fast moving cleavage crack can be established. This time interval for a given steel must depend on the temperature and the amount of overloading experienced in the critical section.

No data are now available to allow a discussion of these quantities. However, it is expected that those steels which have the lower transition temperatures, as determined by the laboratory tests, will be the most effective in suppressing brittle crack formation in ships.

Ship Steel Selection: In the consideration of steel selection for future merchant vessel construction restricted lines of action are possible. The extreme approaches to the ship fracture problem are first, the relaxation of materials fracture specifications with the expected elimination of the fracture problem by control of design and second, the setting up of a fully reliable fracture specification test, with the relaxation of design restrictions.

The latter approach if readily realized would probably prove desirable from the point of view of construction, but the ductile-brittle transition studies which have been completed to date indicate that a construction program based on this philosophy of materials selection would lead to the rejection of a large percentage of the steels which could be supplied for ship construction. This is obviously an unacceptable solution.

The alternative approach to the ship fracture problem, that of controlling ship fractures by design control, has been used in the construction of the Victory ships. These ships continued to operate satisfactorily until the winter of 1951-1952, at which time several serious failures occurred. This suggests that design improvement without consideration for the fracture characteristics of the steel is not the final answer to the ship fracture problem.

It is not the purpose of this discussion to advance a given test for the purposes of specification needs, but in the interests of close coordination of such tests with service failure, two quantities must be given much importance, and these quantities are the intensity of the notch and the duration of loading. Since the effective notch in determining the fracture characteristics of a structure is an extremely acute crack, the notch in a small-scale correlation test specimen should be sharp. The relative duration of loading of the specimen would simulate that experienced by the structure. The testing of even a small test bar over an appropriate range of temperature should then satisfactorily predict the location of the ductile-brittle transition for the ship. The transition temperature so determined alone will not predict the performance of the ship and gives only one extreme value for consideration in anticipating ship performance. Qualitatively, however, there can be no question but that those steels which have the higher transition temperature will fail more readily in a ship structure than will those with the lower transition temperatures. In view of the paucity of data pertaining to the time and loading effects on the development of a cleavage crack in mild steels and to uncertainties about loading conditions in ship service, it does not appear possible at this time to devise a test that will provide full correlation with ship performance.

ACKNOWLEDGMENT

The present report is a review of the salient features of the investigations conducted on medium ship steel under the auspices of the Ship Structure Committee. The reports which have been submitted by the many contractors of these investigations are both numerous and voluminous, and it has not been possible tp present here other than selected material taken from these reports. The selection of material for inclusion in this report has been the responsibility of the authors, but valuable suggestions indicating appropriate deletions and/pr additions have been made by Drs. John Low, Jr., and Finn Jonassen, both of whom were kind enough to examine the manuscript in one or more of its early forms. The writers' associates at the Pennsylvania State College, notably Drs. John R. Low, Jr.; William Lankford, Jr.; John Ransom; T. A. Prater; were closely associated with the early development of the research program that was ultimately completed at that institution.

The writers would like finally to thank Messrs. James McNutt and Fred Bailey for much assistance in placing the manuscript, tabulated material and cuts in final form. Their task has been rather a difficult one as certain of the cuts requested have not been readily available.

BIBLIOGRAPHY

(1) Final Report of the Board to Investigate the Design and Methods of Construction of Welded Steel Merchant Vessels, July 15, 1946.

(2) Technical Progress Report of the Ship Structure Committee, March 1, 1948.

(3) Second Technical Progress Report of the Ship Structure Committee, July 1, 1950.

(4) M. Gensamer, E. P. Klier, T. A. Prater, F. C. Wagner, J. O. Mack and J. L. Fisher: "Correlation of Laboratory Tests with Full Scale Ship Plate Fracture Tests." Ship Structure Committee Report Serial No. SSC-9, March 19, 1947.

(5) A. Le Chatelier: Rapport a la Commission francaise des Methodes d'essais le 22 October 1892. Contrib. pp. 25/46.

(6) P. Lukwik: "Elements der Technologischen Mechanik, Berlin, Julius Springer, 1909.

(7) N. N. Davidenkov and E. M. Shevandin: Jnl. Techn. Phy. IV, 1934.

N. N. Davidenkov: "Dynamic Metal Tests." Second edition, 1936, pp. 158 et. seq.

(8) R. W. Vanderbeck and M. Gensamer: "Evaluating Notch Toughness," Welding Research Supplement, p. 37-s, January 1950.

(9) M. Gensamer: "Strength and Ductility." Trans. A.S.M. 36. p. 30, 1946.

(10) J. Marin, V. L. Dutton and J. H. Faupel: "Hydrostatic Tests of Spherical Shells," Welding Research Supplement, p. 593-s, December, 1948.

(11) H. E. Davis, G. E. Troxell, E. R. Parker, A. Boodberg and M. P. O'Brien "Causes of Cleavage Fracture in Ship Plate: Flat Plate Tests and Additional Tests on Large Tubes." Ship Structure Committee Report Serial No. SSC-8, January 17, 1947.

(12) H. Larson and E. P. Klier: Trans. A.S.M. 43, P. 1033, 1951

(13) H. Neuber: "Theory of Notch Stress: Principles for Exact Stress Calculation" Ann Arbor, Michigan, 1947, pp. 155-175.

(14) K. J. Stodden and E. P. Klier: "Brittle Failure and Size Effect in a Mild Steel," Welding Research Supplement, p. 303-s, June 1950.

(15) E. Orowan, J. F. Nye and W. J. Cairns "Notch Brittleness and Ductile-Fracture in Metals," Theoretical Research, Report No. 16/45, Ministry of Supply, Armament Research. Sept.; July 1945.

(16) G. Sachs and J. D. Lubahn, Welding Research Supplement. 1944

(17) R. S. Zeno and J. R. Low, Jr.: "The Effect of Variation in Notch Severity on the Transition Temperature of Ship Plate Steel in the Notched Bar Impact Test," Welding Research Supplement, p. 145-s, 1948.

(18) A. B. Bagsar: Welding Research Supplement, p. 284-s, October 1949.

(19) R. D. Stout and L. J. McGeady: "The Meaning and Measurement of Transition Temperature," Welding Research Supplement, p. 299-s, 1948.

(20) Osborn, Scotchbrock, Stout and Johnston, "Comparison of Notch Tests and Brittleness Criteria", Welding Research Supplement, p. 24-s, 1949.

(21) R. D. Stout and L. J. McGeady: "Notch Sensitivity of Welded Steel Plate", Welding Research Supplement, p. 1-s, January 1949.

(22) N. N. Davidenkov and P. Sakharov: "On the Influence of Cold Working upon the Brittleness of Steel," Tech. Phy. U.S.S.R. 5, p. 743, 1938.

P. Sakharov: "On the Influence of a Notch upon the Critical Temperature of Brittleness of Cold-Worked Specimens," Tech. Phy. U.S.S.R. 5, p. 758, 1938.

(23) J. M. Lessells and H. E. Jacques: "Effect of Fatigue on Transition Temperature of Steel," Welding Research Supplement, p. 74-s, February 1950.

(24) W. H. Bruckner and N. M. Newmark: "Axial Tension Impact Tests of Structural Steels," Welding Research Supplement, p. 67-s, 1949.

(25) F. Fettweis: "The Notch Impact Test - Development and Critique", Arch. Eisenhüttenw. 10, p. 625, April 1929. (A partial English translation has been published by the Ship Structure Committee)

(26) R. R. Thomas and D. F. Windenberg: "A Study of Slotted Tensile Specimens for Evaluating the Toughness of Structural Steel, Welding Research Supplement, p. 209-s, April 1949.

(27) W. M. Wilson and R. A. Hechtman: "Cleavage Fracture of Ship Plate as Influenced by Size Effect," Ship Structure Committee Report Serial No. SSC-10, June 12, 1947.

(28) S. T. Carpenter and W. P. Roop: "Tensile Tests of Internally Notched Plate Specimens", Welding Research Supplement, p. 161-s, April 1950.

(29) E. P. DeGarmo, J. L. Weiran and M. P. O'Brien: "Causes of Cleavage Fracture in Ship Plate - Hatch Corner Tests" Ship Structure Committee Report No. SSC-5, October 23, 1946.

(30) H. E. Davis, G. E. Troxell, E. R. Parker and M. P. O'Brien: "Behavior of Steel under Conditions of Multiaxial Stress and Effect of Welding and Temperature on this Behavior; Tests of Large Tubular Specimens," OSRD No. 6365, Serial No. M-542, December 6, 1945.

(31) A. Boodberg and E. R. Parker, "Causes of Cleavage Fracture in Ship Plate; High Yield Strength Structural Steel", Ship Structure Committee Report Serial No. SSC-28, September 21, 1949.

(32) E. P. Klier, F. C. Wagner, J. L. Fisher and M. Gensamer: "Correlation of Laboratory Tests with Full Scale Ship Plate Fracture Tests, A Study of Strain Gradients, Ship Structure Committee Report Serial No. SSC-17, 1949.

(33) E. M. MacCutcheon, C. L. Pittiglo and R. H. Raring, "Transition Temperature of Ship Plate in Notch-Tensile Tests", Welding Research Supplement, p. 184-s, April 1950.

(34) N. A. Kahn and E. A. Imbembo, "Further Study of Navy Tear Test", Welding Research Supplement, p. 84-s, February 1950.

TABLES
AND
FIGURES

TABLE A

CHEMICAL ANALYSES OF THE STEELS

CODE	C %	Mn %	P %	S %	Si %	Al %	Ni %	Cu %	Cr %	Mo %	Sn %	N_2 %
A	.26	.50	.012	.039	.03	.012	.02	.03	.03	.006	.003	.004
Br	.18	.73	.008	.030	.07	.015	.05	.07	.03	.006	.012	.005
Bn	.18	.73	.011	.030	.04	.013	.06	.08	.03	.006	.015	.006
C	.24	.48	.012	.026	.05	.016	.02	.03	.03	.005	.003	.009
Dr	.22	.55	.013	.024	.21	.020	.16	.22	.12	.022	.023	.006
Dn	.19	.54	.011	.024	.19	.019	.15	.22	.12	.021	.025	.006
E	.20	.33	.013	.020	.01	.009	.15	.18	.09	.018	.024	.005
F	.18	.82	.012	.031	.15	.054	.04	.05	.03	.008	.021	.006
G	.20	.86	.020	.020	.19	.045	.08	.15	.04	.018	.012	.006
H	.18	.76	.012	.019	.16	.053	.05	.09	.04	.006	.004	.004
N	.17	.53	.011	.020	.25	.077	3.39	.19	.06	.025	.017	.005
Q	.22	1.13	.011	.030	.05	.008	.05	.13	.03	.006	.018	.006

V % $<$ .02; As % $<$ .01 in each steel.

TABLE B

Summary of Test Results —20-In. Diameter Tubes

Specimen	Stress Ratio,[a] T/L	Loading Conditions	Test Temp. °F.	Heat Treatment (1100°F)	Conventional Stress psi.[i]		Nominal Stress,[b] psi.		Average True Stress at Fracture,[c] psi.		Maximum Percent Elongation in 5 in.		Reduction in Wall Thickness, %	Potential Energy at Fracture, ft.-lb.[h]	Nature of Fracture
					Longi-tudinal	Trans-verse	Prop. Limit	Ulti-mate	Long	Trans.	Long	Trans.			
A	2	Internal Pressure	70	Before Welding	26,250	52,500	30,000	52,000	42,500	85,000	1	15.0[j]	30.0	133,000	Initiated by shear in plate about 4 in. from and parallel to weld near midsection; after shearing for about 5 in., crack propagated over considerable length of tube by cleavage.
H	2	"	70	Before and After Welding	24,900	49,800	30,000	62,000	45,000	90,000	1	21.0[j]	32.0	148,500	Practically same as for tube A.
B[d]	2	"	-42	Before Welding	25,650	51,300	40,000	54,000	30,000[e]	60,000[e]	0.2	3.0	3.0	110,000	Cleavage fracture entirely around circumferential end weld.
C[d]	1	Axial load int. press.	70	Before Welding	55,100	51,300	30,000	56,000	60,000[e]	59,500[e]	4.4	4.4	9.0	109,500	Shear for 6 in. (premature);[f] after repair by welding, shear for 4 in., then cleavage.[g]
D[d]	1	"	70	"	56,800	53,100	30,000	56,500	60,500[e]	56,000[e]	3.5	4.0	7.5	102,000	Cleavage fracture originating in weld about 48 in. from mid-section and propagating spirally around tube.
E	1	"	70	"	56,800	51,000	30,000	61,500	69,000	72,000	9.2	10.6	20.0	143,000	Cleavage fracture originating in weld 2 in. from mid-section and propagating completely around tube. No shattering.
F	1	"	-44	Before Welding	45,400	44,500	40,000	44,500	45,500	45,500	1.6	2.0	3.5	86,500	Cleavage fracture originating in weld 24 in. from mid-section. Specimen shattered into many pieces.
O[k]	1	"	-40	"	48,760	48,600	34,000	50,000	49,100	50,600	4.2	3.8	6.0	98,000	Cleavage fracture originating at longitudinal weld 22-in. from mid-section proceeding along the heat affected zone parallel to the weld and then around the tube at both ends.
I	1	"	-39	Before and After Welding	62,500	51,400	40,000	65,000	85,500	88,500	17.4	18.7	31.0	201,000	Cleavage fracture originating in weld 4 in. from mid-section. Specimen shattered into many pieces.
L	1	"	-42	"	58,600	54,300	37,000	56,000	62,000	59,900	5.7	6.3	10.8	205,000	Cleavage fracture originating near top of the tube at the defect in the plate, propagating around upper portion and downward parallel to the weld. Specimen shattered into many pieces.
J	1	"	-38	None	59,700	59,300	25,000	59,000	61,000	64,500	3.0	3.0	6.7	160,500	Cleavage fracture originating in weld 28 in. from mid-section. Specimen shattered into many pieces.
G	1/2	Axial load, int. press.	-44	Before Welding	50,800	24,700	42,000	49,500	50,000	25,000	2.0	0.3	2.0	38,000	Cleavage fracture originating at defect in plate, 90° from weld, 44 in. from mid-section, and propagating around specimen. No shattering.

[a] T = circumferential stress; L = longitudinal stress.

[b] Nominal stress computed on basis of original wall thickness but with respect to greatest diameter obtained at the designated load condition.

[c] Computed as load on a given section divided by actual cross-sectional area, except as noted in footnote *e* for specimens failing prematurely. Underlined values indicate direction of stress presumed to govern failure.

[d] Failure occurred at or near ends or end connections, presumably due to high complex stresses caused by bending induced by end restraint. However, results are significant in that they indicate average stress levels attained before localized conditions caused failure.

[e] Values given are those for mid-section of tube at instant of failure.

[f] Shear fracture 6 in. long, crossing longitudinal weld at 1/8 in. from circumferential end weld. Fracture started inside of tube, in circumferential weld.

[g] Fracture 4 in. long (apparently shear) at root of circumferential weld, starting about 8 in. from nearest longitudinal weld; then cleavage fracture extending completely around specimen at angle of about 70° from axis.

[h] Compression energy in liquid and concrete plugs, and elastic energy in specimen.

[i] Computed on basis of original diameter and original thickness.

[j] Computed from thickness measurements at 1/4 in. intervals over 5-in. length across fracture at point of origin.

[k] Welded with NRC-2A electrodes.

TABLE C

TRANSITION TEMPERATURES OF PROJECT STEELS
AS DETERMINED BY VARIOUS NOTCHED TESTS

Type of Test	Temperature °F For Midpoint of Transition Range										Temperature - °F For Upper Limit of Transition Range									
	Energy Absorption										% Fibrous Fracture									
	C	E	A	Bn	Dn	Dr	Br	Q	H	N	C	E	A	Bn	Dn	Dr	Br	Q	H	N
Charpy Impact Std. V-Notch	100	140	100	30	20	40	0	0	0	-50	—	—	—	—	—	—	—	—	—	—
Tear Test Keyhole Notch	127	130	60	—	55	55	45	—	30	—	127	130	62	—	55	55	45	—	30	—
Prestrained Charpy 10% Tens: Keyhole Notch	95	85	60	30	0	20	20	—	-20	—	—	—	—	—	—	—	—	—	—	—
Notched Tension (5/8" Wide Section)	—	—	—	—	—	—	—	—	—	—	125	100	95	95	40	75	-30	45	75	—
3" Tension Sheared Edge	—	—	—	—	—	—	—	—	—	—	105	55	35	—	—	—	—	—	10	—
Slow-Bend: Schnadt Type .01"R. Milled Notch	110	85	50	25	25	25	-25	-20	-35	-30	120	85	50	25	25	25	-25	-15	-35	-30
Slow-Bend: Schnadt Type .0015"R. Pressed Notch	87	72	55	82	15	42	-15	-17	-20	—	107	87	55	82	15	42	-15	-15	-20	—
72" Wide Tension Internal Notch	90	95	30	33	23	23	30	—	20	-45	90	?	38	30	?	?	50	—	20	-25
12" Wide Tension Internal Notch (Swarthmore Data)	89	81	48	17	15	—	8	—	—	—	102	85	50	17	15	—	13	—	—	—
12" Wide Tension Internal Notch (California and Illinois Data)	90	91	25	15	15	40	5	0	-15	-64	105	101	35	30	15	40	25	? Q.S. 25	30	-45
3" Tension Edge-Notched	—	—	—	—	—	—	—	—	—	—	90	120	45	?	—	32	30	35	35	?
Prestrained Charpy 5% Tens: Keyhole	65	60	45	0	-25	0	10	—	-35	—	—	—	—	—	—	—	—	—	—	—
Prestrained Charpy 2% Tens: Keyhole	55	70	40	0	-55	-30	-5	—	-55	—	—	—	—	—	—	—	—	—	—	—
Charpy Impact Full Thickness Sawcut Notch	50	75	60	35	-30	-20	10	15	0	-100	—	—	—	—	—	—	—	—	—	—
Charpy Impact Std. Keyhole Notch	10	30	0	-20	-60	-60	-30	-55	-50	-220	—	—	—	—	—	—	—	—	—	—

Type of Test	Energy Absorption										% Fibrous Fracture									
	C	E	A	Bn	Dn	Dr	Br	Q	H	N	C	E	A	Bn	Dn	Dr	Br	Q	H	N
Charpy Impact Std. V-Notch	200	200	160	160	80	120	50	70	70	35	—	—	—	—	—	—	—	—	—	—
Tear Test Keyhole Notch	135	140	70	—	70	60	60	—	50	—	135	140	70	—	70	60	60	—	50	—
Prestrained Charpy 10% Tens: Keyhole Notch	140	105	75	55	70	70	35	—	75	—	—	—	—	—	—	—	—	—	—	—
Notched Tension (5/8" Wide Section)	—	—	—	—	—	—	—	—	—	—	130	105	110	105	40	80	-20	80	100	—
3" Tension Sheared Edge	—	—	—	—	—	—	—	—	—	—	122	65	40	—	—	—	—	—	27	—
Slow-Bend: Schnadt Type .01"R. Milled Notch	120	85	60	35	30	50	-10	0	-20	-20	125	85	55	35	30	50	-10	0	-20	-20
Slow-Bend: Schnadt Type .0015"R. Pressed Notch	?	95	65	100	30	60	0	-5	0	—	130	95	65	100	30	60	0	-5	0	—
72" Wide Tension Internal Notch	100	110	45	33	30	?	50	—	25	-32	102	140	45	30	?	?	70	—	25	0
12" Wide Tension Internal Notch (Swarthmore Data)	97	92	58	25	20	—	14	—	—	—	116	106	58	25	20	—	14	—	—	—
12" Wide Tension Internal Notch (California and Illinois Data)	100	100	35	35	30	41	15	15 Q.S. 15	15	-25	120	?	50	50	?	?	50	15 Q.S. 65	65	-25
3" Tension Edge-Notched	—	—	—	—	—	—	—	—	—	—	102	127	62	70	—	35	40	50	40	25
Prestrained Charpy 5% Tens: Keyhole	140	105	75	55	70	70	35	—	10	—	—	—	—	—	—	—	—	—	—	—
Prestrained Charpy 2% Tens: Keyhole	140	105	60	75	70	70	35	—	35	—	—	—	—	—	—	—	—	—	—	—
Charpy Impact Full Thickness Sawcut Notch	145	175	140	110	80	110	85	70	70	35	—	—	—	—	—	—	—	—	—	—
Charpy Impact Std. Keyhole Notch	120	120	70	120	120	120	15	35	35	35	—	—	—	—	—	—	—	—	—	—

Table D - Chemical Analysis in % of Specimens from PIERRE S. DUPONT and PONAGANSET

Plate	C	Mn	Si	P	S	Cu	N	Type steel*
DU	0.26	0.33	0.02	0.011	0.038	..	..	..
PBDP	0.14	0.38	0.00	0.020	0.035	0.16	0.005	Rim
PBDS	0.15	0.40	0.00	0.020	0.030	0.17	0.004	Rim
PAD	0.22	0.47	0.04	0.021	0.035	0.03	0.004	S-K
PCDP	0.14	0.41	0.01	0.027	0.030	0.10	0.004	Rim
PJSS	0.29	0.45	0.10	0.015	0.040	0.03	0.0045	S-K

* Rimmed, semikilled (S-K)

Table E - Mechanical Properties of Steel from PIERRE S. DUPONT and PONAGANSET (1-In. Wide Full-Thickness Specimens)

Specimen	Gage, in.	Tensile strength psi.	Yield point, psi	Elongation in 8 in., %	Bend test
DU	3/4	60,200	34,400	28.2	..
PBDP	13/16	52,300	31,900	32.5	OK
PBDS	13/16	55,600	32,600	31.0	OK
PAD	13/16	59,700	30,500	25.0	OK
PCDP	13/16	54,500	34,500	28.0	OK
PJSS	3/4	65,200	37,100	27.5	OK

Table F - Transition Temperature in °F. of Steels as Determined by Various Tests

Steel	No. Tests	T.T., Energy to rupture	T.T., fracture appearance	1/8 in., hole	Hack Saw	Keyhole Charpy 15 ft.-lb.	V-Notch Charpy 15 ft.-lb.	Navy Tear Test
DU	7	37	37	..	107	..	62	..
PBDP	11	46	46	71	..	9	..	90
PBDS	11	60	60	127	..	18	..	110
PAD	11	104	102	152	..	12	..	150
PCDP	11	54	55	54	..	-3	..	90
PJSS	11	58	60	89	..	-6	..	90

TABLE G

PROPERTIES AND COMPOSITIONS OF HIGH YIELD STRENGTH STRUCTURAL STEELS USED IN THE INVESTIGATION

STEEL NO.	1	2	3	4	B**	C
TYPE HEAT TREATMENT	Alloy Quenched & Drawn*	Alloy Quenched & Drawn	Alloy Quenched & Drawn	Alloy Quenched & Drawn	Mild Semi Killed as-rolled	Mild Semi Killed as-rolled
PHYSICAL PROPERTIES						
Yield Strength Psi. Average	66,000	80,000	80,000	84,000	36,000	39,000
Ultimate Strength Psi. Average	89,000	97,000	100,000	100,000	60,000	67,400
Elongation % in 2" Average	26	22	20	23	26	25.5+
Reduction in Area % Average	64	60	60	68	63	-
APPROXIMATE CHEMICAL COMPOSITION						
Carbon	.19	.14	.16	.16	.15	.24
Manganese	1.08	.75	1.45	.27	.77	.48
Silicon	.24	.77	.21	.17	.05	.05
Molybdenum	.42	.16	.48	.20	-	.005
Chromium	-	.60	-	1.13	-	.03
Zirconium	-	.09	-	-	-	-
Phosphorus	.014	.023	.017	.014	.010	.012
Sulphur	.023	.028	.038	.021	.029	.026
Vanadium	-	-	.08	-	-	-
Nickel	-	-	.53	2.32	-	.02

* Steel 1 was also used in a normalized condition for some of the tests
** Mild Steel Br properties included for comparison
*** + Elongation in 8"

TABLE H

APPROXIMATE TRANSITION TEMPERATURES OF HIGH YIELD STRENGTH STRUCTURAL STEELS DETERMINED BY MEANS OF DIFFERENT SPECIMENS

STEELS	1	2	3	4	B
TYPE OF SPECIMEN	APPROXIMATE TRANSITION TEMPERATURES				
3" Edge Notched	-10°F	+18°F	-102°F	-108°F	+20°F
12" Centrally Notched	+5°F	+20°F	-95°F	-102°F	+18°F
Restrained Welded	+40°F	+75°F	-50°F	-65°F	+58°F

TABLE I

Composition, Tensile and Tear-Test Properties of Ship Plate Steels, Medium, Semikilled, 48-S-5, Normal Manganese (Mn/C<3)

Description				Composition, %					Static tensile properties			Tear-test properties				
Heat code	Plate code	Plate thickness, in.	Condition	C	Mn	Si	Al	N	Yield point, psi.	Tensile strength, psi.	Elongation, %, 8 in.	Maximum load, lb./in.*	Energy to start, ft.-lb./in.*	Energy to prop., ft.-lb./in.*	Transition temp., °F.	Mn/C
5	G2	1/8	R	0.25	0.42	0.08	0.003	0.004	...	...	...	56,000	1140	750	50	1.7
5	G3	3/4	R	0.25	0.42	0.08	0.003	0.004	...	...	...	52,600	1060	860	100	1.7
5	G4	1	R	0.24	0.42	0.08	0.003	0.004	...	...	...	50,900	1320	980	120	1.7
6	"A"	1/4	R	0.25	0.49	0.04	0.004	0.004	34,090	58,640	33.4	48,300	930	640	70	2.0
7	"C"	1/4	R	0.25	0.51	0.05	0.015	0.009	35,500	65,240	30.4	51,800	880	610	135	2.0
8	S7	1/4	R	0.21	0.49	0.08	0.002	0.005	35,800	63,200	35.5	48,000	800	730	120	2.3
9	S6	1/4	R	0.20	0.55	0.10	−0.002	0.005	34,900	66,000	30.0	53,800	1060	880	100	2.8
10	S9	1/4	R	0.18	0.50	0.07	−0.002	0.004	32,600	57,900	34.5	53,000	1550	1000	80	2.8
11	S10	1/4	R	0.19	0.54	0.12	−0.006	0.004	33,300	61,400	31.0	56,000	1190	960	90	2.8
12	S11	1/4	R	0.20	0.55	0.06	−0.006	0.004	31,300	59,400	31.0	49,200	910	760	90	2.8
13	S8	1/4	R	0.14	0.46	0.07	−0.002	0.005	32,300	57,400	32.0	46,400	950	780	90	2.9

* Average of all tests conducted above transition temperature.

Composition, Tensile and Tear-Test Properties of Ship Plate Steels, Medium, Semikilled, ABS-B, Manganese 0.60/0.90 (Mn/C>3)

Description				Composition, %					Static tensile properties			Tear-test Properties				
Heat code	Plate code	Plate thick., in.	Condition	C	Mn	Si	Al	N	Y. P. (P.S.I.)	T. S. (P.S.I.)	Elong. %, 8"	Max. load,* lbs./in.	Energy to start,* ft. lbs./in.	Energy to prop.,* ft. lbs./in.	Transition temp., °F.	Mn/C
14	M29B	5/8	R	0.22	0.90	0.03	0.004	0.006	40,180	68,030	27.5	55,700	1110	870	90	4.1
14	M29B	5/8	N	0.22	0.90	0.03	0.004	0.006	...	...	...	56,900	1210	780	60	4.1
14	M29A	1	R	0.22	0.90	0.03	0.008	0.004	38,830	63,820	31.7	57,100	1530	1100	120	4.1
14	M29A	1	N	0.22	0.90	0.03	0.008	0.004	...	...	...	...	...	...	>70	4.1
15	G5	1/2	R	0.18	0.96	0.05	0.006	0.004	...	...	...	57,100	1450	940	30	5.3
15	G6	3/4	R	0.18	0.96	0.05	0.005	0.003	...	...	...	56,900	1690	1040	50	5.3
15	G7	1	R	0.18	0.96	0.04	0.006	0.003	...	...	...	57,000	1970	1150	80	5.3
15	G8	1 1/2	R	0.18	0.96	0.04	0.007	0.003	...	...	...	59,100	2410	1150	130	5.3
16	M37	5/8	R	0.20	0.74	0.07	0.008	0.004	...	...	...	53,800	1290	740	50	3.7
16	M37	5/8	N	0.20	0.74	0.07	0.008	0.004	...	...	...	53,100	1290	900	<70	3.7
17-1	M38A	5/8	R	0.19	0.72	0.08	0.005	0.005	...	...	...	53,100	1310	880	60	3.8
17-1	M38A	5/8	N	0.19	0.72	0.08	0.005	0.005	...	...	...	53,600	1320	890	60	3.8
17-2	M38B	5/8	R	0.19	0.72	0.08	0.005	0.005	...	...	...	52,900	1260	770	60	3.8
17-2	M38B	5/8	N	0.19	0.72	0.08	0.005	0.005	...	...	...	54,000	1460	880	<60	3.8
18	M39	5/8	R	0.21	0.82	0.05	0.005	0.004	35,540	63,400	31.7	54,600	1320	950	40	3.9
18	M39	5/8	N	0.21	0.82	0.05	0.005	0.004	...	...	...	55,100	1420	980	<40	3.9
19-1	M34A	5/8	R	0.22	0.89	0.07	0.009	0.005	40,100	65,560	30.2	53,500	1090	770	60	4.0
19-1	M34A	5/8	N	0.22	0.89	0.07	0.009	0.005	...	...	...	54,800	1130	850	70	4.0
19-2	M34B	5/8	R	0.22	0.89	0.07	0.006	0.004	...	...	...	54,100	1140	800	70	4.0
19-2	M34B	5/8	N	0.22	0.89	0.07	0.006	0.004	...	...	...	52,400	1180	830	<70	4.0
20	M30	5/8	R	0.22	0.90	0.03	0.006	0.006	39,900	70,470	28.0	57,000	1140	780	80	4.1
20	M30	5/8	N	0.22	0.90	0.03	0.006	0.006	...	...	...	57,500	1190	830	80	4.1
21	S2	3/4	R	0.17	0.60	0.07	−0.003	0.005	31,370	57,970	32.8	52,900	1400	1050	110	3.5
21	S3**	3/4	R	0.17	0.60	0.07	0.028	0.005	31,600	58,000	31.8	53,000	1350	1010	80	3.5
22	S21	3/4	R	0.22	0.81	0.08	−0.006	0.004	37,900	68,300	26.0	56,200	1190	960	70	3.7
22	S14**	3/4	R	0.22	0.81	0.07	0.04	0.004	36,700	66,400	31.0	56,900	1140	950	60	3.7
23	S23	3/4	R	0.20	0.75	0.05	−0.006	0.005	34,200	66,200	30.0	53,000	1030	920	100	3.8
23	S15**	3/4	R	0.20	0.75	0.06	0.05	0.004	34,000	62,600	31.0	53,400	1050	810	30	3.8
24	S1	3/4	R	0.17	0.66	0.08	−0.003	0.005	31,780	58,720	32.4	51,500	1170	1000	100	3.9
25	S13	3/4	R	0.17	0.68	0.07	−0.006	0.004	34,200	60,200	33.5	53,500	1360	1050	90	4.0
25	S17**	3/4	R	0.17	0.68	0.07	0.04	0.004	34,100	60,600	33.0	51,500	1260	940	40	4.0
26	S22	3/4	R	0.19	0.77	0.09	−0.006	0.004	35,000	63,800	32.0	59,900	1420	1010	100	4.1
26	S12**	3/4	R	0.19	0.77	0.07	0.04	0.004	34,700	64,100	28.0	57,200	1230	880	40	4.1
27	S20	3/4	R	0.18	0.73	0.07	−0.006	0.004	34,500	62,100	33.0	53,900	1220	990	80	4.1
27	S16**	3/4	R	0.18	0.73	0.08	0.03	0.004	36,600	62,000	33.5	53,600	1210	920	50	4.1
28	S19	3/4	R	0.19	0.78	0.09	−0.006	0.005	35,300	64,900	32.0	55,100	1190	1020	80	4.1
29	S18	3/4	R	0.17	0.73	0.05	−0.006	0.005	33,500	62,100	32.0	52,100	1220	970	100	4.3
30	"B"	3/4	R	0.16	0.76	0.05	0.001	0.005	32,750	56,700	33.5	52,700	1430	840	60	4.7
31	S5	3/4	R	0.17	0.90	0.09	−0.005	0.005	36,600	56,000	29.5	54,300	1090	1030	70	5.3
31	S4**	3/4	R	0.17	0.90	0.10	0.04	0.004	36,250	65,100	30.8	56,600	1080	770	−20	5.3
32-1	M23A	1	R	0.33	0.76	0.08	0.005	0.006	37,150	67,120	29.7	55,300	1280	840	120	3.3
32-1	M23A	1	N	0.33	0.76	0.08	0.005	0.006	38,700	65,200	49.0(2")	55,200	1370	870	110	3.3
32-2	M23B	1	R	0.33	0.76	0.08	0.006	0.005	38,410	66,800	30.2	52,600	1220	920	130	3.3
32-2	M23B	1	N	0.33	0.76	0.08	0.006	0.005	...	...	...	53,500	1380	960	70	3.3
33-1	M22A	1	R	0.22	0.70	0.06	0.007	0.005	...	...	...	54,300	1390	890	120	3.4
33-1	M22A	1	N	0.22	0.76	0.06	0.007	0.005	...	...	...	53,800	1460	1040	90	3.4
33-2	M22B	1	R	0.22	0.76	0.06	0.014	0.004	...	...	...	53,200	1490	1060	130	3.4
33-2	M22B	1	N	0.22	0.76	0.06	0.014	0.004	...	...	...	54,600	1700	1070	80	3.4
34	M28	1	R	0.22	0.74	0.19	0.025	0.005	39,410	67,620	31.5	55,200	1350	830	70	3.4
34	M28	1	N	0.22	0.74	0.19	0.025	0.005	...	...	...	55,700	1550	900	<50	3.4
35-1	M18A	1	R	0.19	0.69	0.06	0.009	0.004	...	...	...	52,600	1240	930	120	3.5
35-1	M18A	1	N	0.19	0.69	0.06	0.009	0.004	...	...	...	51,700	1290	900	<70	3.5
35-2	M18B	1	R	0.19	0.69	0.06	0.014	0.003	38,560	64,020	27.5	50,900	1490	910	100	3.5
35-2	M18B	1	N	0.19	0.69	0.06	0.014	0.003	...	...	...	50,200	1410	910	70	3.5
36-1	M21A	1	R	0.24	0.76	0.07	0.007	0.004	36,580	66,780	30.5	54,300	1260	720	110	3.5
36-1	M21A	1	N	0.24	0.76	0.07	0.007	0.004	...	...	...	54,700	1470	880	70	3.5
36-2	M21B	1	R	0.24	0.76	0.07	0.012	0.004	...	...	...	54,700	1450	950	120	3.5
36-2	M21B	1	N	0.24	0.76	0.07	0.012	0.004	...	...	...	54,400	1420	900	60	3.5
37	M32	1	R	0.21	0.76	0.03	0.009	0.004	38,110	64,420	30.2	53,700	1400	960	110	3.6
37	M32	1	N	0.21	0.76	0.03	0.009	0.004	...	...	...	51,500	1400	940	70	3.6
38-1	M19A	1	R	0.24	0.87	0.07	0.006	0.004	...	...	...	55,300	1360	890	120	3.7
38-1	M19A	1	N	0.24	0.87	0.07	0.006	0.004	...	...	...	...	...	...	>100	3.7
38-2	M19B	1	R	0.24	0.87	0.07	0.007	0.004	...	...	...	52,900	1270	990	110	3.7
38-2	M19B	1	N	0.24	0.87	0.07	0.007	0.004	...	...	...	51,900	1330	940	60	3.7
39	M36	1	R	0.19	0.70	0.04	0.017	0.006	40,140	65,800	30.0	53,700	1590	980	110	3.7
39	M36	1	N	0.19	0.70	0.04	0.017	0.006	...	...	...	52,900	1570	1010	60	3.7
40-1	M24A	1	R	0.20	0.75	0.09	0.006	0.004	...	...	...	50,000	1060	770	50	3.8
40-1	M24A	1	N	0.20	0.75	0.09	0.006	0.004	...	...	...	50,900	1240	820	40	3.8
40-2	M24B	1	R	0.20	0.75	0.09	0.012	0.008	...	...	...	54,100	1130	900	140	3.8
40-2	M24B	1	N	0.20	0.75	0.09	0.012	0.008	...	...	...	54,300	1400	920	90	3.8
41	M26	1	R	0.19	0.72	0.09	0.016	0.005	...	...	...	54,200	1510	920	100	3.8
41	M26	1	N	0.19	0.72	0.09	0.016	0.005	...	...	...	53,800	1550	1020	<70	3.8
42-1	M25A	1	R	0.19	0.75	0.08	0.012	0.005	...	...	...	49,800	1400	730	100	3.9
42-1	M25A	1	N	0.19	0.75	0.08	0.012	0.005	...	...	...	51,200	1440	940	60	3.9
42-2	M25B	1	R	0.19	0.75	0.08	0.009	0.005	...	...	...	53,100	1340	860	100	3.9
42-2	M25B	1	N	0.19	0.75	0.08	0.009	0.005	...	...	...	...	...	...	>80	3.9
43	M27	1	R	0.21	0.81	0.07	0.021	0.006	38,650	63,820	33.5	52,600	1420	1010	100	3.9
43	M27	1	N	0.21	0.81	0.07	0.021	0.006	...	...	...	51,300	1340	980	70	3.9
44	M35	1	R	0.18	0.71	0.02	0.004	0.005	33,380	62,120	32.7	54,000	1530	970	140	3.9
44	M35	1	N	0.18	0.71	0.02	0.004	0.005	...	...	...	52,900	1670	1010	100	3.9
45	M31	1	R	0.21	0.86	0.08	0.007	0.005	38,390	67,520	30.5	57,000	1570	1090	120	4.1
45	M31	1	N	0.21	0.86	0.08	0.007	0.005	...	...	...	54,300	1560	1000	70	4.1
46-1	M20A	1	R	0.21	0.79	0.06	0.007	0.005	38,260	65,710	28.0	54,600	1420	930	100	4.2
46-1	M20A	1	N	0.21	0.79	0.06	0.007	0.005	...	...	...	53,400	1420	1020	80	4.2
46-2	M20B	1	R	0.21	0.79	0.06	0.007	0.007	37,160	66,130	31.0	55,600	1470	730	90	4.2
46-2	M20B	1	N	0.21	0.79	0.06	0.007	0.007	...	...	...	55,400	1490	1040	80	4.2
47	M33	1	R	0.21	0.90	0.08	0.006	0.005	...	...	...	55,300	1610	960	100	4.3
47	M33	1	N	0.21	0.90	0.08	0.006	0.005	...	...	...	55,200	1640	940	60	4.3

TABLE J

Composition, Tensile and Tear-Test Properties of Ship Plate Steels, Medium, Rimmed

Description				Composition, %					Static tensile properties			Tear test properties				
Heat code	Plate code	Plate thickness, in.	Condition	C	Mn	Si	Al	N	Yield point, psi.	Tensile strength, psi.	Elongation, %, 8 in.	Maximum load, lb./in.*	Energy to start, ft.-lb./in.*	Energy to prop., ft.-lb./in.*	Transition Temp., ° F.	Mn/C
												49,000	1010	810	0	1.8
1	"E"	1/2	R	0.19	0.35	0.01	0.003	0.003	...	...	...	45,400	870	680	140	1.8
1	"E"	3/4	R	0.23	0.37	0.004	−0.002	0.004	30,950	58,430	30.6	47,900	890	660	100	1.9
2	Cy	3/4	R	0.18	0.34	0.01	...	0.004	37,340	61,440	26.0	48,200	1100	880	100	2.5
3	Cz	3/4	R	0.16	0.40	0.01	...	0.004	35,550	57,310	30.0	48,900	1210	850	80	3.4
4	Cx	3/4	R	0.14	0.47	0.01	...	0.004	36,830	57,320	33.0					

Composition, Tensile and Tear-Test Properties of Ship Plate Steels, Medium, Fully Killed (Si or Al)

Description				Composition, %					Static tensile properties			Tear-test properties				
Heat code	Plate code	Plate thickness, in.	Condition	C	Mn	Si	Al	N	Yield point, psi.	Tensile strength, psi.	Elongation, %, 8 in.	Maximum load, lb./in.*	Energy to start, ft.-lb./in.*	Energy to prop., ft.-lb./in.*	Transition temp., ° F.	Mn/C
48	"Dn"	1/2	N	0.20	0.55	0.23	0.022	0.003	...	...	...	52,700	1230	930	30	3.0
48	"Dr"	3/4	R	0.19	0.55	0.25	0.015	0.005	37,600	65,050	30.3	55,800	1170	750	60	3.0
48	"Dn"	3/4	N	0.20	0.55	0.23	0.02	0.005	34,700	59,550	31.9	54,700	1270	840	70	3.0
49	M2	5/8	R	0.26	0.38	0.23	−0.006	0.004	...	...	...	53,800	935	455	70	1.4
50	M1	5/8	R	0.22	0.38	0.26	−0.006	0.004	...	...	...	52,300	1000	675	40	1.7
51-1	M4A	5/8	R	0.23	0.40	0.19	...	0.004	...	...	...	54,600	1170	710	80	1.7
51-1	M4A	5/8	N	0.23	0.40	0.19	...	0.004	...	...	...	56,600	1240	790	<70	1.7
51-2	M4B	5/8	R	0.23	0.40	0.19	...	0.004	...	...	...	54,000	1070	780	90	1.7
51-2	M4B	5/8	N	0.23	0.40	0.19	...	0.004	...	...	...	58,300	1420	820	<70	1.7
52	M3	5/8	R	0.24	0.44	0.19	−0.006	0.006	...	...	...	52,100	835	655	80	1.9
53-1	M6A	5/8	R	0.23	0.43	0.19	...	0.003	...	...	...	53,700	975	735	70	1.9
53-1	M6A	5/8	N	0.23	0.43	0.19	...	0.003	...	...	...	56,500	1280	720	<70	1.9
53-2	M6B	5/8	R	0.23	0.43	0.19	...	0.003	...	...	...	54,100	1030	735	60	1.9
53-2	M6B	5/8	N	0.23	0.43	0.19	...	0.003	...	...	...	53,700	1140	740	<60	1.9
54-1	M12A	5/8	R	0.26	0.46	0.21	...	0.005	...	...	...	53,800	1090	740	60	1.9
54-2	M12B	5/8	R	0.26	0.46	0.21	...	0.005	...	...	...	51,800	885	670	<40	1.9
55-1	M17A	5/8	R	0.25	0.47	0.21	0.004	0.004	...	...	...	55,700	1000	740	70	1.9
55-1	M17A	5/8	N	0.25	0.47	0.21	0.004	0.004	...	...	...	55,700	1140	830	<70	1.9
55-2	M17B	5/8	R	0.25	0.47	0.22	...	0.005	...	...	...	55,000	1040	750	70	1.9
55-2	M17B	5/8	N	0.25	0.47	0.22	...	0.005	...	...	...	57,000	1190	800	<70	1.9
56-1	M5A	5/8	R	0.24	0.47	0.20	...	0.005	...	...	...	56,200	1025	745	70	2.0
56-1	M5A	5/8	N	0.24	0.47	0.20	...	0.005	...	...	...	59,500	1310	700	<70	2.0
56-2	M5B	5/8	R	0.24	0.47	0.20	...	0.005	...	...	...	55,000	985	720	70	2.0
56-2	M5B	5/8	N	0.24	0.47	0.20	...	0.005	...	...	...	56,700	1200	770	<70	2.0
57	M13	5/8	R	0.22	0.47	0.24	...	0.004	...	...	...	56,000	1200	760	<70	2.1
58	M16	5/8	R	0.24	0.52	0.22	...	0.005	...	...	...	54,200	1170	790	<70	2.2
59-1	M11A	5/8	R	0.21	0.49	0.22	...	0.005	...	...	...	53,400	1065	740	<70	2.3
59-2	M11B	5/8	R	0.21	0.49	0.22	...	0.005	...	...	...	54,500	1110	740	60	2.3
60	M14	5/8	R	0.19	0.44	0.20	...	0.005	...	...	...	52,500	1100	750	<70	2.3
61	M15	5/8	R	0.20	0.47	0.22	...	0.005	...	...	...	53,100	1240	860	<40	2.3
62-1	M10A	5/8	R	0.19	0.48	0.23	...	0.005	...	...	...	53,300	1030	720	30	2.5
62-2	M10B	5/8	R	0.19	0.48	0.23	...	0.005	...	...	...	53,400	1065	740	30	2.5
63-1	M7A	5/8	R	0.17	0.48	0.21	...	0.004	...	...	...	53,000	1230	840	50	2.8
63-2	M7B	5/8	R	0.17	0.48	0.21	...	0.004	...	...	...	52,400	1220	870	50	2.8
64-1	M9A	5/8	R	0.19	0.63	0.23	...	0.005	...	...	...	55,200	1170	795	30	3.3
64-2	M9B	5/8	R	0.19	0.63	0.23	...	0.005	...	...	...	54,600	1175	810	30	3.3
65-1	M8A	5/8	R	0.19	0.51	0.24	...	0.005	...	...	...	53,600	1040	700	30	3.7
65-2	M8B	5/8	R	0.19	0.51	0.24	...	0.005	...	...	...	53,500	1110	755	50	3.7
66	W	3/4	R	0.21	0.52	0.23	0.006	0.005	37,230	62,540	30.3	55,400	1320	870	60	2.6
67	"H"	3/4	R	0.17	0.78	0.16	0.037	0.005	35,000	62,550	29.8	55,000	1330	810	50	4.5

Composition, Tensile and Tear-Test Properties of Ship Plate Steels, High-Tensile, Vanity-Type, 48-S-5

Description				Composition, %					Static tensile properties			Tear-test properties				
Heat code	Plate code	Plate thickness, in.	Condition	C	Mn	Si	V	Ti	Yield point, psi.	Tensile strength, psi.	Elongation, %	Maximum load, lb./in.*	Energy to start, ft.-lb./in.*	Energy to prop., ft.-lb./in.*	Transition temp., ° F.	Mn/C
68	1X4	7/8	R	0.18	1.23	0.30	0.05	0.010	60,100	85,300	20.0	67,200	975	610	50	6.8
68	2X5	1	R	0.18	1.23	0.31	0.05	0.009	55,300	81,200	22.0	63,000	965	500	40	6.8
68-1	3X7	1 1/4	R	0.18	1.23	0.35	0.05	0.011	51,400	79,100	24.3	62,200	875	385	70	6.8
68-1	3X7	1 1/4	SR	0.18	1.23	0.35	0.05	0.011	...	...	...	60,700	790	350	80	6.8
68-2	4X7	1 1/4	R	0.18	1.23	0.31	0.05	0.012	50,200	79,000	24.3	61,300	860	390	60	6.8
68-2	4X7	1 1/4	N	0.18	1.23	0.31	0.05	0.012	55,000	77,400	29.0	59,500	940	460	−70	6.8
69	2Z1	1/2	R	0.15	1.15	0.25	0.05	0.034	56,000	79,740	24.7	69,100	1180	850	30	7.7
69	2Z1	1/2	N	0.15	1.15	0.25	0.05	0.034	...	...	...	65,400	1630	1000	0	7.7
69	1Z2	5/8	R	0.15	1.15	0.25	0.05	0.034	55,050	79,360	26.0	68,600	1190	950	60	7.7
69	1Z2	5/8	N	0.15	1.15	0.25	0.05	0.034	...	...	...	64,500	1590	1300	−30	7.7
70	21X4	7/8	R	0.15	1.25	0.25	0.04	0.007	57,200	78,500	26.0	62,500	880	725	40	8.3
70-1	19X7	1 1/4	R	0.15	1.25	0.24	0.04	0.007	55,000	78,900	25.3	61,200	905	500	100	8.3
70-1	19X7	1 1/4	SR	0.15	1.25	0.24	0.04	0.007	...	...	...	...	...	...	>80	8.3
70-2	18X7	1 1/4	R	0.15	1.25	0.23	0.04	0.007	53,200	73,800	26.8	59,600	905	500	20	8.3
70-2	18X7	1 1/4	SR	0.15	1.25	0.23	0.04	0.007	...	...	...	58,300	830	420	20	8.3
71	3Z1	1/2	R	0.16	0.98	0.18	0.04	0.025	49,750	70,430	27.0	60,300	1220	950	−30	6.1
71	3Z1	1/2	N	0.16	0.98	0.18	0.04	0.025	...	...	...	57,200	1190	930	−40	6.1
72	4Y2	5/8	R	...	...	...	...	...	55,000	78,000	23.0	71,600	1330	970	130	...
72	4Y2	5/8	N	...	...	...	...	...	53,700	71,600	27.0	69,700	1870	1050	−20	...
73	5Y2	5/8	R	0.15	1.19	0.33	0.04	0.009	56,800	79,200	24.0	68,400	1180	980	110	8.5
74	1Y2	5/8	R	0.15	1.15	0.30	0.04	0.006	50,800	72,700	44.0†	64,500	1060	960	70	7.7
74	1Y2	5/8	N	0.15	1.15	0.30	0.04	0.006	51,000	73,000	49.5†	64,000	1440	820	−20	7.7
75-1	25X2	5/8	SR	0.16	1.22	0.25	0.078	0.007	59,600	77,200	43.0†	65,300	1000	940	70	7.6
75-2	26X2	5/8	SR	0.16	1.22	0.25	0.078	0.007	58,600	78,000	42.0†	66,100	950	870	50	7.6
76-1	6Y2A	5/8	R	0.14	1.00	0.24	0.04	0.024	48,800	70,000	47.5†	66,100	1550	940	60	7.2
76-2	6Y2B	5/8	R	0.14	1.00	0.26	0.04	0.011	49,100	70,900	46.5†	66,800	1420	820	60	7.2
77-1	23X2	5/8	SR	0.16	1.30	0.26	0.072	0.007	53,400	74,800	48.0†	66,900	1050	890	60	8.1
77-2	27X2	5/8	SR	0.16	1.30	0.26	0.072	0.007	56,700	76,600	45.0†	66,000	1060	900	40	8.1
78	24X2	5/8	SR	0.15	1.25	0.25	0.064	0.008	59,200	77,700	42.0†	67,800	1110	770	30	8.3
79	29X2	5/8	R	0.13	1.16	0.24	0.062	0.007	57,500	82,300	18.3	63,900	600	370	<0	8.9
80	30X2	5/8	R	0.14	1.20	0.25	0.07	0.006	59,600	83,400	18.5	62,000	670	290	−20	8.6
81	31X2	5/8	R	0.14	1.21	0.26	0.07	0.007	58,800	83,200	22.5	63,600	600	340	−20	8.6
82	28X2	5/8	R	0.16	1.02	0.27	0.064	0.008	54,200	77,000	25.0	62,700	770	580	−50	6.4
83	2Y5	1	R	0.20	1.07	0.27	0.04	0.006	50,000	76,200	23.0	62,300	1170	740	70	5.4
83	2Y5	1	N	0.20	1.07	0.27	0.04	0.006	53,700	75,600	28.0	58,100	1060	780	−40	5.4
84	3Y5	1	R	0.19	1.18	0.33	0.05	0.005	52,200	77,800	24.0	70,900	1360	720	60	6.2
84	3Y5	1	N	0.19	1.18	0.33	0.05	0.005	...	...	...	67,800	1340	1020	0	6.2
85	16X7	1 1/4	R	0.19	1.27	0.23	0.04	0.007	52,000	85,900	21.5	59,900	725	355	120	6.7
85	16X7	1 1/4	N	0.19	1.27	0.23	0.04	0.007	57,000	81,300	27.0	57,300	700	360	−50	6.7
86-1	12X7	1 1/4	R	0.16	1.23	0.34	0.06	0.010	52,900	77,100	25.5	58,000	835	455	80	7.7
86-2	13X7	1 1/4	R	0.16	1.23	0.33	0.07	0.010	53,200	76,900	25.0	61,500	965	495	90	7.7
86-2	13X7	1 1/4	N	0.16	1.23	0.33	0.07	0.010	52,800	73,200	29.5	58,500	1090	540	−60	7.7
87-1	11X7	1 1/4	R	0.17	1.20	0.24	0.05	0.008	54,900	79,500	24.5	62,800	1060	525	80	7.1
87-2	15X7	1 1/4	R	0.17	1.20	0.23	0.05	0.008	58,800	75,800	24.0	60,000	900	410	50	7.1
88	14X7	1 1/4	R	0.15	1.30	0.25	0.04	0.006	53,100	78,400	24.8	62,600	1110	570	70	8.7
89-1	10X7	1 1/4	R	0.20	1.19	0.28	0.05	0.010	52,500	81,800	25.0	58,600	765	345	60	6.0
89-2	9X7	1 1/4	R	0.19	1.18	0.30	0.05	0.011	55,500	77,300	25.0	57,000	785	370	15	6.0
90	20X7	1 1/4	R	0.13	1.01	0.25	0.04	0.007	47,400	66,900	28.0	56,200	1235	690	50	7.8
91	17X7	1 1/4	R	0.14	1.05	0.24	0.04	0.007	48,300	70,700	28.5	65,500	1700	710	45	7.5
92	5X7	1 1/4	R	0.19	1.29	0.27	0.05	0.010	56,900	81,600	38.0†	56,700	675	295	40	6.8
93-1	8X7	1 1/4	R	0.17	1.26	0.34	0.05	0.010	53,600	77,900	26.0	62,500	1150	500	10	7.4
93-2	7X7	1 1/4	R	0.17	1.26	0.24	0.05	0.009	56,700	77,100	24.0	60,600	1005	515	10	7.4
93-2	7X7	1 1/4	N	0.17	1.26	0.24	0.05	0.009	49,900	71,500	29.0	65,500	810	440	−40	7.4
94	6X7	1 1/4	R	0.19	1.27	0.28	0.05	0.010	61,200	81,800	47.0†	65,800	1135	565	−80	6.7

* Average of all tests conducted above transition temperature.
† Values marked with dagger represent % Elongation in 2 in.; all others in 8 in.

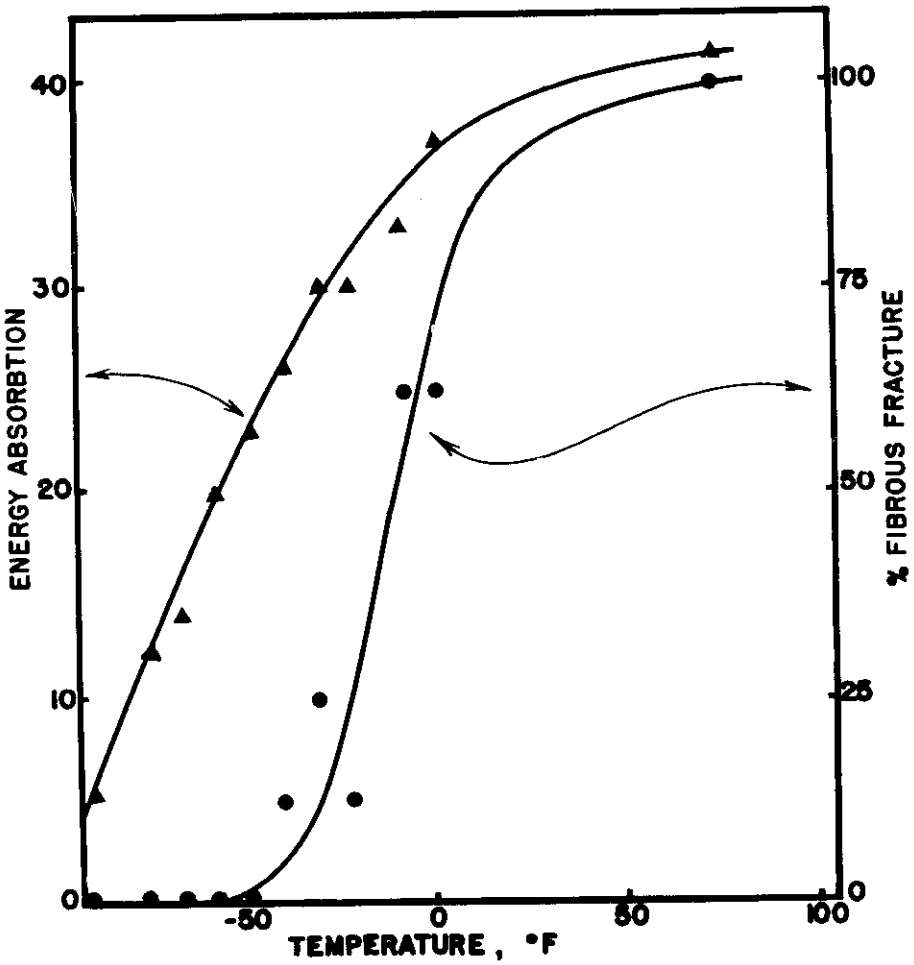

FIG. 1. The transitions in energy absorption and fracture appearance in the Charpy keyhole impact specimen. Steel D_r

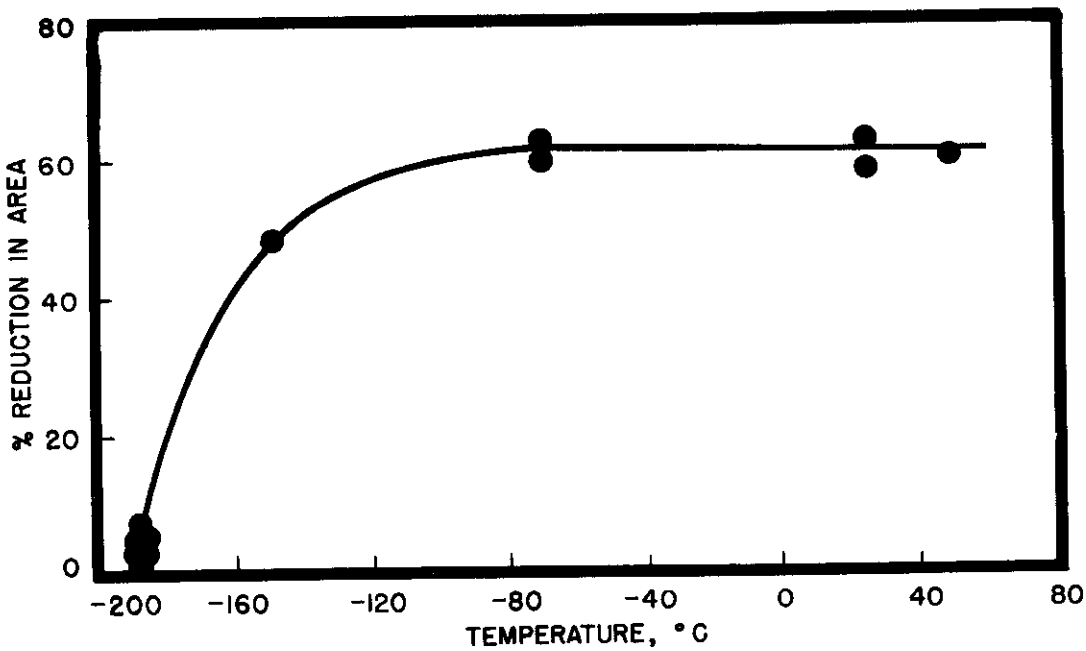

FIG. 2. The per cent reduction in area versus temperature of testing. Steel E.

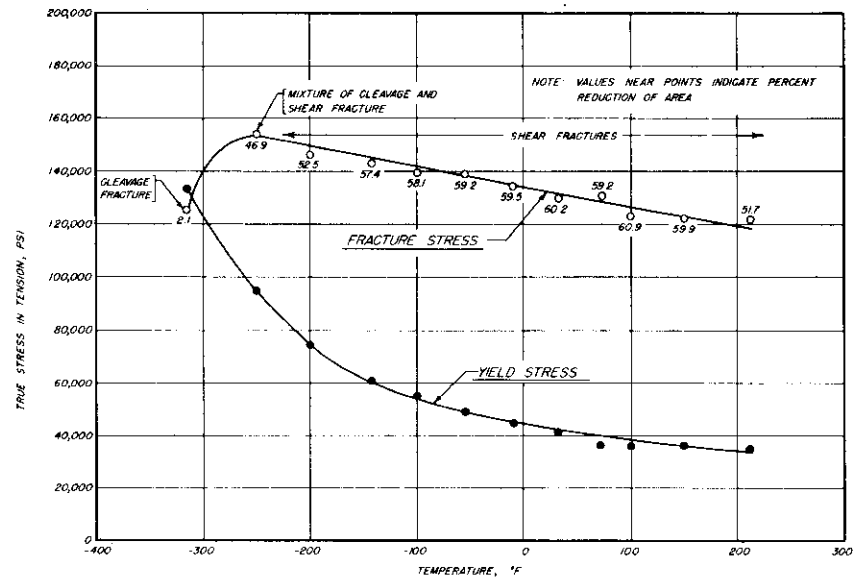

FIG. 3. EFFECT OF TEMPERATURE ON TENSILE PROPERTIES OF STEEL "C" IN THE "AS ROLLED" CONDITION.

C = 0.25 % Mn = 0.49 %

3/8-INCH DIAMETER TENSILE BARS

DWG. 44E278

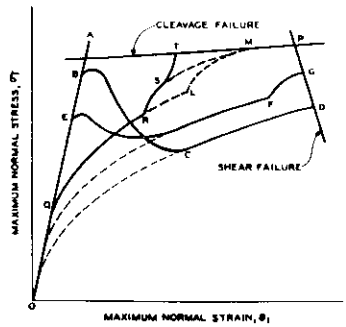

FIG. 4. *Hypothetical flow and fracture curves depicting conditions leading to ductility and fracture transitions*

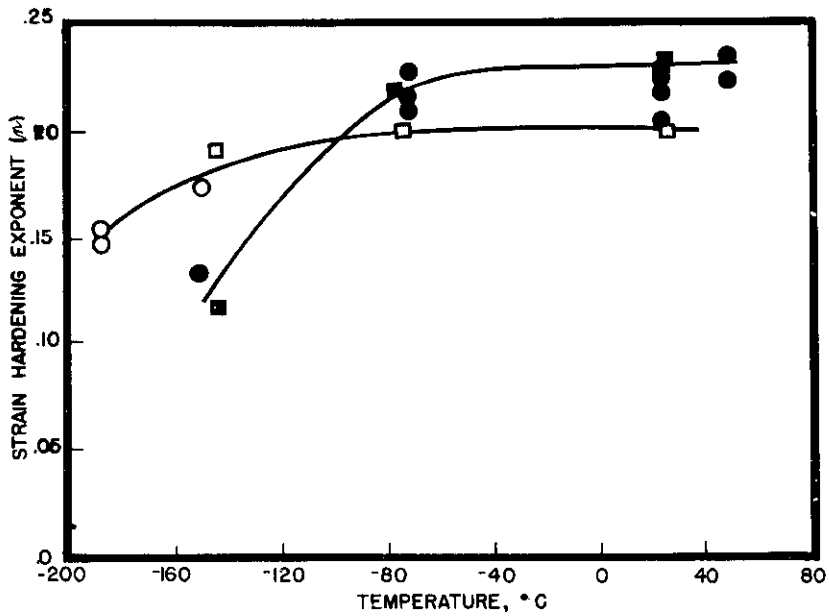

FIG. 5. The strain hardening exponent (n) versus temperature for Steel F (filled figures) and Steel H. Circles are longitudinal specimens and squares transverse specimens.

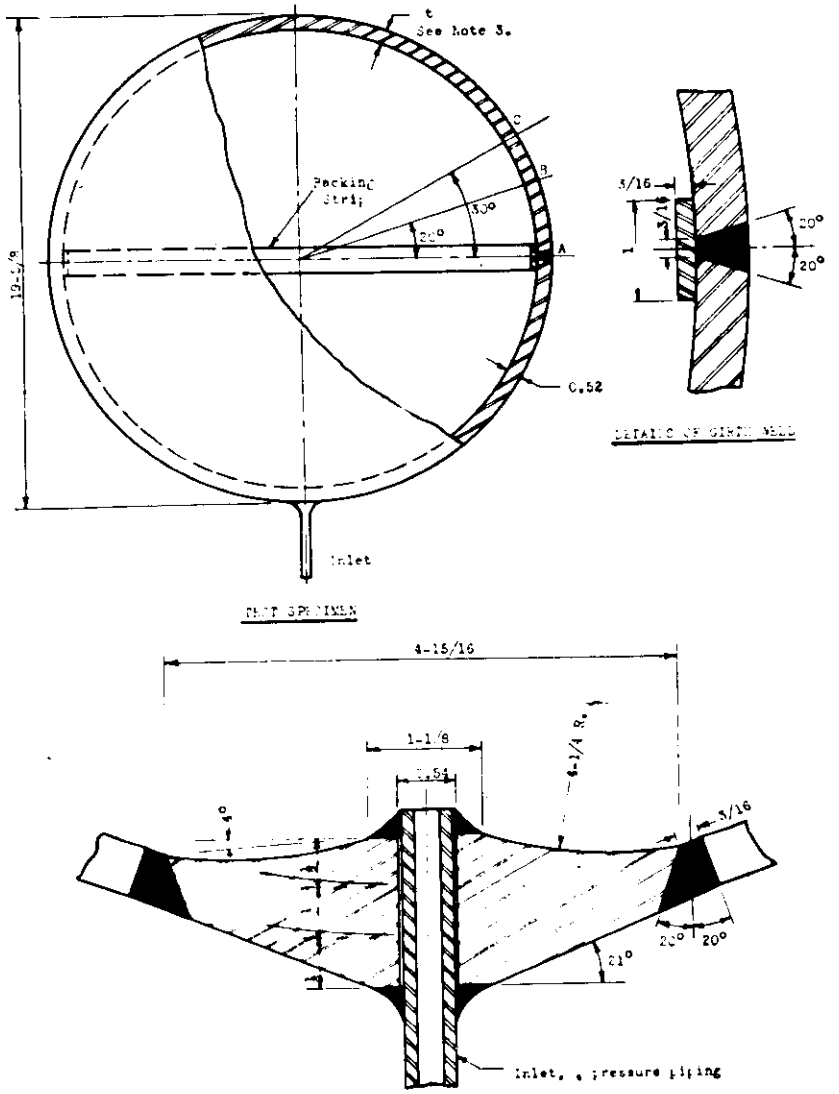

FIG. 6. *Spherical test specimen*

Notes: (1) Wall thickness varied from 0.52-in. ± 0.002 at *A* to 0.50-in. ± 0.002 at *B* for specimens 1, 2 and 3. (2) Wall thickness varied from 0.52-in. ± 0.002 at *A* to 0.40-in. ± 0.002 at *C* for specimens 4, 5 and 6. (3) Specimens 1, 2 and 3: *t* = 0.50-in. ± 0.002; specimens 4, 5 and 6: *t* = 0.40-in. ± 0.002

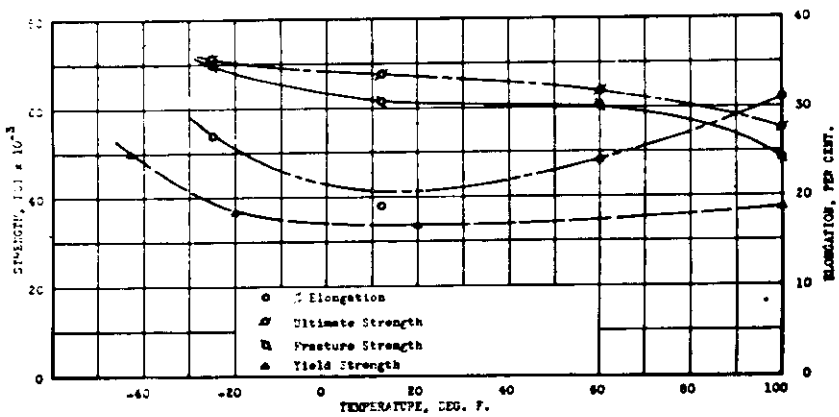

FIG. 7. *Variation of nominal biaxial properties with temperature*

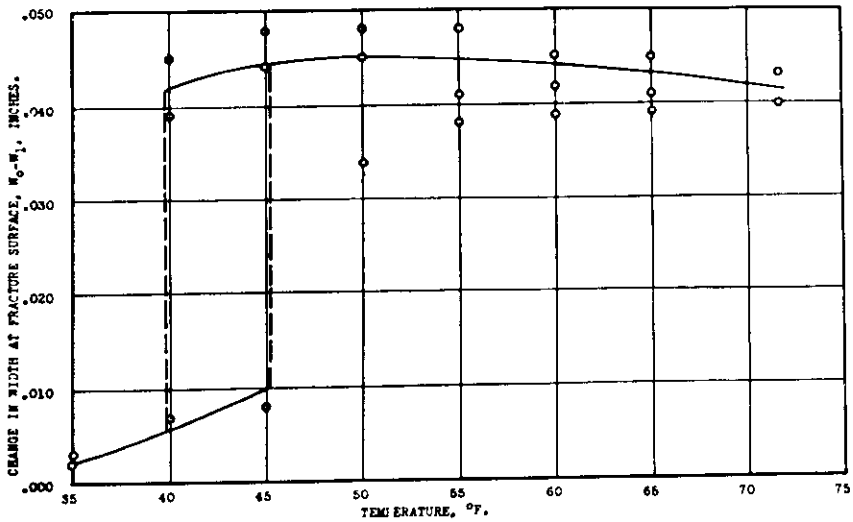

Slow bend test results. $W_0 - W_1$ vs. temperature

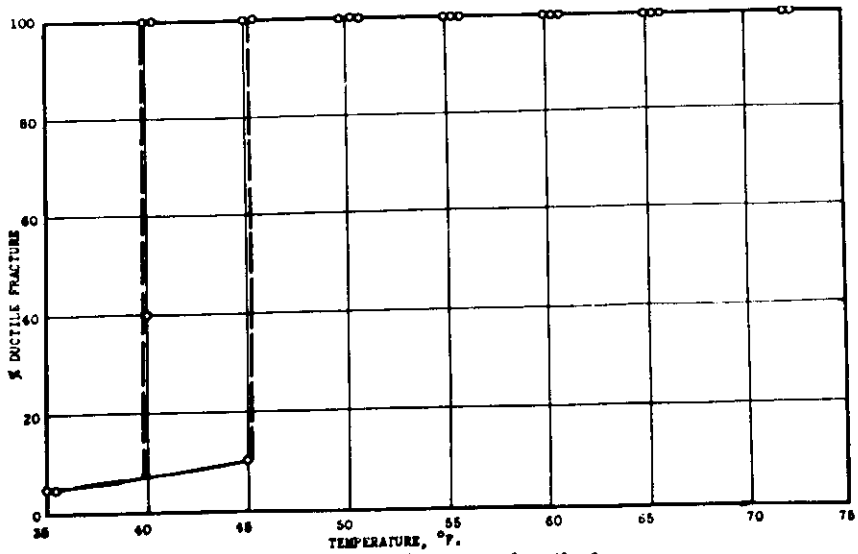

Slow bend test results. Per cent ductile fracture vs. temperature

FIG. 8. Slow bend test results.

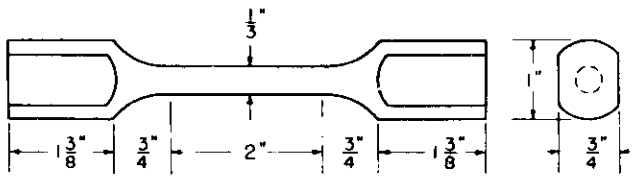

FIG. 9. Torsion Specimen

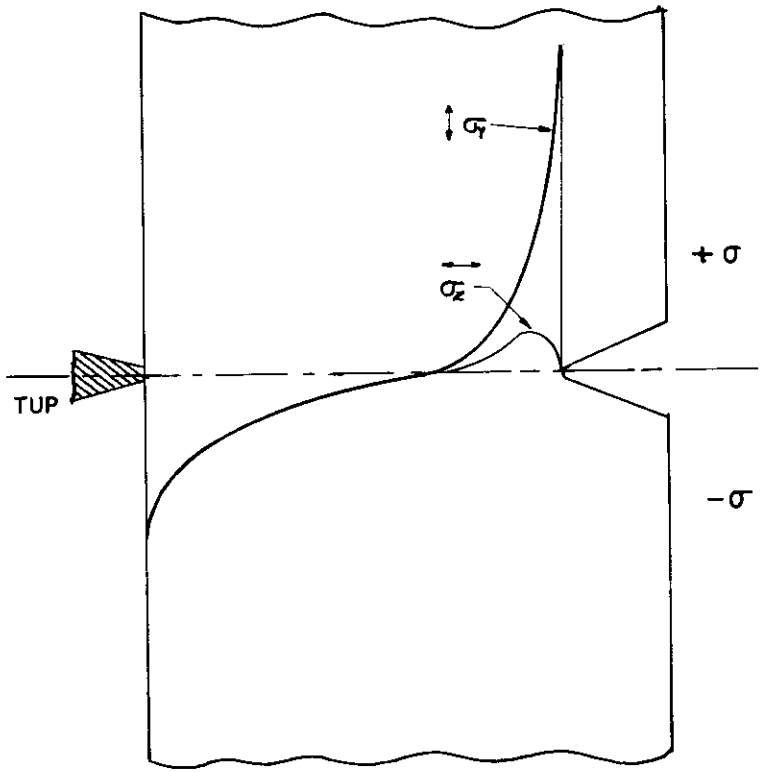

FIG. 10. Distribution of elastic stress at the base of the notch in a notch-bend test bar.

FIG. 11. Charpy keyhole notch specimens.

FIG. 12. Charpy V-notch specimens.

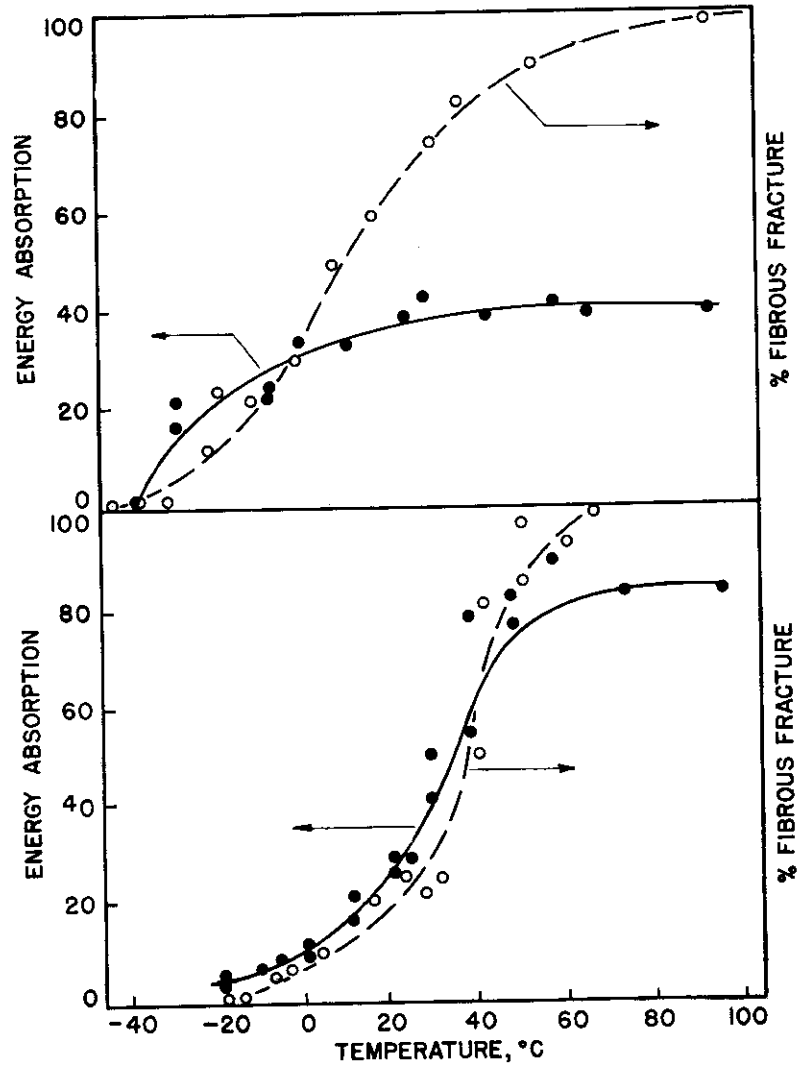

FIGS. 11 and 12. The transitions in energy absorption and fracture appearance for a selected mild steel.

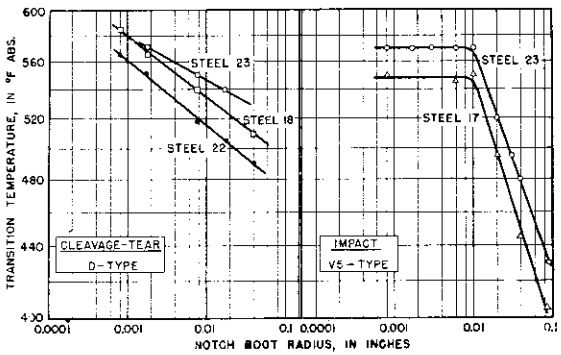

FIG. 13. The change in transition temperature versus notch root radius—Charpy V-notch specimens (right hand plot). (Bagsar, ref. (18))

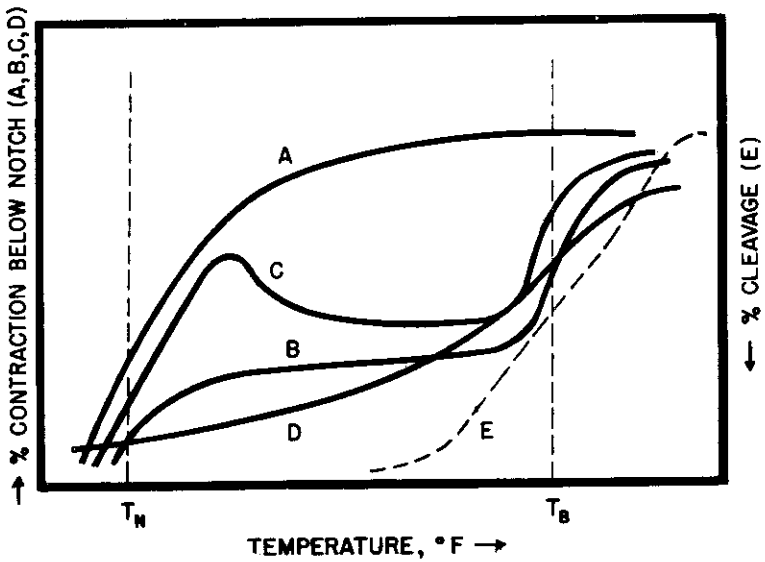

FIG. 14. Diagram showing types of transition curves obtained on notched specimens.

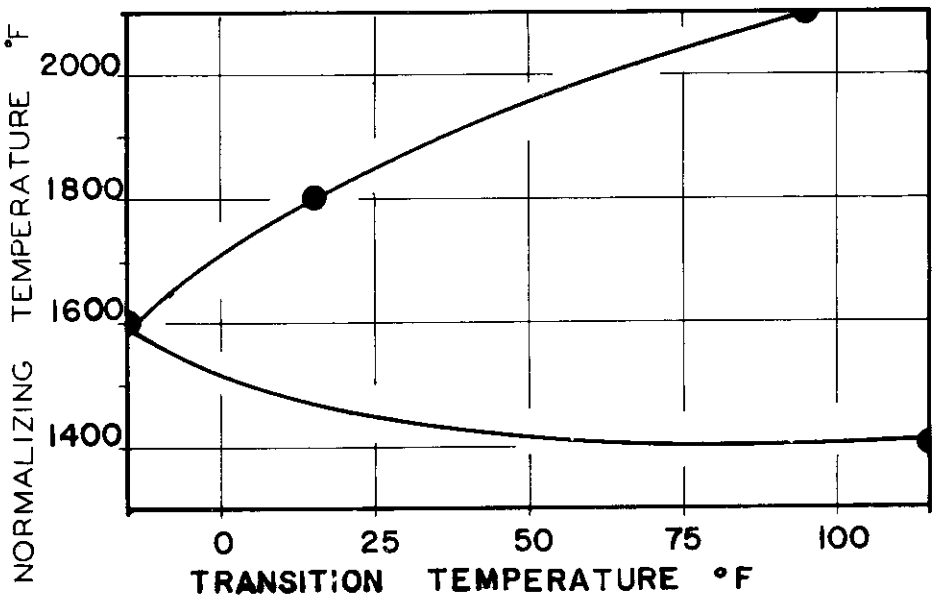

FIG. 15. Influence of normalizing on Lehigh Bend Test transition as indicated by fracture appearance. Silicon-killed steel, 0.25%C, 0.66%Mn, 0.19%Si.

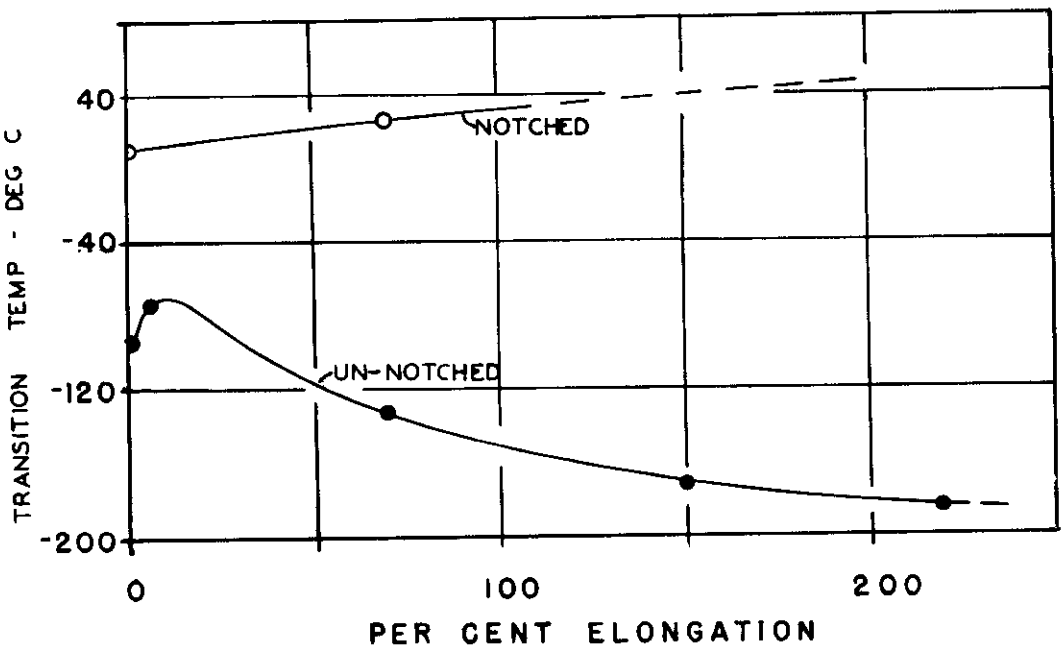

FIG. 16. Influence of pre-strain on the transition temperature of notched and un-notched mild steel impact specimens.

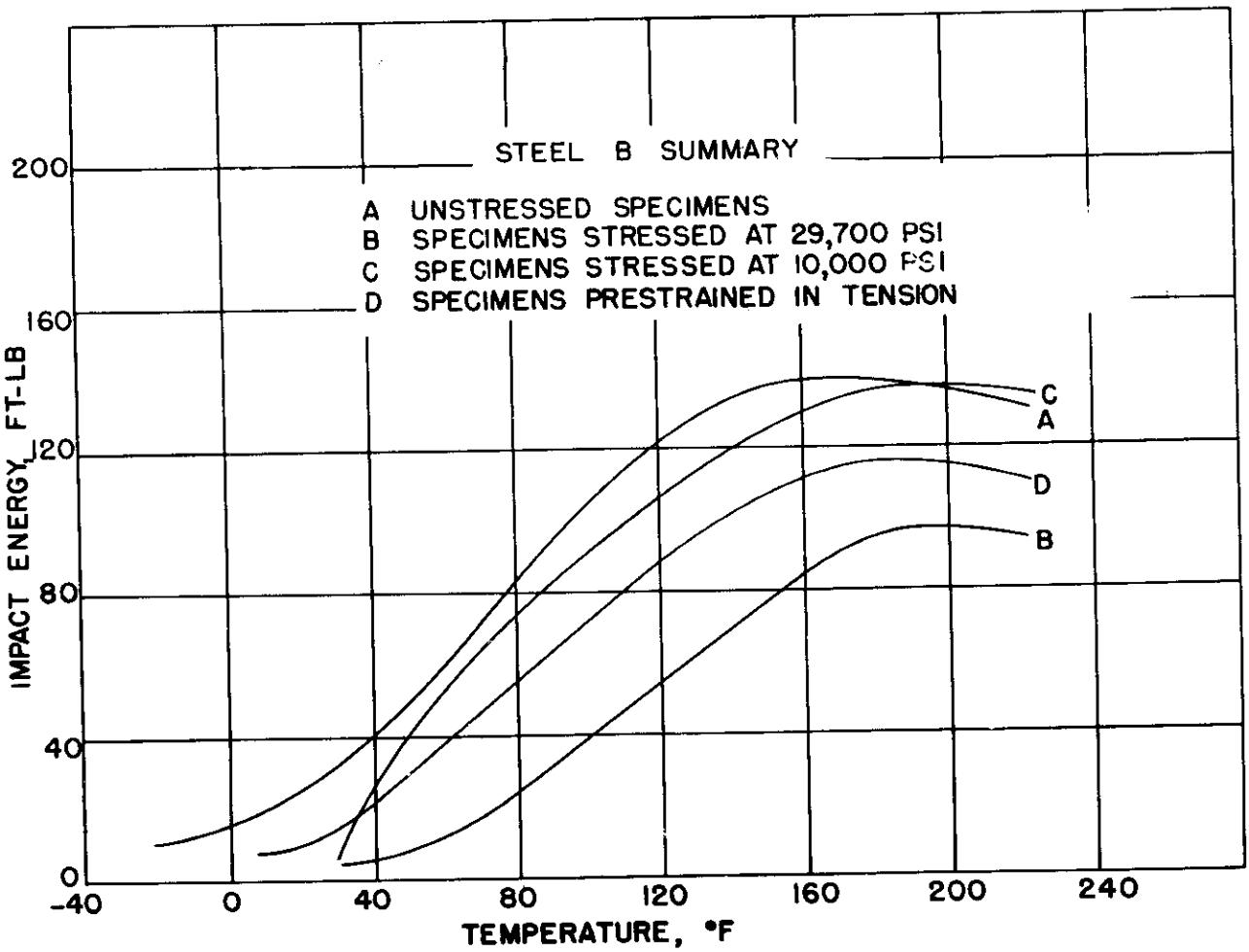

FIG. 17. Effect of fatigue on notched impact strength. (Endurance limit of notched specimens approx. 26,000 p.s.i.)
Curve B - 105,000 cycles of stress.
Curve C - 1,000,000 cycles.

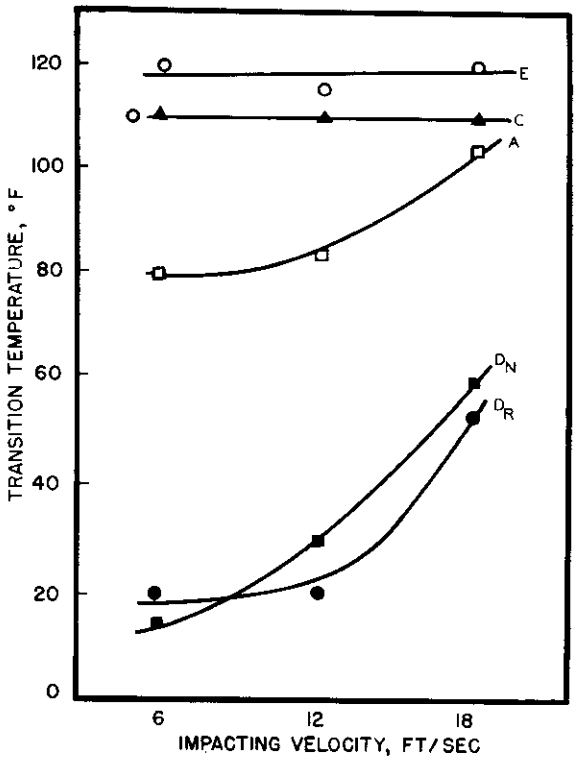

FIG. 18. The transition temperature versus impacting velocity for selected project steels in tension impact. Adapted from Bruckner and Newmark, (24).

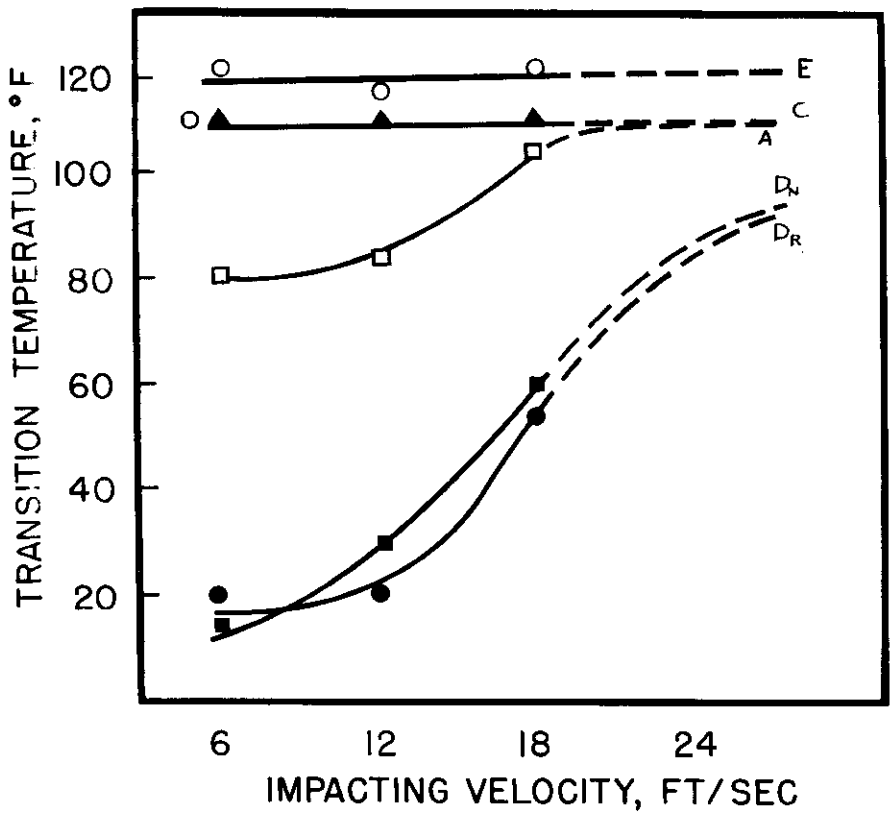

FIG. 19. A suggested extrapolation of the curves of Fig. 18.

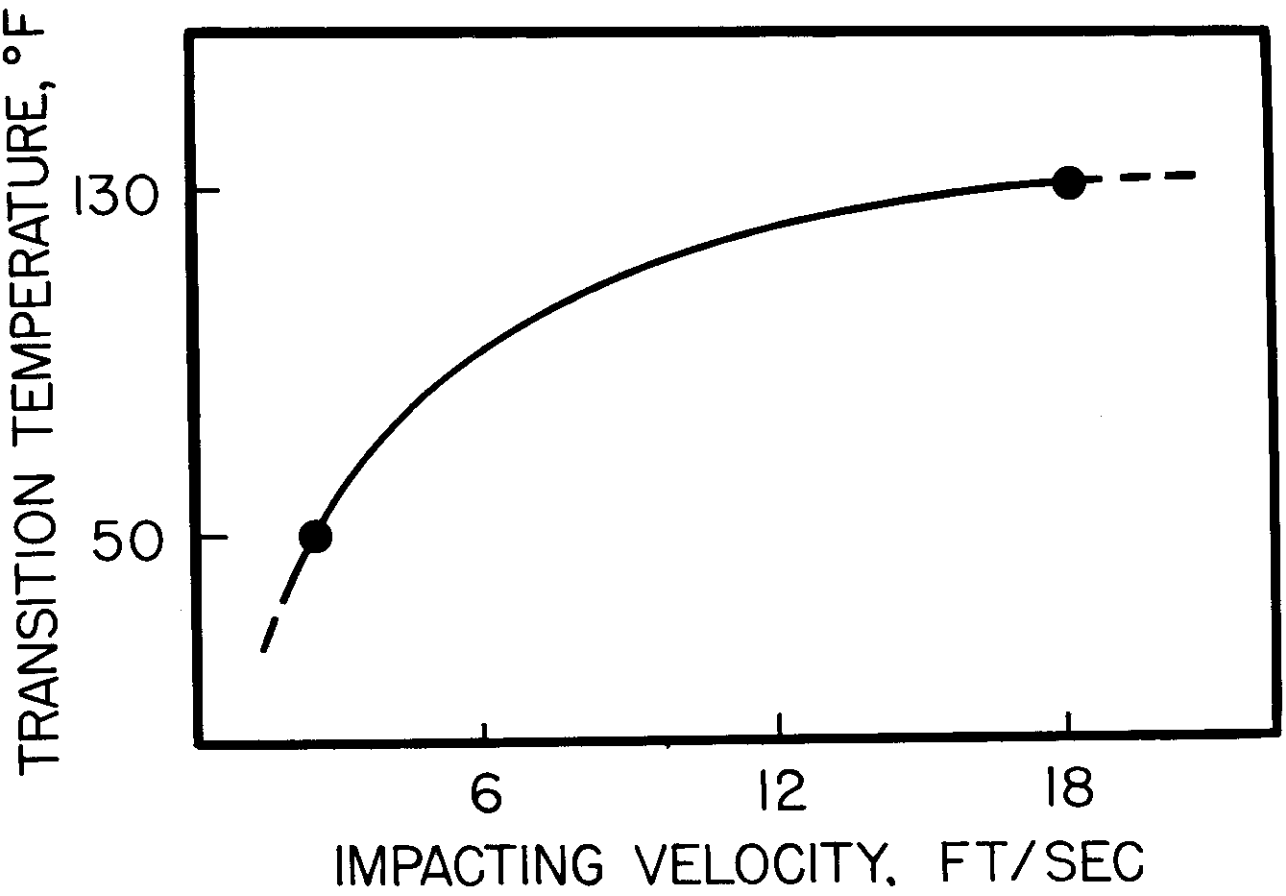

FIG. 20. Suggested variation of transition temperature in the Charpy V-notch impact test with impacting velocity. The two experimental points were determined respectively in slow bending and impact bending.

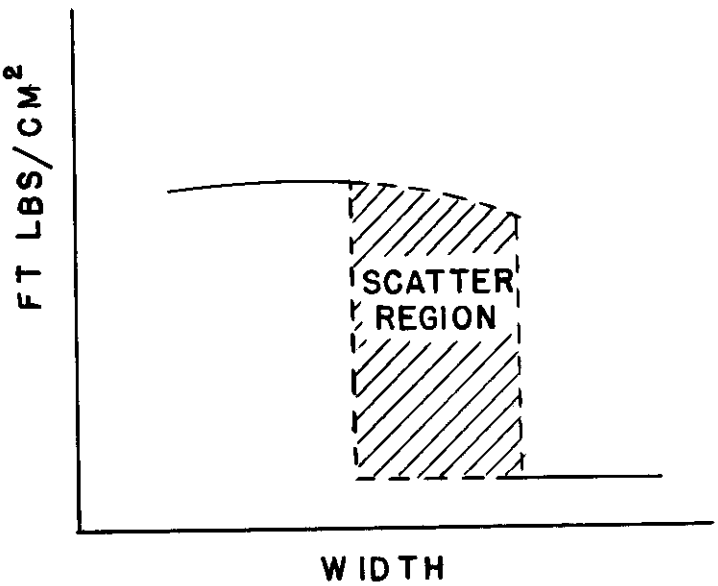

FIG. 21. Influence of specimen width on absorbed energy at constant temperature.

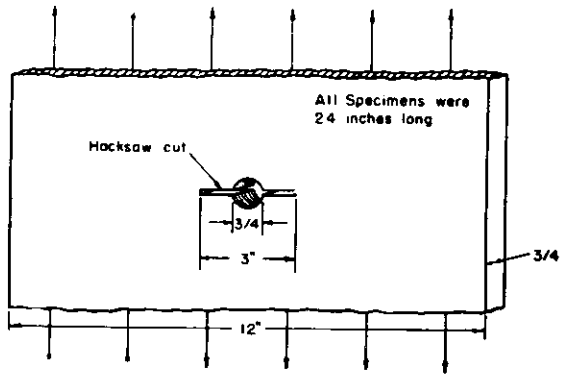

FIG. 22. Form of Taylor Model Basin tensile test specimens.

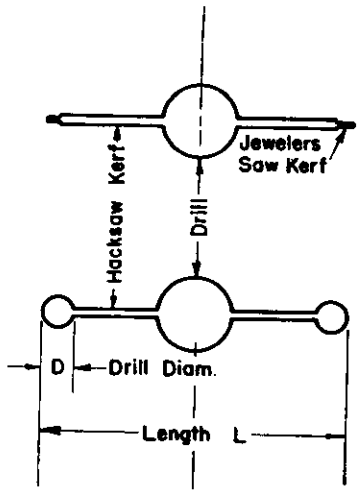

FIG. 23. Details of slot-Taylor Model Basin specimen

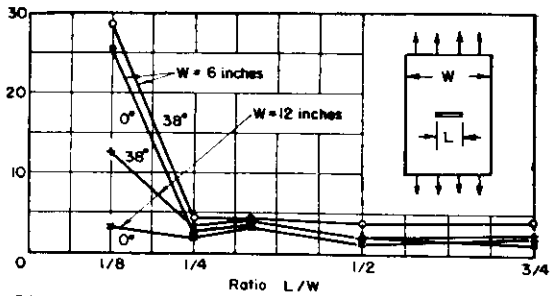

FIG. 24.—Effect of Ratio of Length of Slot to Width of Plate on Energy Absorbed. Results Are for Steel E Specimens Notched with a Jeweler's Saw

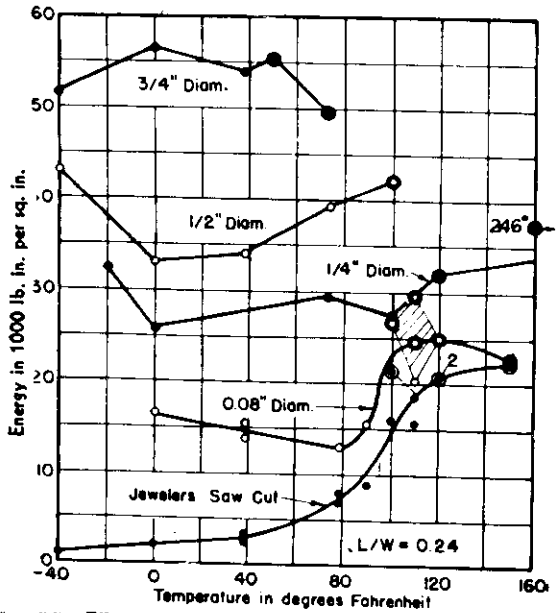

FIG. 25.—Effect of Temperature on Energy Absorbed for Specimens of Steel E

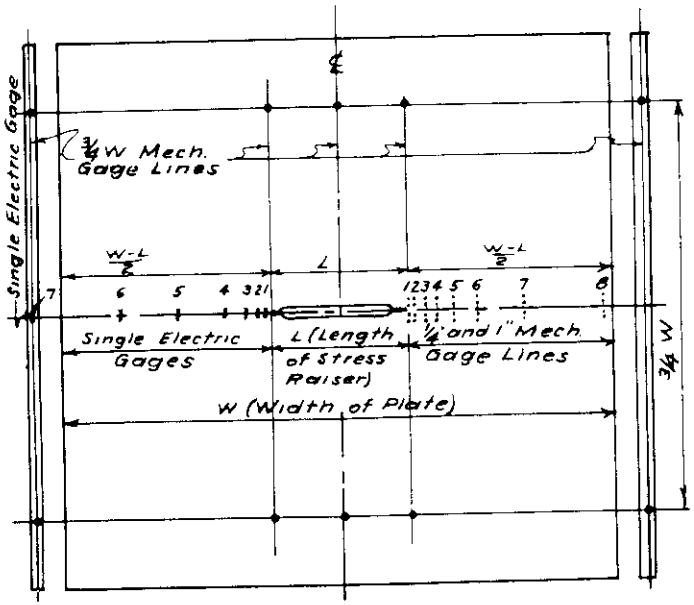

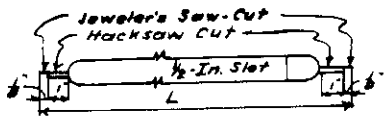

SKETCH OF WIDE PLATE SPECIMENS AND TYPE OF STRESS-RAISER

FIGURE 26

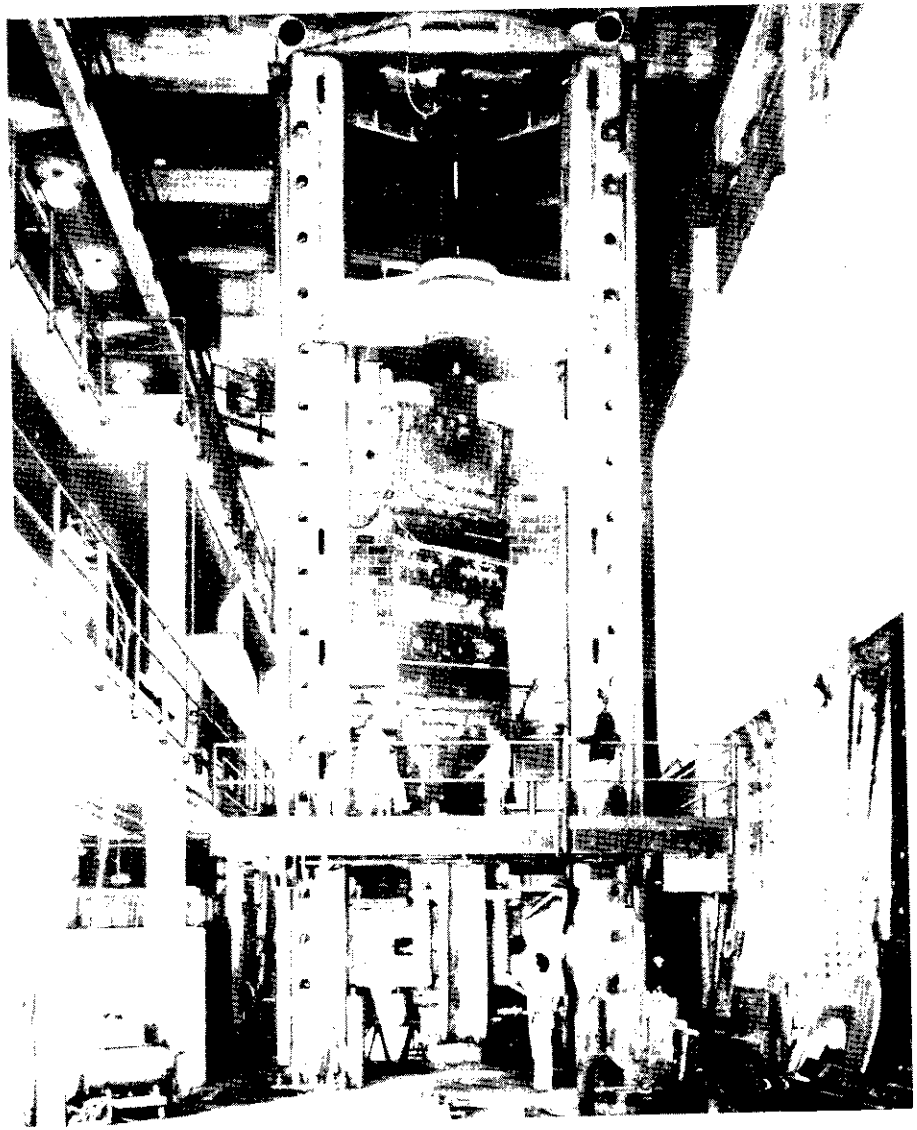

FIGURE 27. 72-IN. SPECIMEN IN 3,000,000-LB. TESTING MACHINE

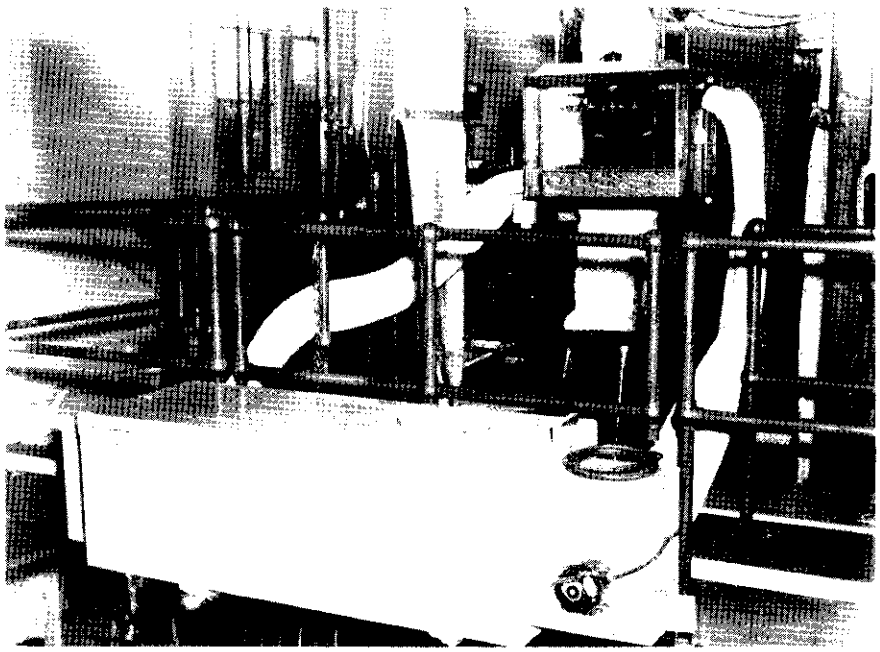

FIG. 28. Specimen cooling mechanism.

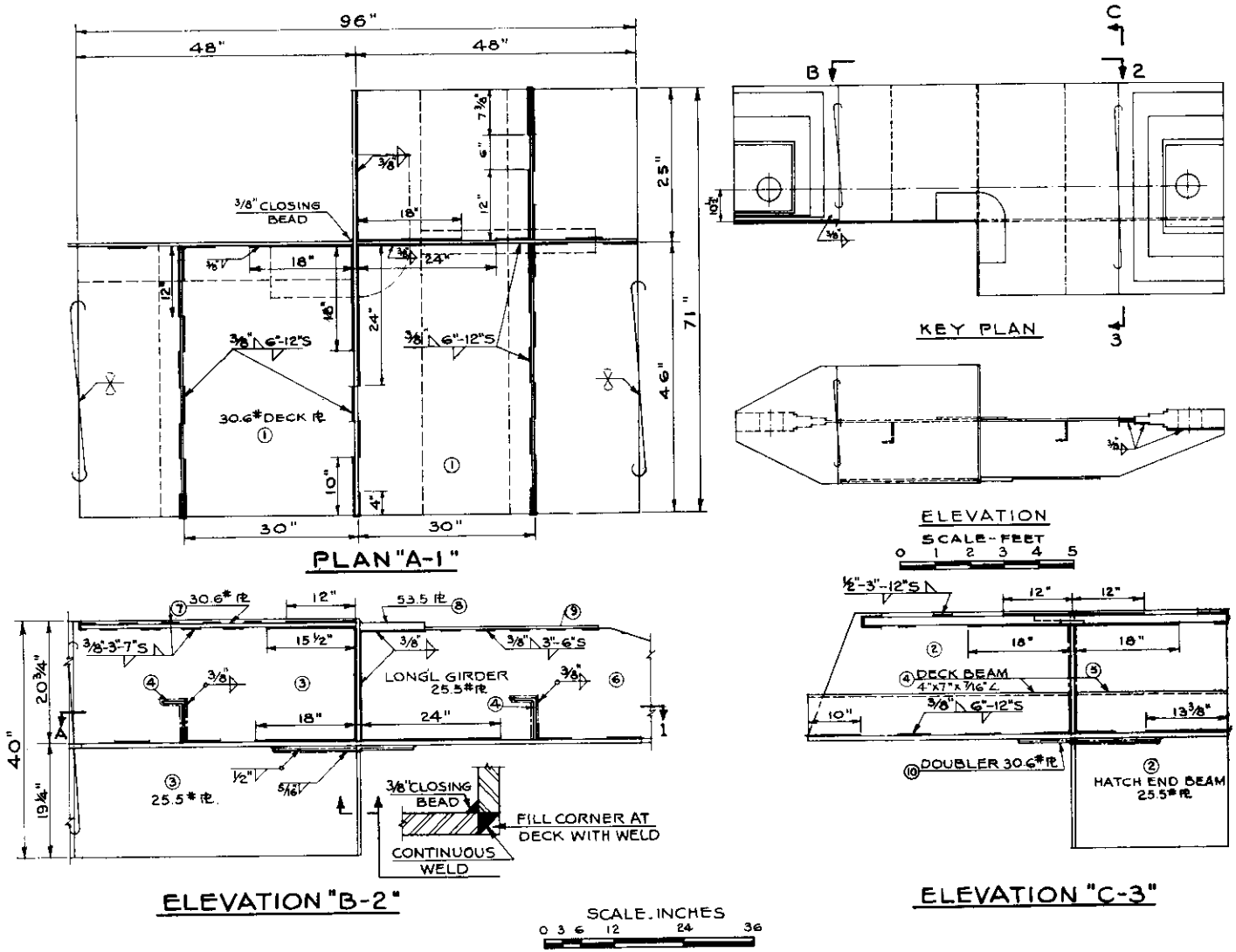

UNIVERSITY OF CALIFORNIA WELDING RESEARCH - NRC - 92 B 310 ENGINEERING BLDG. BERKELEY, CALIF.	REVISED DESIGN OF THE FULL SCALE HATCH CORNER MODEL	SCALE: AS SHOWN DR. BY: R. SISSON CH. BY:	APPROVED 6/11/45 / /

FIG. 29

FIG. 30. Specimen 4: Overall view from above

FIG. 31. Specimen 4: Overall view from below

FIGS. 30 and 31. Hatch corner tests.

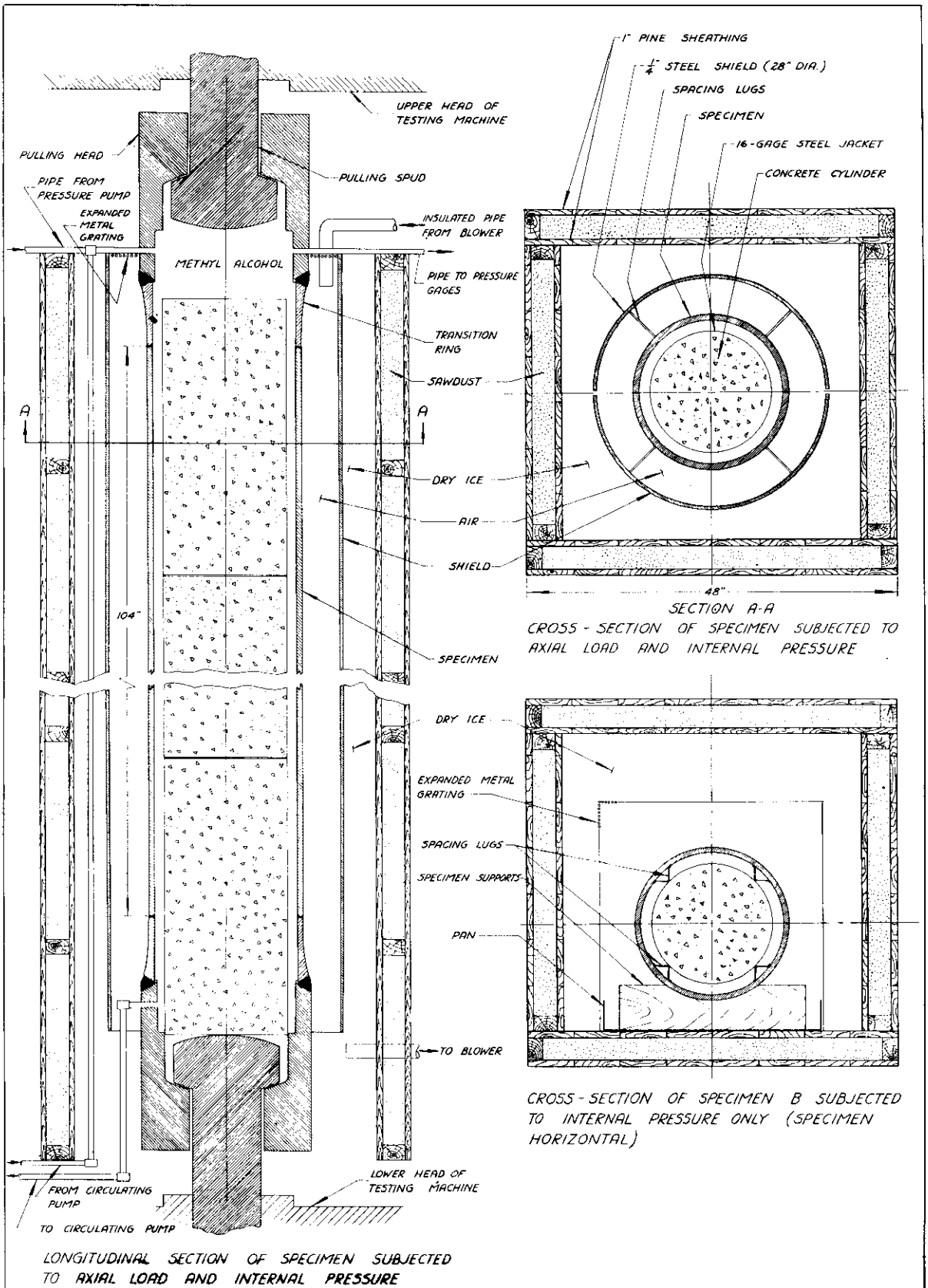

FIG. 32. Sections of apparatus for tests of 20" Diameter tubes at low temperatures.

43D-78

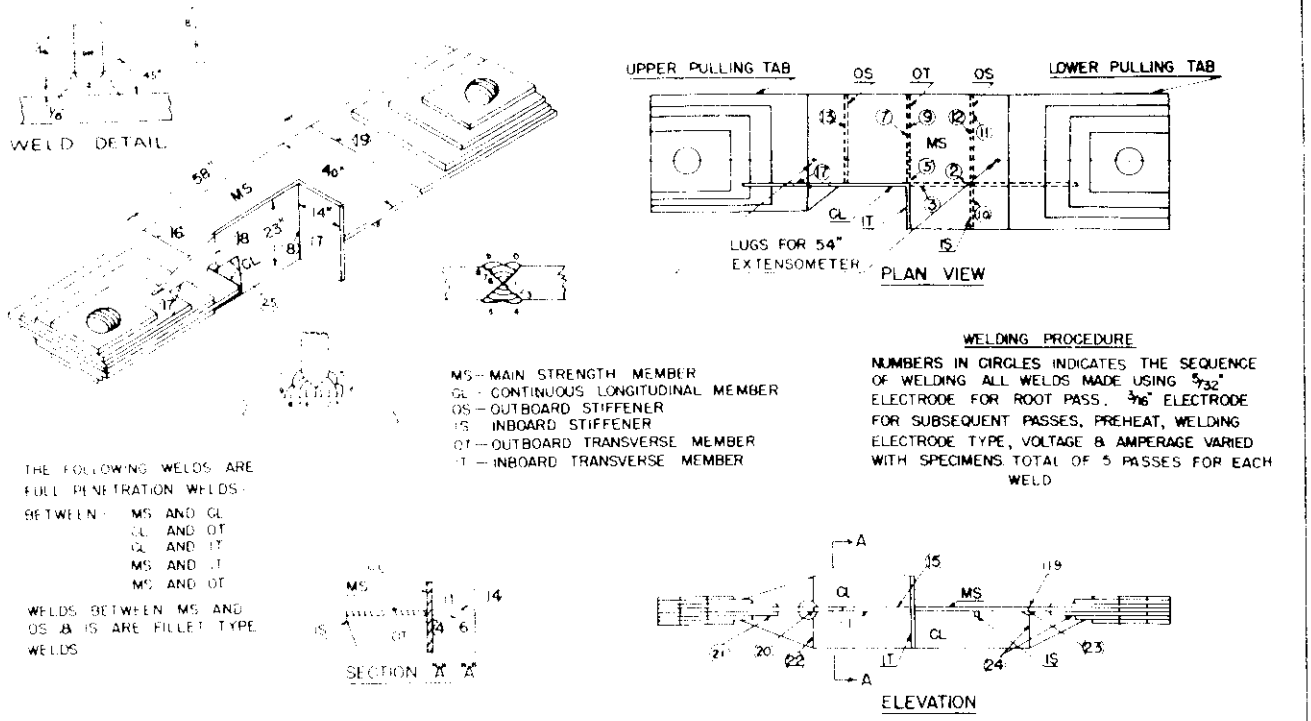

RESTRAINED WELDED SPECIMEN USED FOR TESTS OF HIGH YIELD STRENGTH STRUCTURAL STEELS.

Fig. 7a. Restrained weld specimen in testing machine showing pin ends and extensometer.

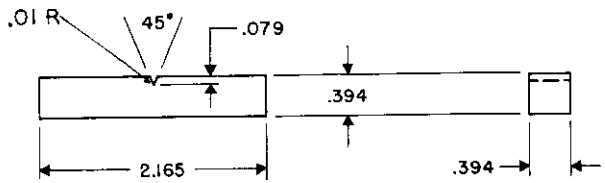

STANDARD "V" NOTCH

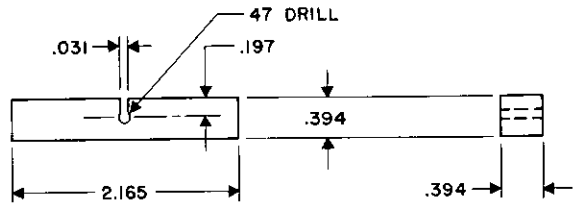

STANDARD KEYHOLE NOTCH

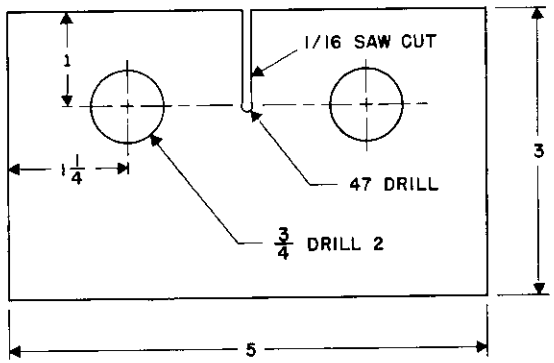

NAVY TEAR TEST KEYHOLE NOTCH

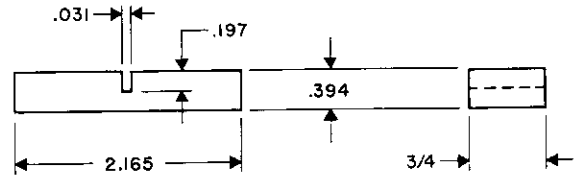

SAW CUT NOTCH

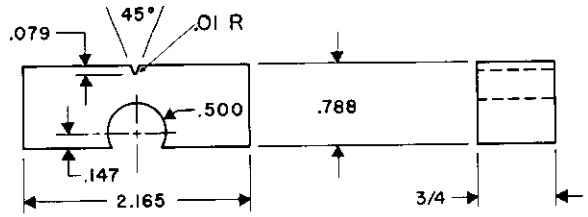

SLOW BEND TEST

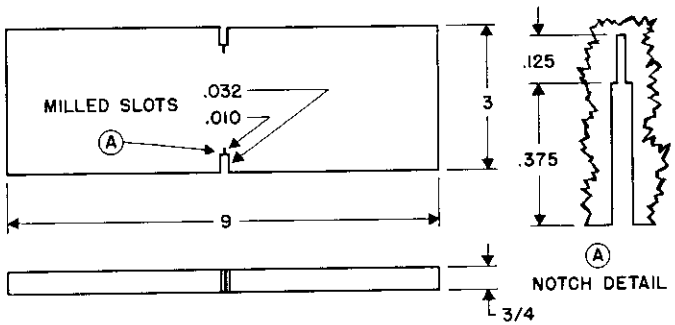

3 IN. EDGE-NOTCHED TENSION TEST

FIG. 35 LABORATORY TEST SPECIMENS EMPLOYED FOR CORRELATION WITH LARGE PLATE TEST RESULTS

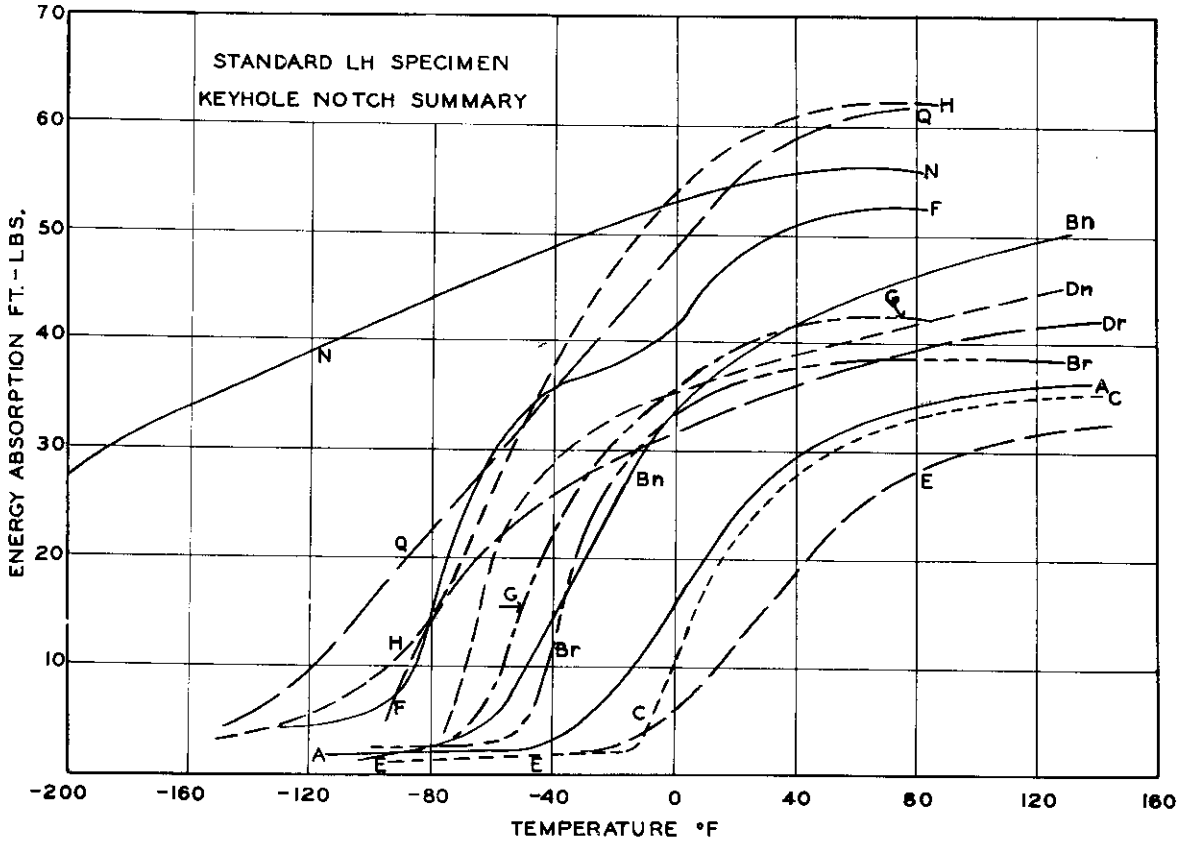

FIG. 36. Keyhole Notch Summary.

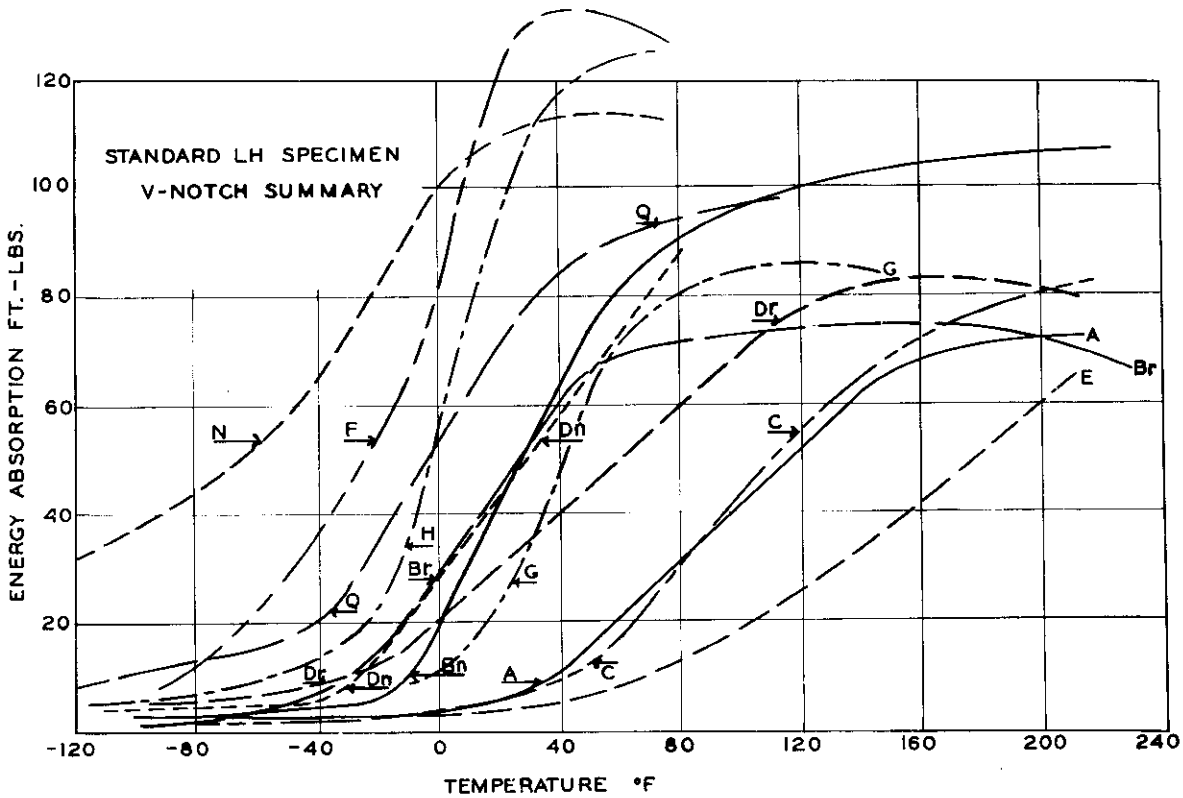

FIG. 37. V-Notch Summary

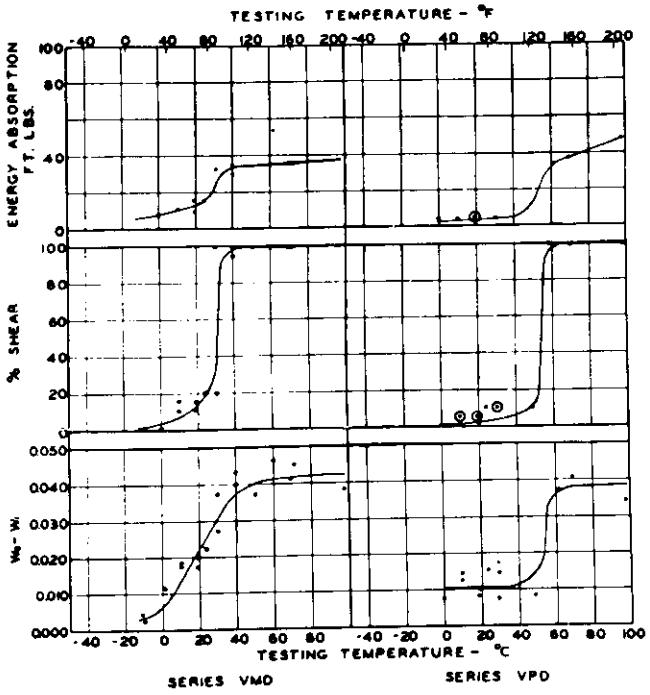

FIG. 38. Energy absorption, fracture appearance, and lateral contraction vs. testing temperature for V-notch milled and V-notch pressed (both Schnadt modification) Charpy impact specimens. Mild steel. (Ref. (14))

% Axial Compression	Aging Treatment	Transition Temp., °F. Steel A 25%	Steel A 50%	Steel C 25%	Steel C 50%
5	R.T., 1 hr.	0	30	15	40
5	R.T., 6 hr.	−10	35	20	40
5	R.T., 12 hr.	20	35	10	35
5	R.T., 36 hr.	10	35	10	45
5	R.T., 1 wk.	20	40	0	35
5	R.T., 4 wk.	20	40	20	45
10	R.T., 1 hr.	15	45	30	50
10	R.T., 6 hr.	15	35	20	55
10	R.T., 12 hr.	15	45	25	60
10	R.T., 36 hr.	20	40	20	45
10	R.T., 1 wk.	15	45	..	..
10	R.T., 4 wk.	40	65	35	55
10	250° C., ½ hr.	70	100	65	85
10	250° C., 1½ hr.	55	85	60	95
10	250° C., 4 hr.	55	90	..	..
10	250° C., 30 hr.	70	100	65	95

FIG. 39. Charpy V-notch impact transition temperature in °F at 25 and 50% maximum energy absorption for specimens prestrained in compression. R.T. is room temperature. (Ref. (35))

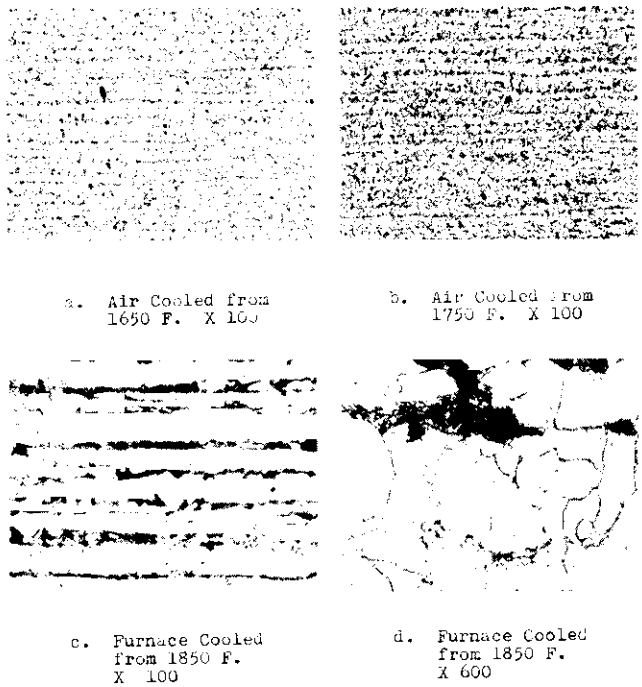

a. Air Cooled from 1650 F. X 100

b. Air Cooled from 1750 F. X 100

c. Furnace Cooled from 1850 F. X 100

d. Furnace Cooled from 1850 F. X 600

Photomicrographs of Steel N
After Different Heat Treatments

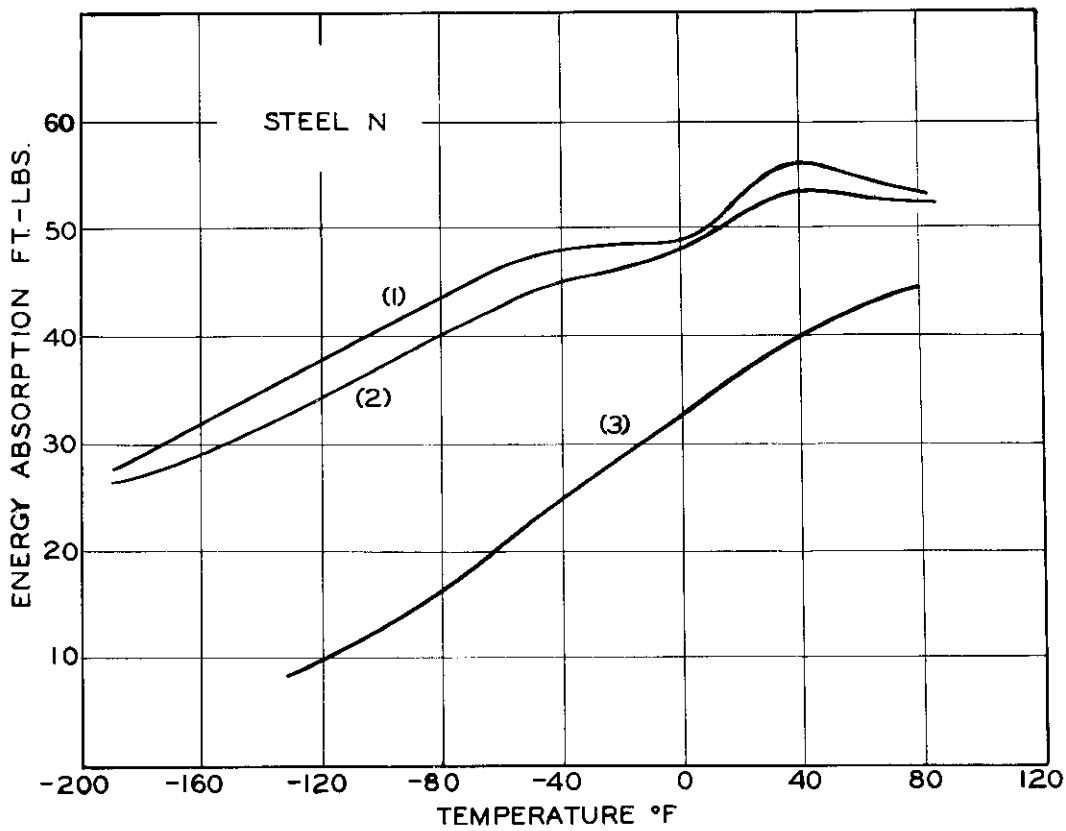

FIG. 40. Charpy keyhole tests of Steel N following different heat treatments. Curve (1) refers to treatment (a) above, curve (2) to treatment (b) etc. (Ref. (35))

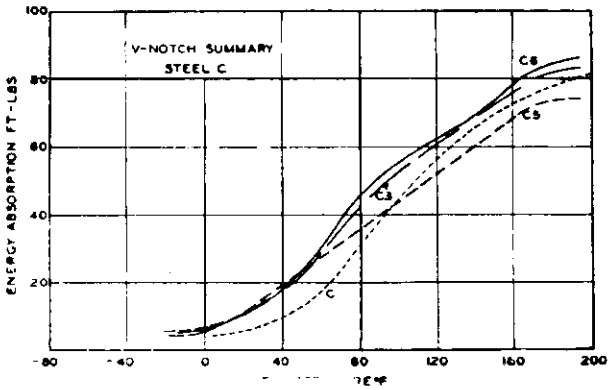

FIG. 41.

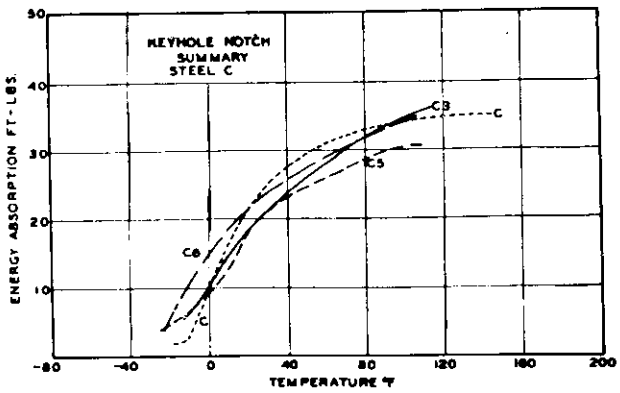

FIG. 42.

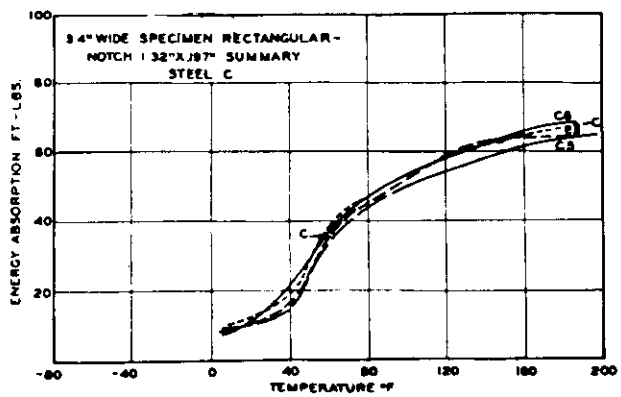

FIG. 43.

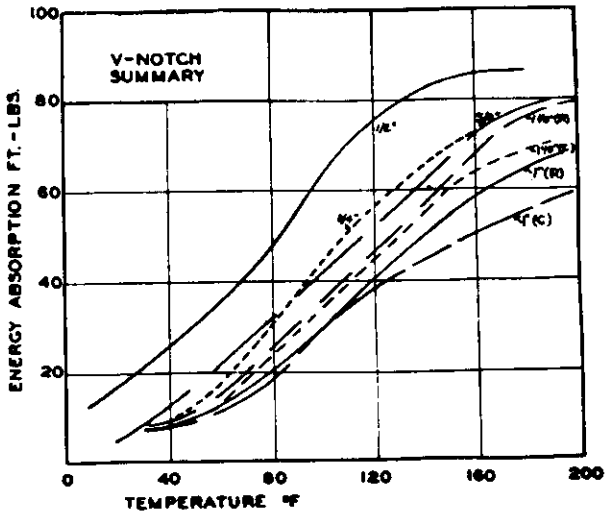

FIG. 44.

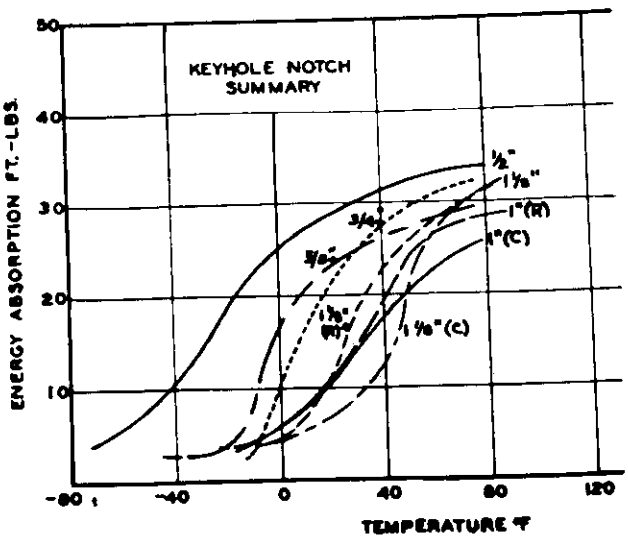

FIG. 45.

FIGS. 41-45. The influence of plate thickness and variations from plate to plate of constant thickness on notched bar test results. All steel from one heat. Project Steel C. R=specimens from plate surface. Others at mid-thickness.

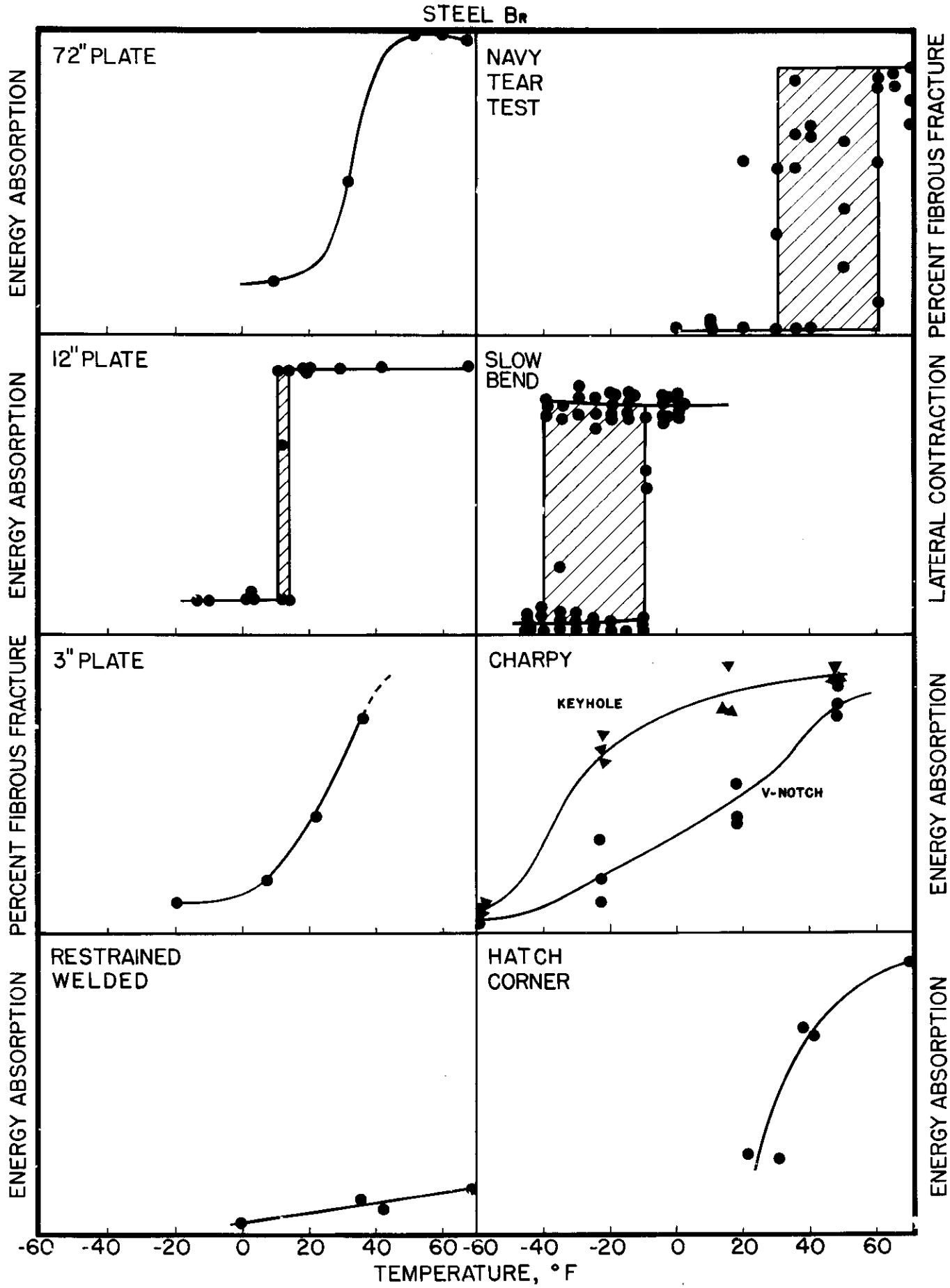
STEEL BR
72" PLATE
NAVY TEAR TEST
12" PLATE
SLOW BEND
3" PLATE
CHARPY
KEYHOLE
V-NOTCH
RESTRAINED WELDED
HATCH CORNER
ENERGY ABSORPTION
PERCENT FIBROUS FRACTURE
LATERAL CONTRACTION
-60 -40 -20 0 20 40 60
TEMPERATURE, °F

FIG. 46

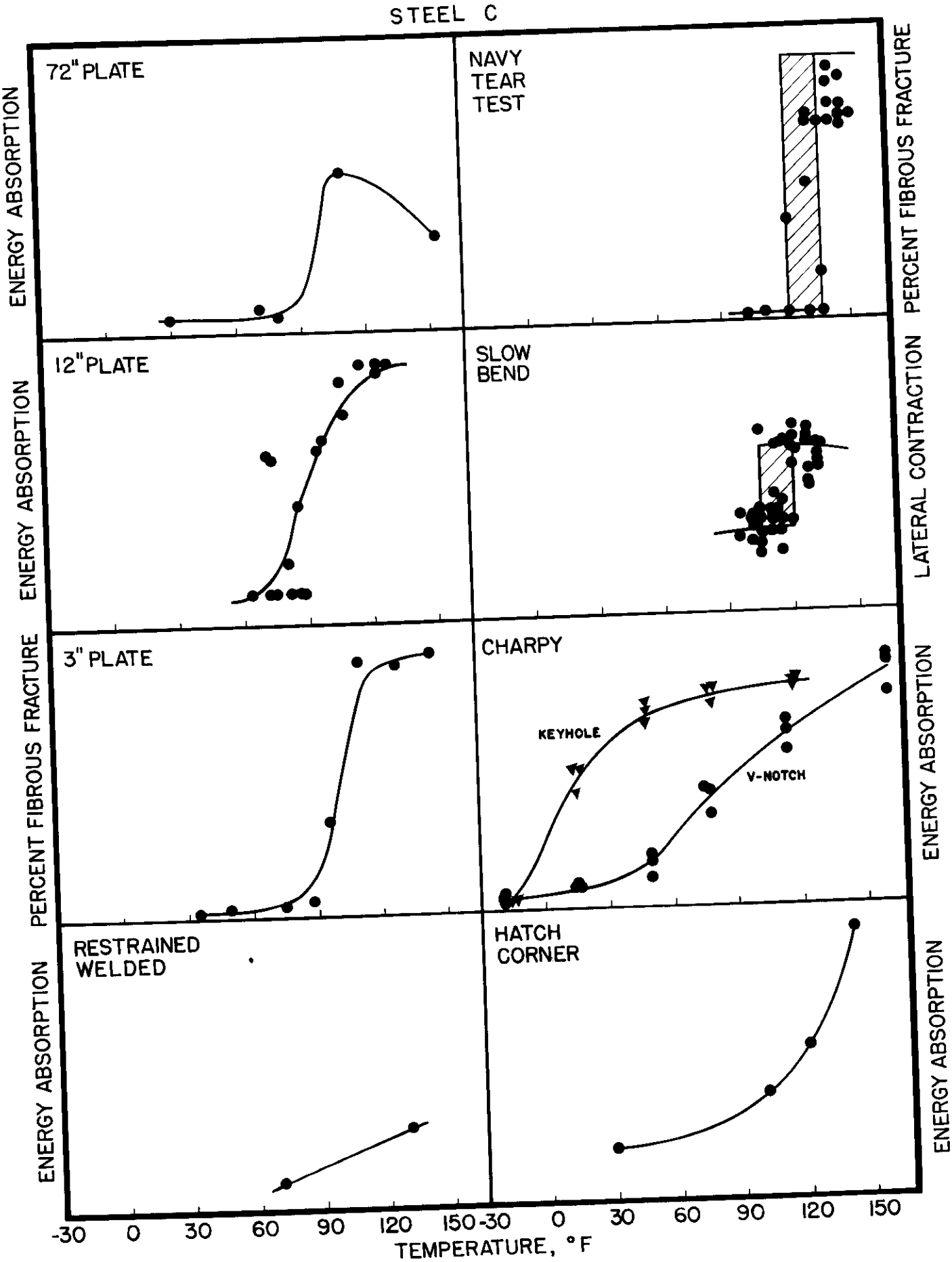
STEEL C
72" PLATE
NAVY TEAR TEST
12" PLATE
SLOW BEND
3" PLATE
CHARPY
KEYHOLE
V-NOTCH
RESTRAINED WELDED
HATCH CORNER
ENERGY ABSORPTION
PERCENT FIBROUS FRACTURE
LATERAL CONTRACTION
-30 0 30 60 90 120 150
TEMPERATURE, °F

FIG. 47

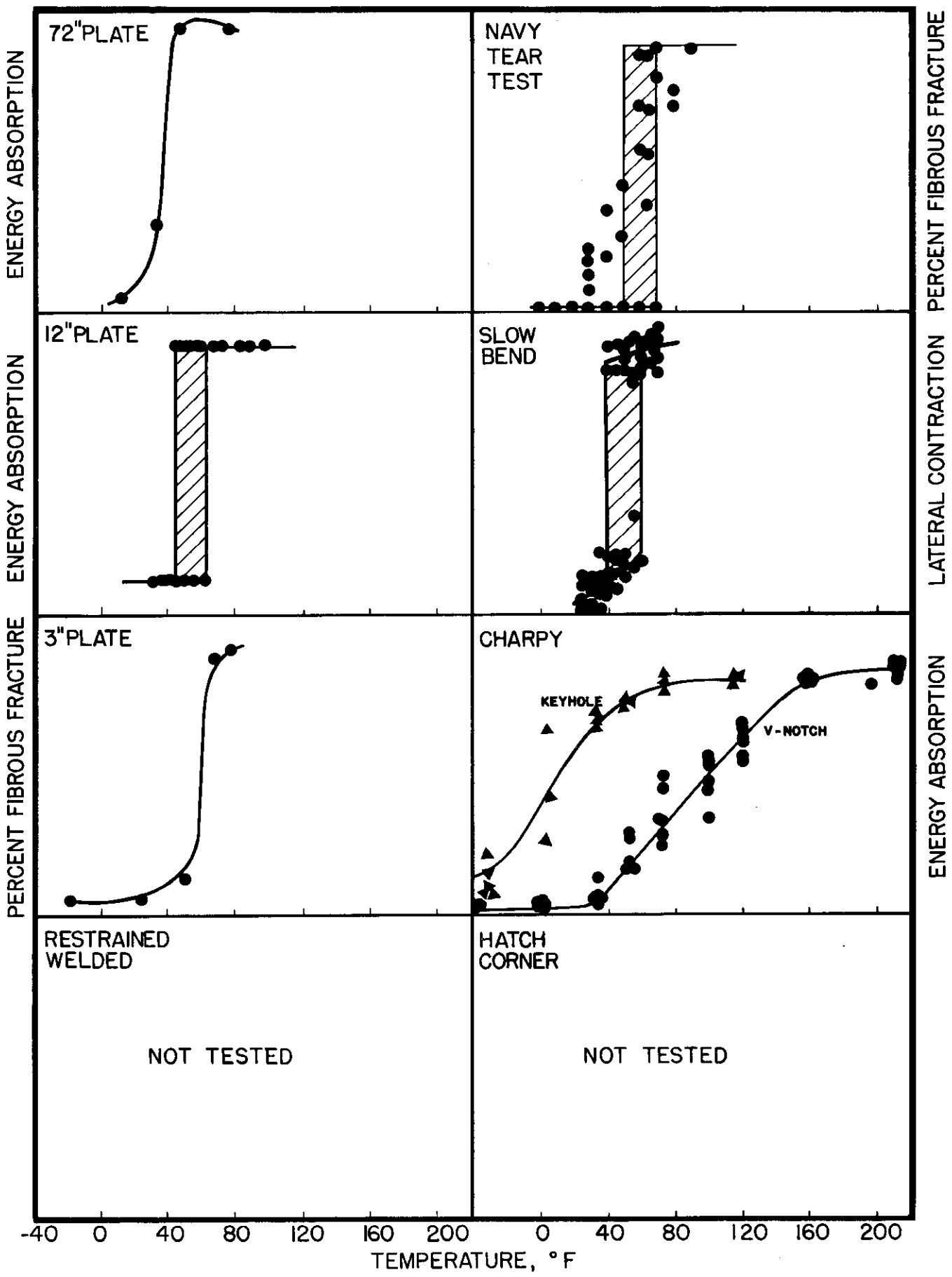
STEEL A
72"PLATE
NAVY
TEAR
TEST
12"PLATE
SLOW
BEND
3"PLATE
CHARPY
KEYHOLE
V-NOTCH
RESTRAINED
WELDED
NOT TESTED
HATCH
CORNER
NOT TESTED
ENERGY ABSORPTION
ENERGY ABSORPTION
PERCENT FIBROUS FRACTURE
PERCENT FIBROUS FRACTURE
LATERAL CONTRACTION
ENERGY ABSORPTION
-40 0 40 80 120 160 200
0 40 80 120 160 200
TEMPERATURE, °F

FIG. 48

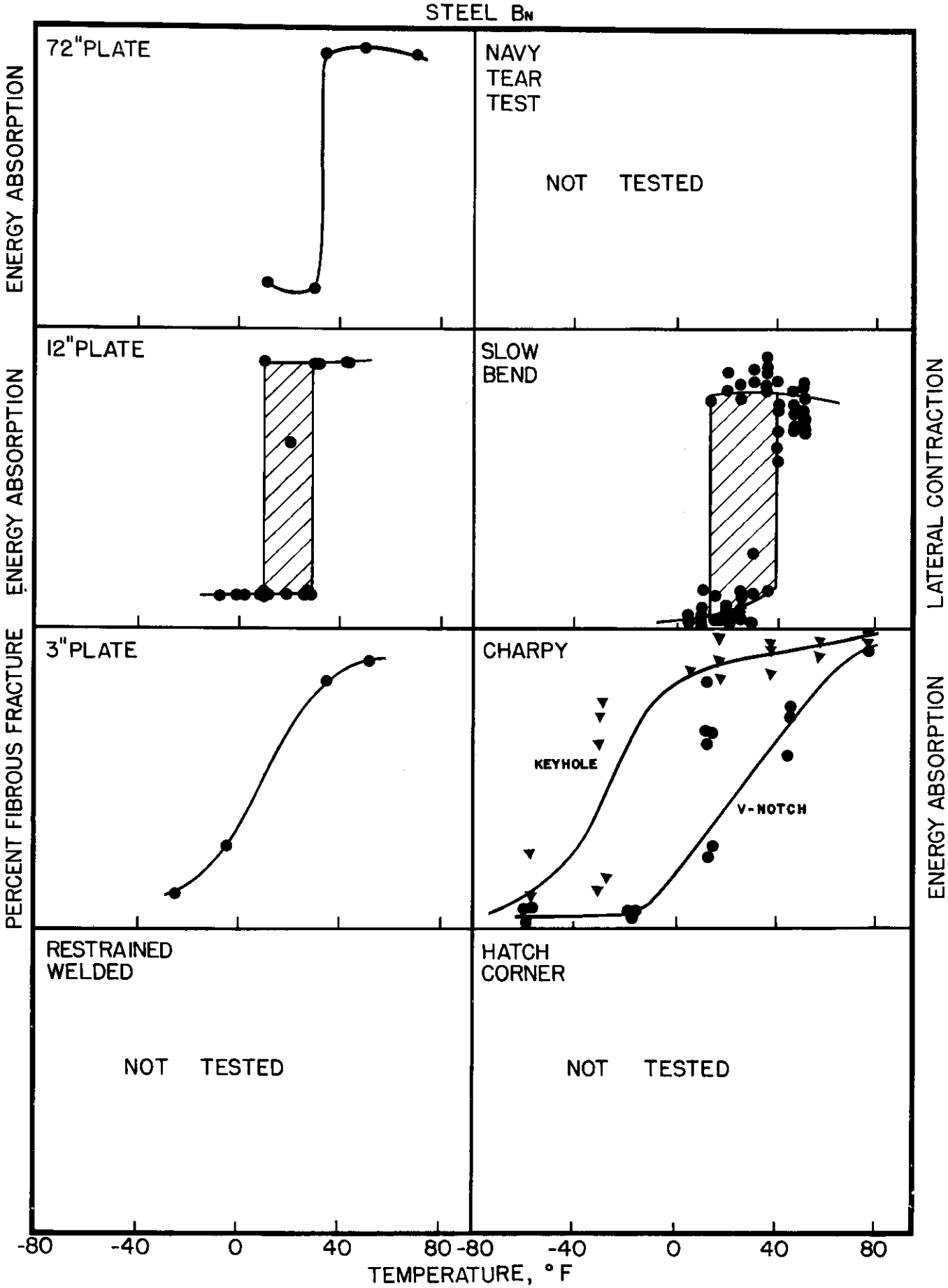
STEEL BN
72"PLATE
NAVY
TEAR
TEST
NOT TESTED
12"PLATE
SLOW
BEND
3"PLATE
CHARPY
KEYHOLE
V-NOTCH
RESTRAINED
WELDED
NOT TESTED
HATCH
CORNER
NOT TESTED
ENERGY ABSORPTION
ENERGY ABSORPTION
PERCENT FIBROUS FRACTURE
LATERAL CONTRACTION
ENERGY ABSORPTION
-80 -40 0 40 80 -80 -40 0 40 80
TEMPERATURE, °F

FIG. 49

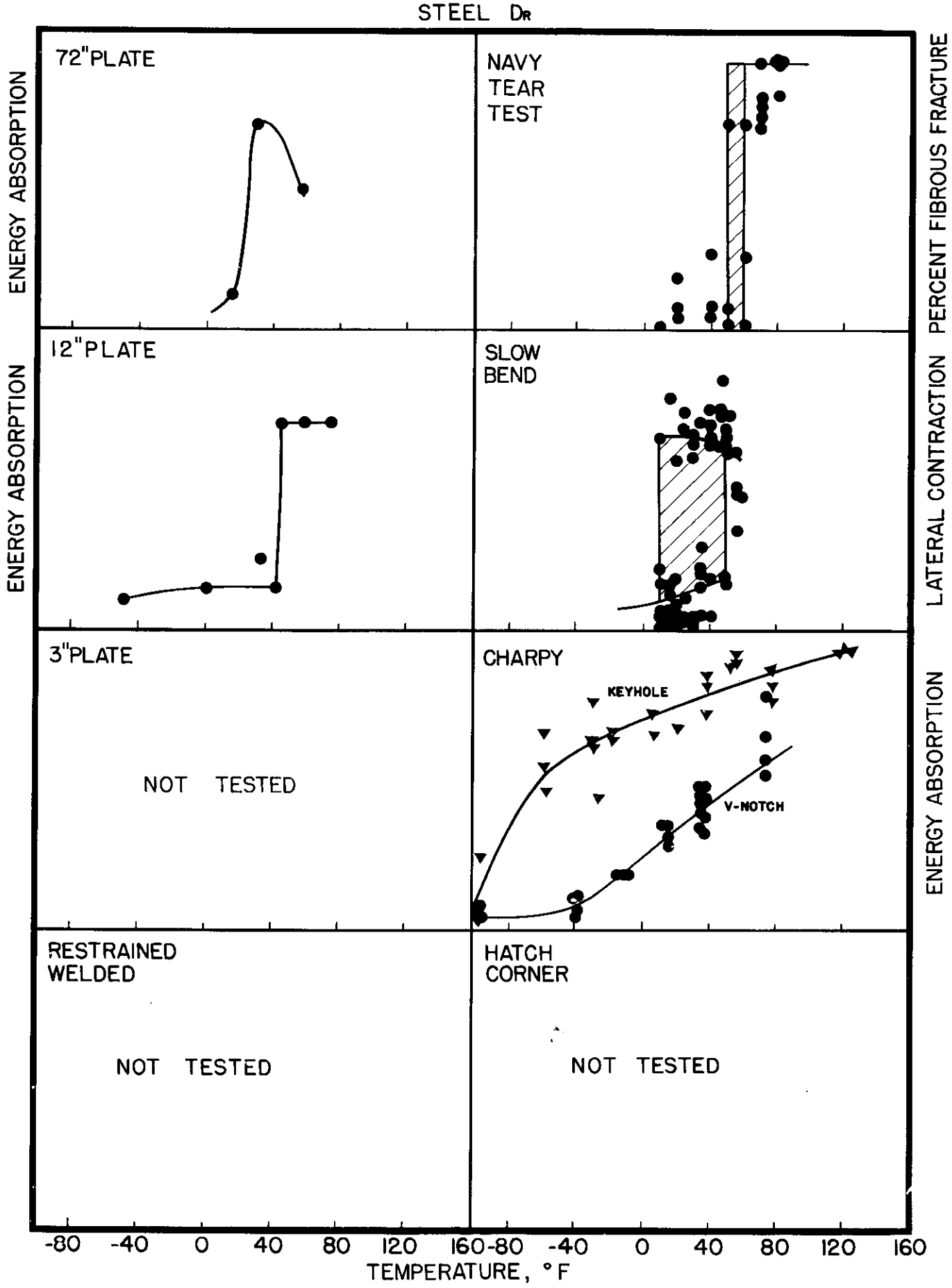
STEEL DR
72"PLATE
NAVY
TEAR
TEST
12"PLATE
SLOW
BEND
3"PLATE
NOT TESTED
CHARPY
KEYHOLE
V-NOTCH
RESTRAINED
WELDED
NOT TESTED
HATCH
CORNER
NOT TESTED
ENERGY ABSORPTION
ENERGY ABSORPTION
PERCENT FIBROUS FRACTURE
LATERAL CONTRACTION
ENERGY ABSORPTION
-80 -40 0 40 80 120 160 -80 -40 0 40 80 120 160
TEMPERATURE, °F

FIG. 50

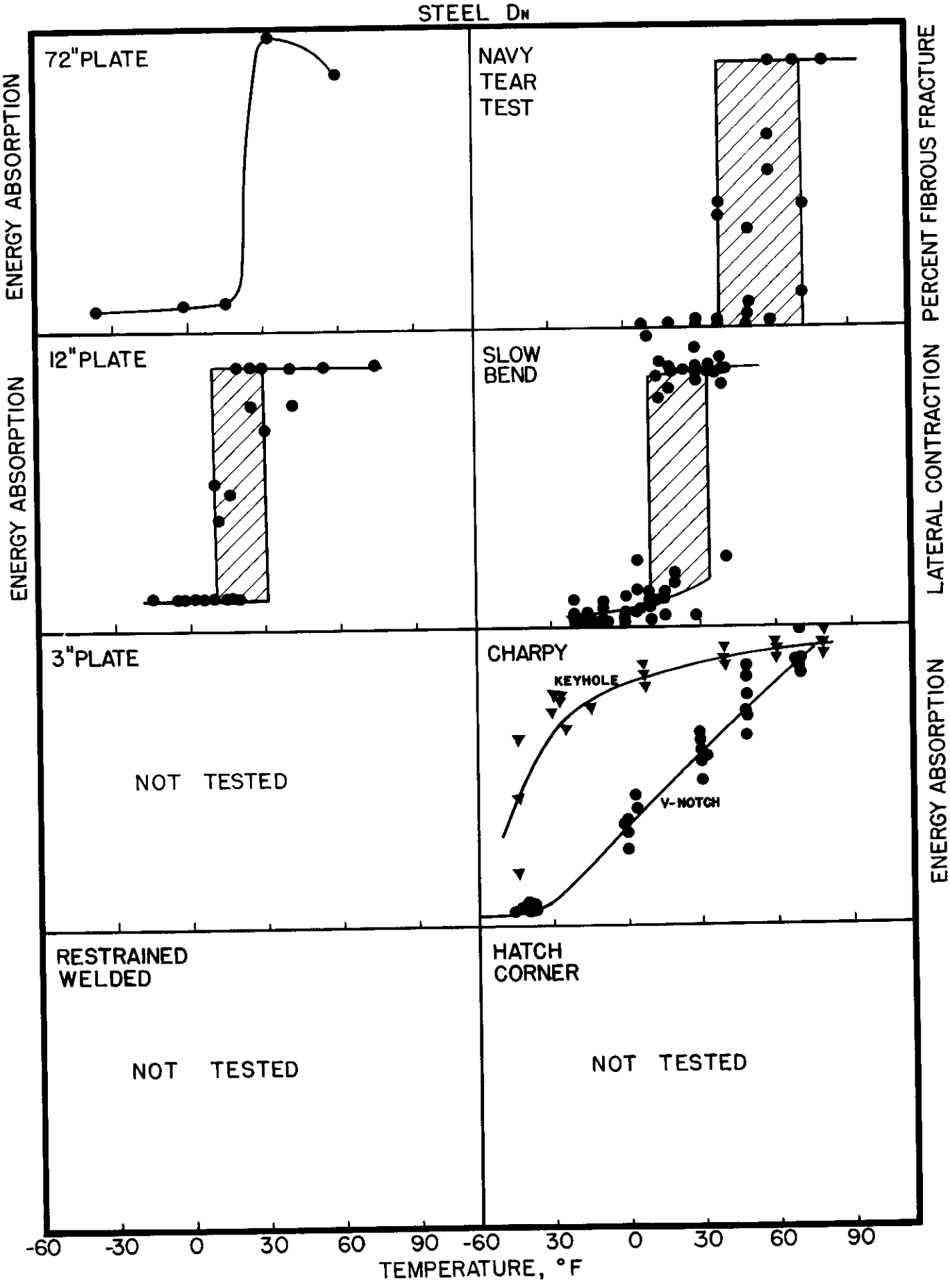
STEEL DN
72"PLATE
NAVY
TEAR
TEST
12"PLATE
SLOW
BEND
3"PLATE
NOT TESTED
CHARPY
KEYHOLE
V-NOTCH
RESTRAINED
WELDED
NOT TESTED
HATCH
CORNER
NOT TESTED
ENERGY ABSORPTION
ENERGY ABSORPTION
LATERAL CONTRACTION
PERCENT FIBROUS FRACTURE
ENERGY ABSORPTION
-60 -30 0 30 60 90 -60 30 0 30 60 90
TEMPERATURE, °F

FIG. 51

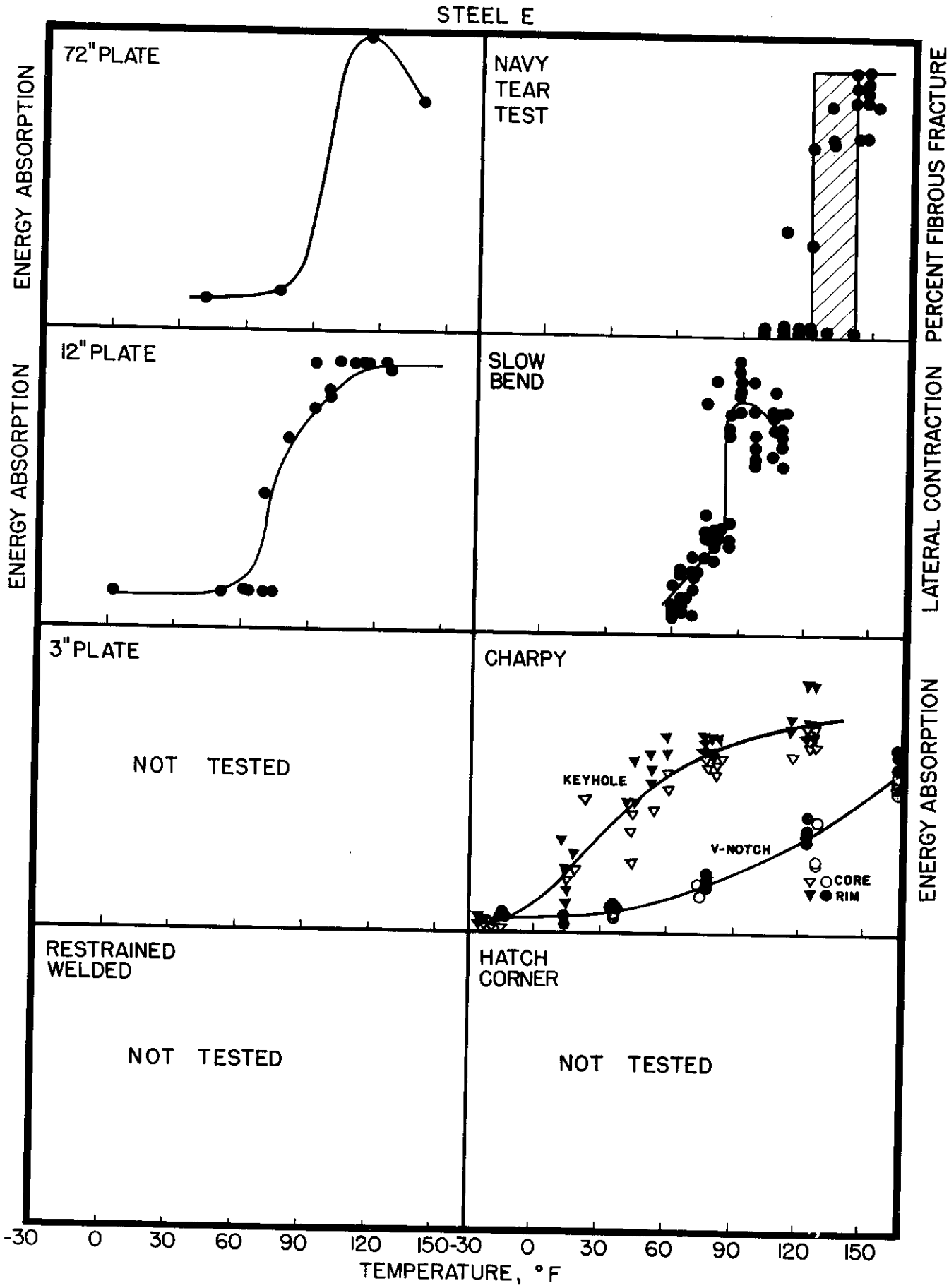
STEEL E
72" PLATE
NAVY TEAR TEST
12" PLATE
SLOW BEND
3" PLATE
NOT TESTED
CHARPY
KEYHOLE
V-NOTCH
CORE
RIM
RESTRAINED WELDED
NOT TESTED
HATCH CORNER
NOT TESTED
ENERGY ABSORPTION
ENERGY ABSORPTION
PERCENT FIBROUS FRACTURE
LATERAL CONTRACTION
ENERGY ABSORPTION
-30 0 30 60 90 120 150
-30 0 30 60 90 120 150
TEMPERATURE, °F

FIG. 52

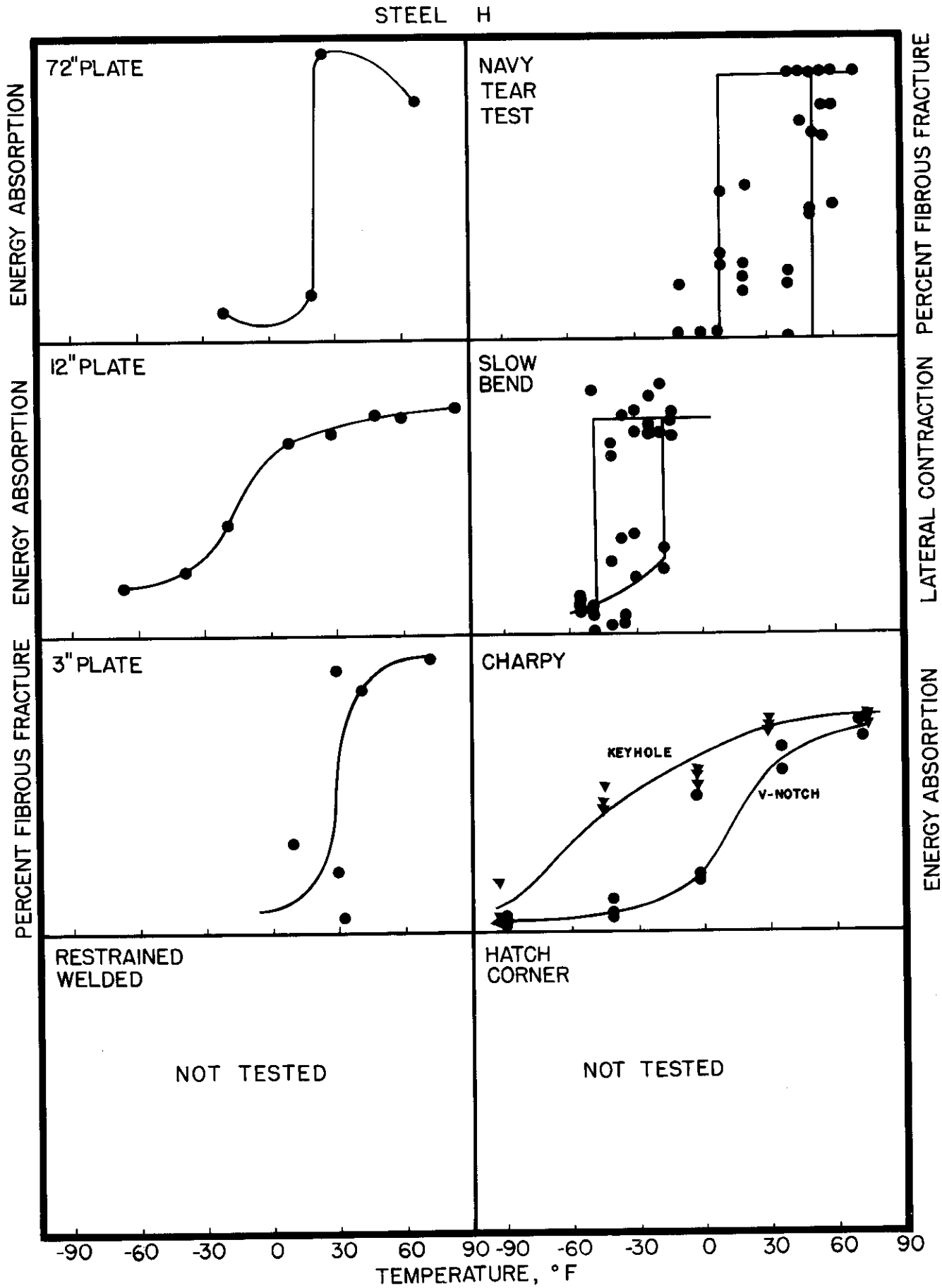
STEEL H
72" PLATE
NAVY TEAR TEST
12" PLATE
SLOW BEND
3" PLATE
CHARPY
KEYHOLE
V-NOTCH
RESTRAINED WELDED
NOT TESTED
HATCH CORNER
NOT TESTED
ENERGY ABSORPTION
PERCENT FIBROUS FRACTURE
ENERGY ABSORPTION
LATERAL CONTRACTION
PERCENT FIBROUS FRACTURE
ENERGY ABSORPTION
-90 -60 -30 0 30 60 90 -90 -60 -30 0 30 60 90
TEMPERATURE, °F

FIG. 53

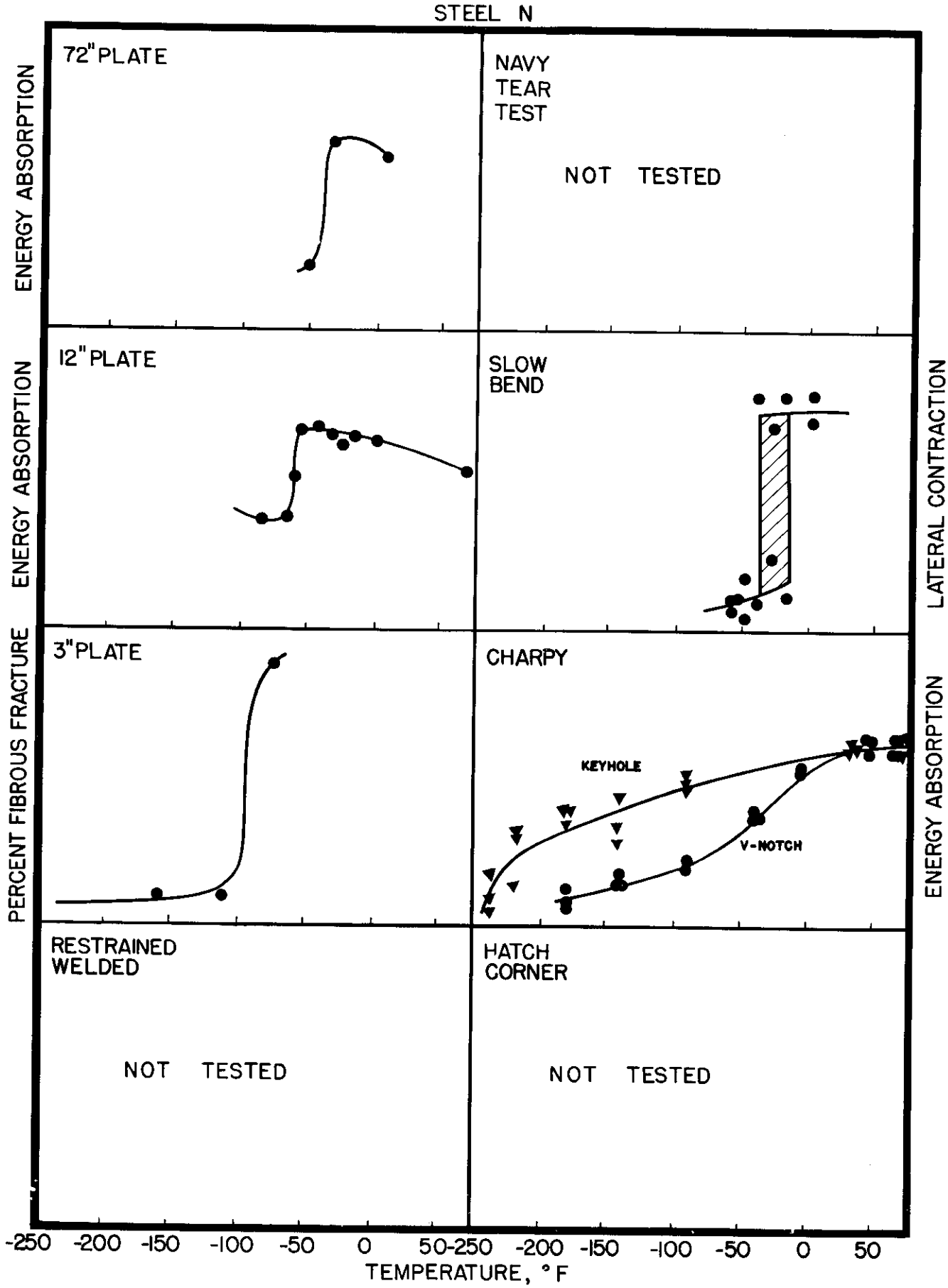
STEEL N
72" PLATE
NAVY TEAR TEST
NOT TESTED
12" PLATE
SLOW BEND
3" PLATE
CHARPY
KEYHOLE
V-NOTCH
RESTRAINED WELDED
NOT TESTED
HATCH CORNER
NOT TESTED
ENERGY ABSORPTION
ENERGY ABSORPTION
PERCENT FIBROUS FRACTURE
LATERAL CONTRACTION
ENERGY ABSORPTION
-250 -200 -150 -100 -50 0 50
-250 -200 -150 -100 -50 0 50
TEMPERATURE, °F

FIG. 54

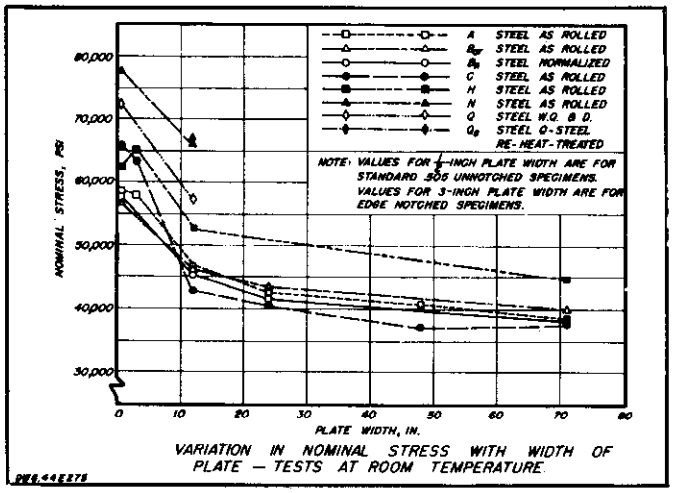

VARIATION IN NOMINAL STRESS WITH WIDTH OF PLATE — TESTS AT ROOM TEMPERATURE.

DWG. 44 E 276

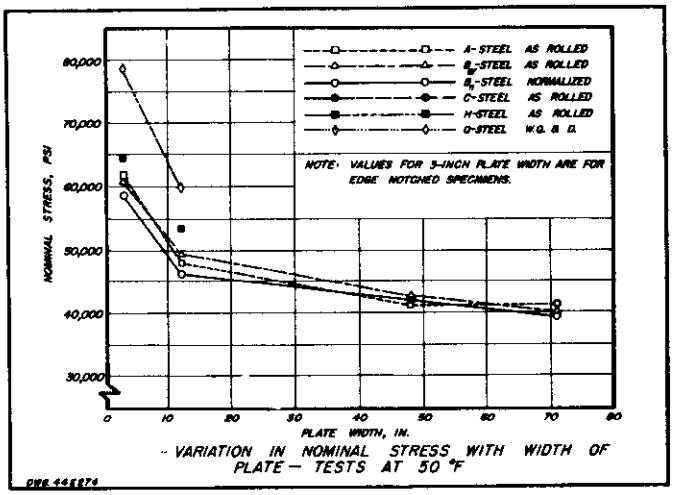

VARIATION IN NOMINAL STRESS WITH WIDTH OF PLATE — TESTS AT 50 °F

DWG. 44 E 274

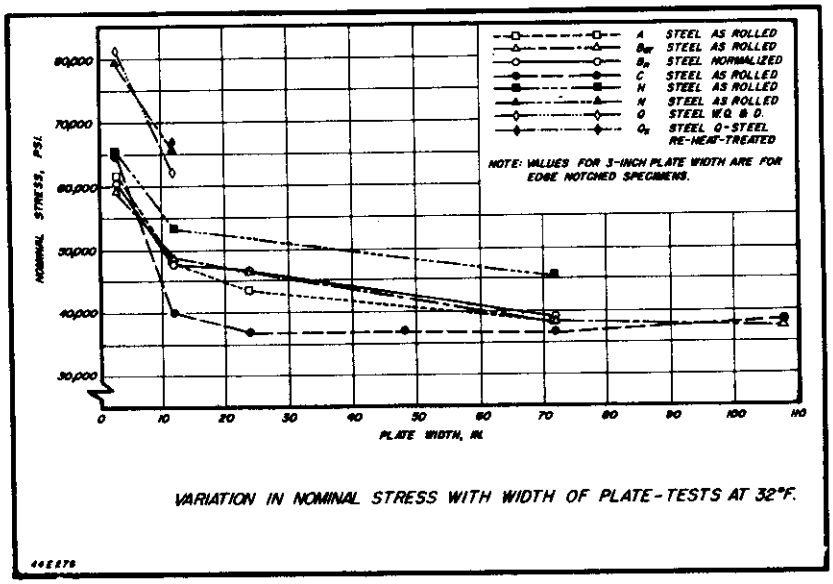

VARIATION IN NOMINAL STRESS WITH WIDTH OF PLATE-TESTS AT 32°F.

44 E 275

FIG. 55. Wide plate test results.

HATCH CORNER TESTS

MAXIMUM NOMINAL STRESS AND ENERGY ABSORPTION

(All tests at 70°F.)

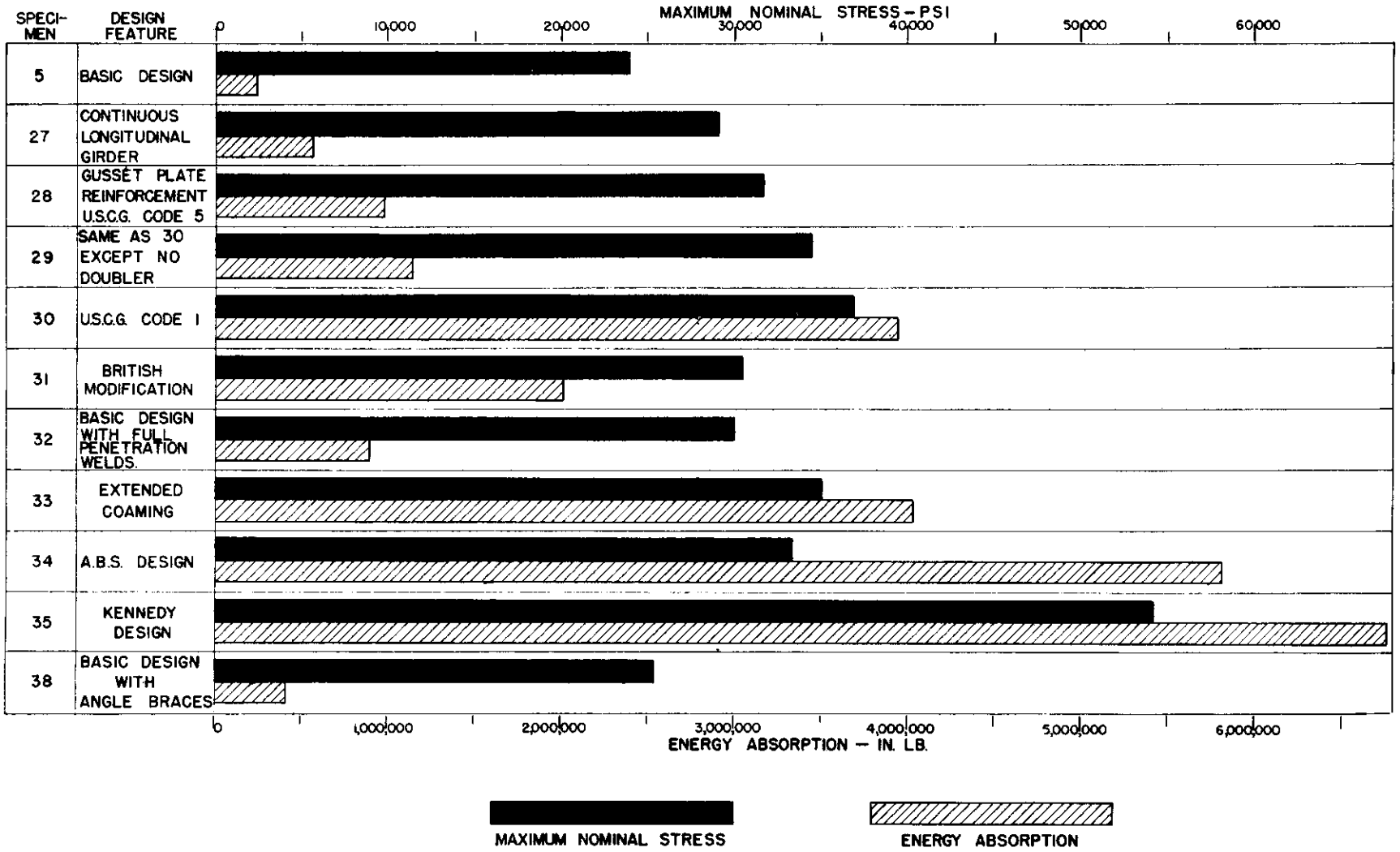

FIG. 56.

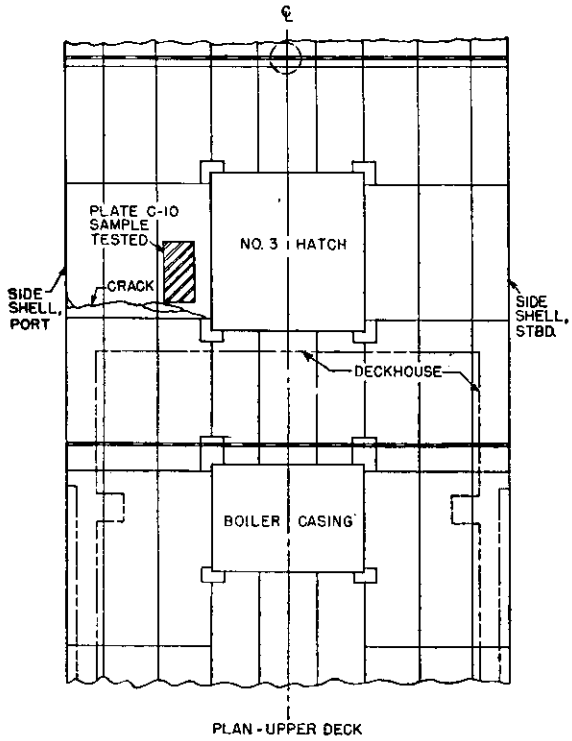

Fig. 57 "Pierre S. Dupont"—Plan view of the upper deck showing the plate removed for testing and the adjacent crack

The crack started in a weld near the corner of No. 3 hatch and was one of several major cracks involved in the casualty

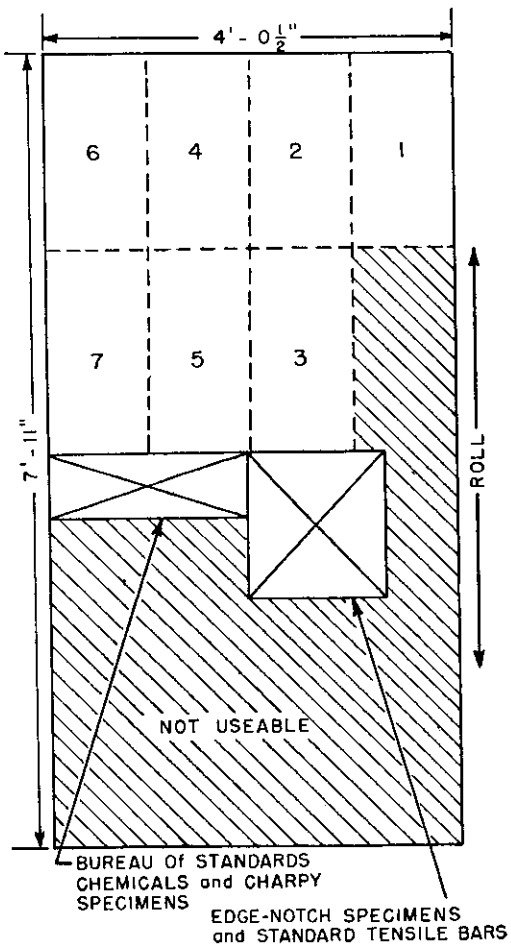

Fig. 58 "Pierre S. Dupont"—Sample from deck plate C-10 showing location of test specimens

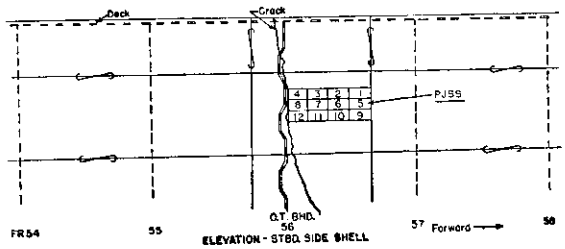

Fig. 59 "Ponaganset"—Elevation of the starboard side-shell showing the location of test specimens in the topside strake

The crack started near the starboard side of the ship in the main deck, which is at the top of the illustration

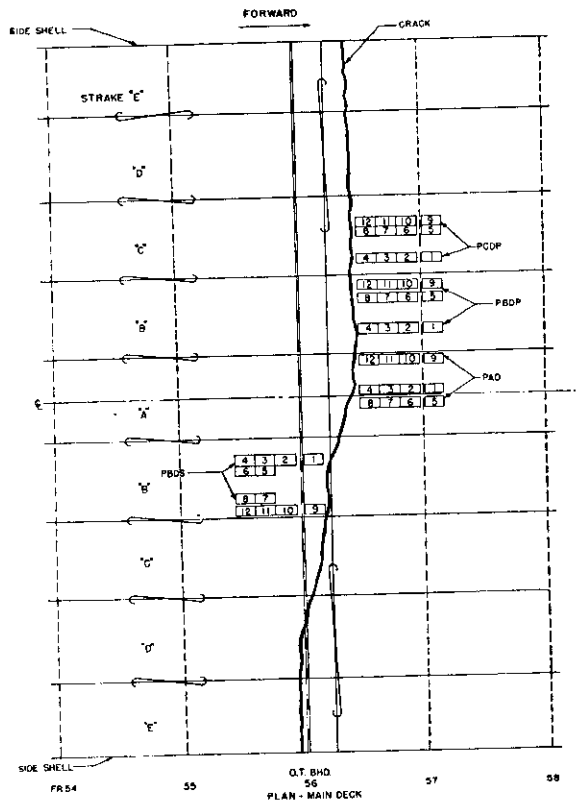

Fig. 60 "Ponaganset"—Plan view of main deck showing the location of test specimens

The crack started in the overlap of two fillet welds around appendages on the main deck. The starting point is about 1 ft. from the starboard side which is at the bottom of the illustration

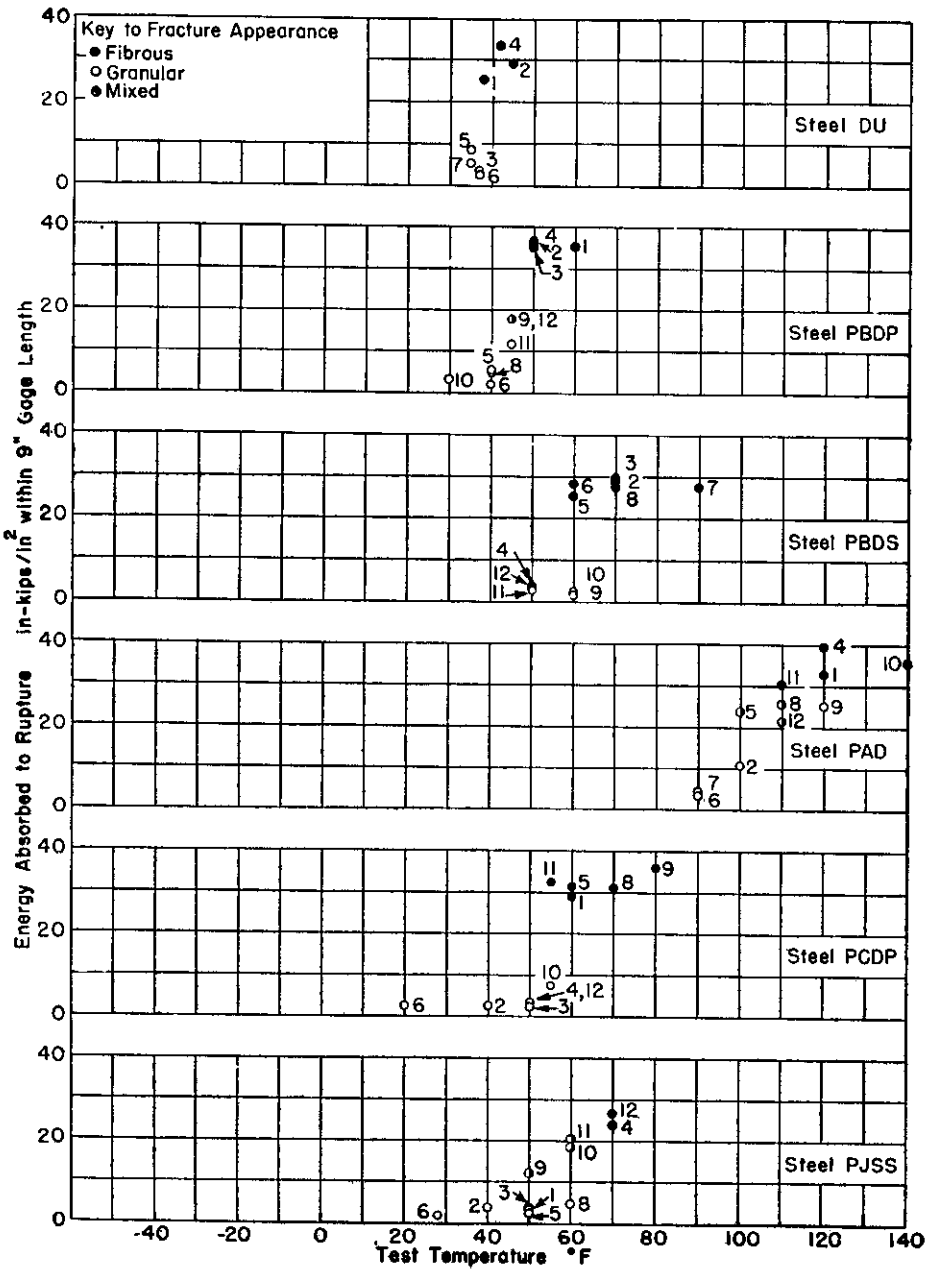

FIG. 61. Twelve-inch wide specimens. Results of tests of samples removed from fractured ships. 3/4 or 13/16 inch thick plate.

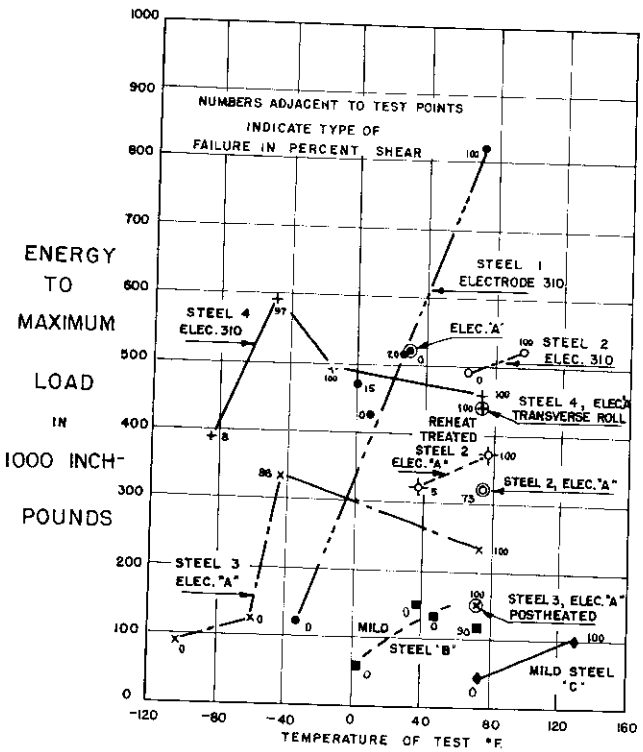

FIG. 62a ENERGY TO MAXIMUM LOAD VS. TEMPERATURE RELATION FOR RESTRAINED WELDED SPECIMENS OF HIGH YIELD STRENGTH STRUCTURAL STEELS.
RESULTS OF TESTS OF SPECIMENS MADE FROM MILD STEEL WITH E-6020 ELECTRODE ARE SHOWN FOR COMPARISON.

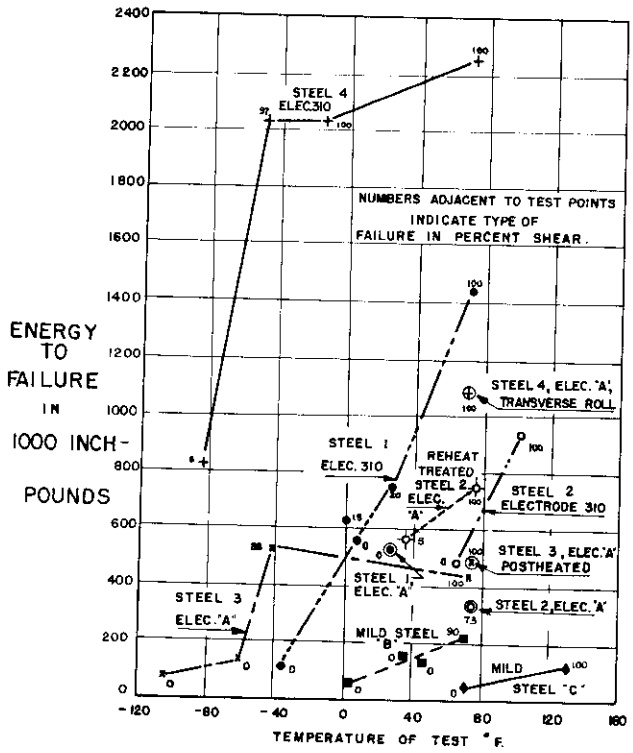

FIG. 62b ENERGY TO FAILURE VS. TEMPERATURE RELATION FOR RESTRAINED WELDED SPECIMENS OF HIGH YIELD STRENGTH STRUCTURAL STEELS.
RESULTS OF TESTS OF SPECIMENS MADE FROM MILD STEEL WITH E-6020 ELECTRODE ARE SHOWN FOR COMPARISON.

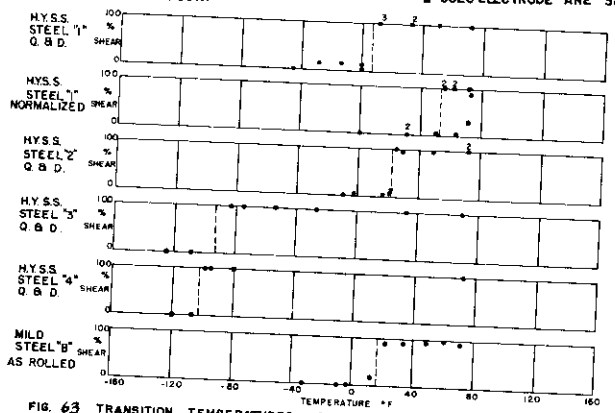

FIG. 63 TRANSITION TEMPERATURES FOR H.Y.S.S. STEELS & MILD STEEL B AS DETERMINED BY 12" CENTRALLY NOTCHED SPECIMENS

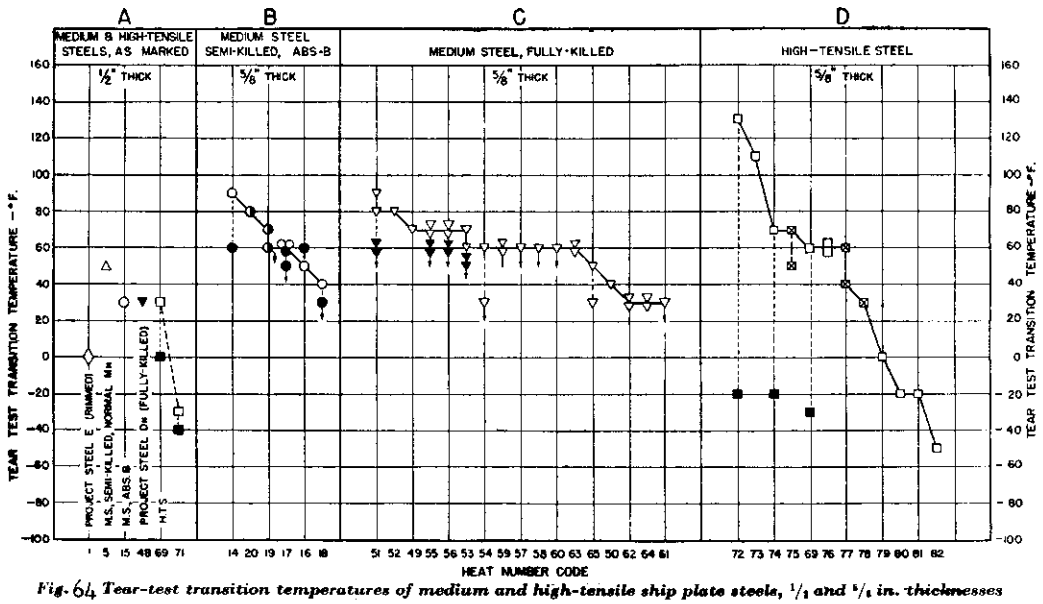

Fig. 64 Tear-test transition temperatures of medium and high-tensile ship plate steels, $^1/_2$ and $^5/_8$ in. thicknesses

Solid points—normalized; x, shown in a square in illustration—stress relieved; all others, as-rolled

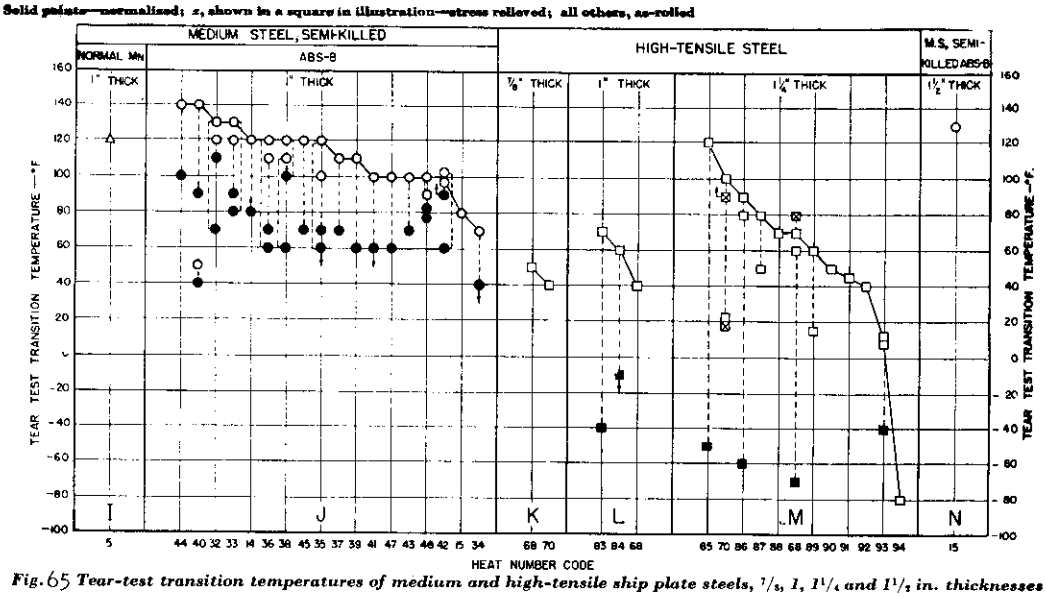

Fig. 65 Tear-test transition temperatures of medium and high-tensile ship plate steels, $^7/_8$, 1, $1^1/_4$ and $1^1/_2$ in. thicknesses

Solid points—normalized; x, shown in a square in illustration—stress relieved; all others, as-rolled

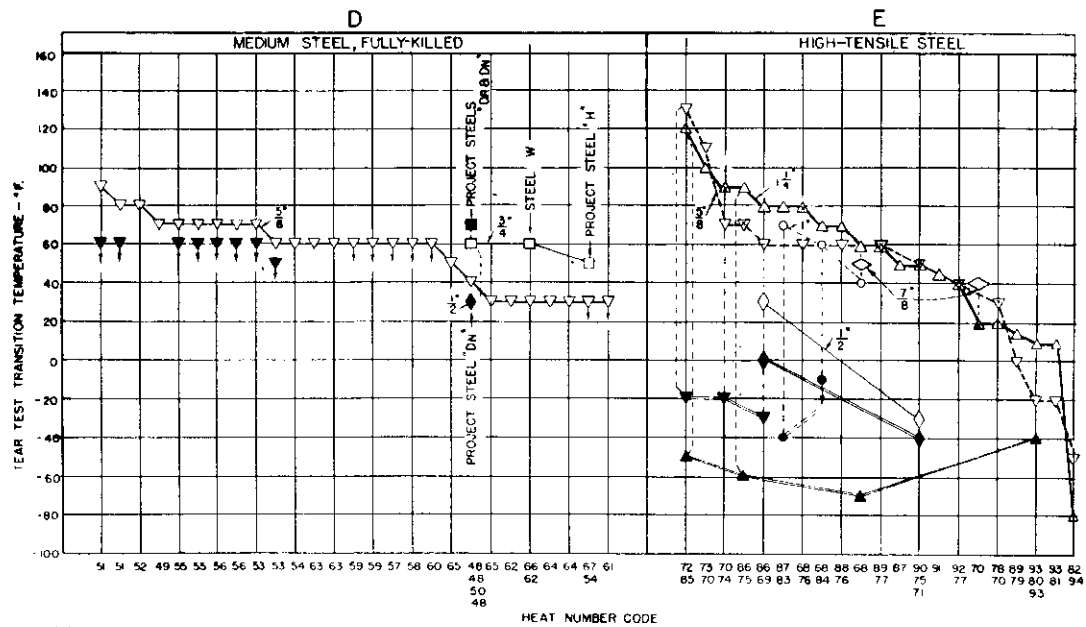

Fig. 66 Tear-test transition temperatures of medium and high-tensile ship plate steels, $^1/_2$, $^5/_8$, $^3/_4$, $^7/_8$, and $1^1/_4$ in. thicknesses

Solid points—normalized; x, in inverted triangle, or x, in triangle, in illustration—stress relieved; all others, as-rolled

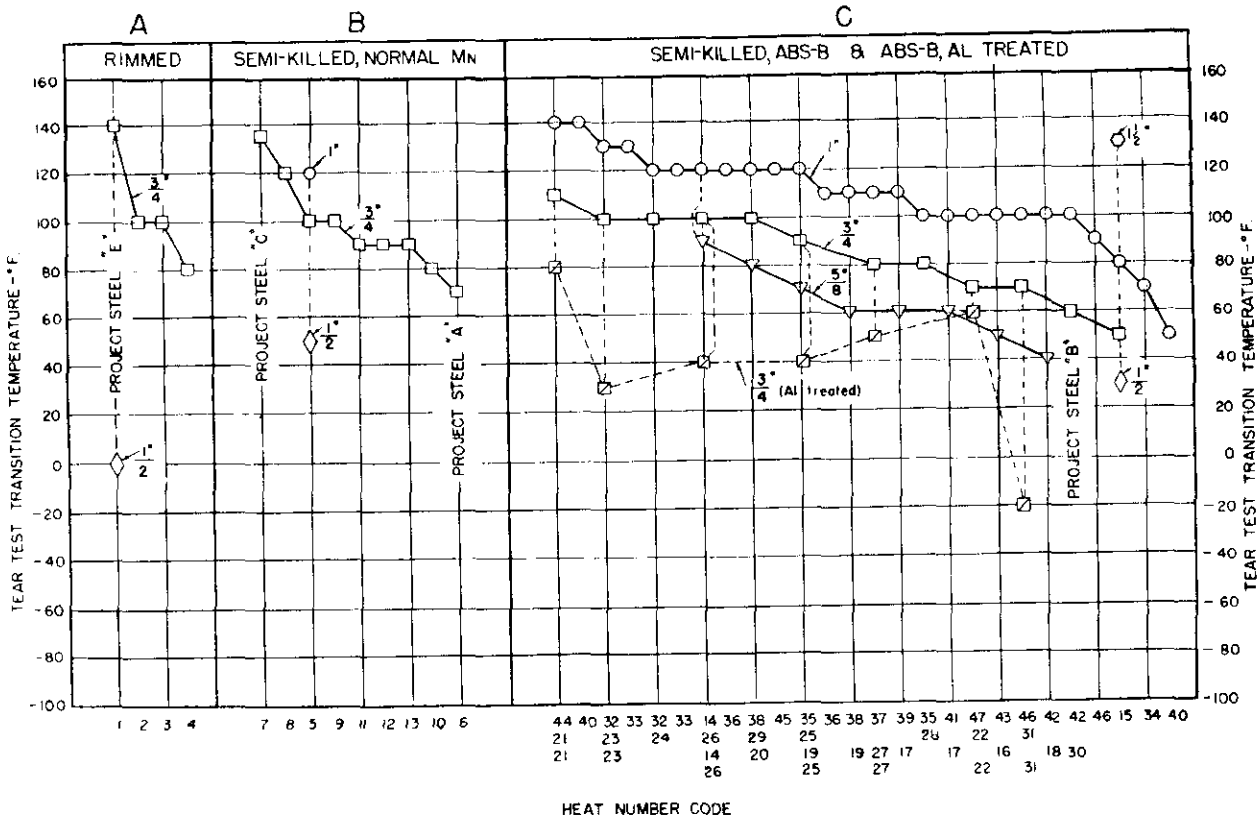

Fig. 67 Tear-test transition temperatures of medium ship plate steels 1/2, 5/8, 3/4, 1 and 1 1/2 in. thicknesses, as-rolled condition

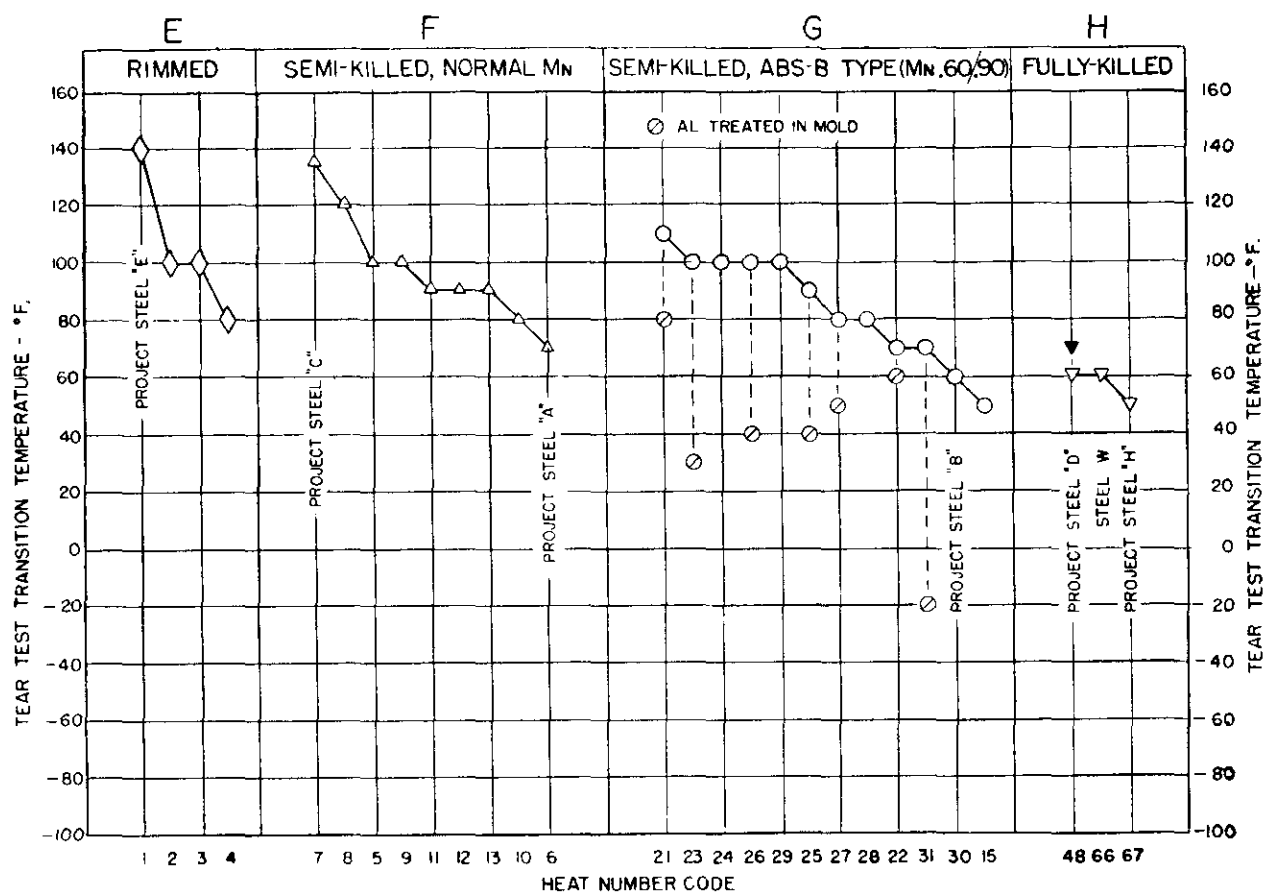

Fig. 68 Tear-test transition temperatures of medium steel ship plate, 3/4 in. thickness

Solid points—normalized; all others, as-rolled

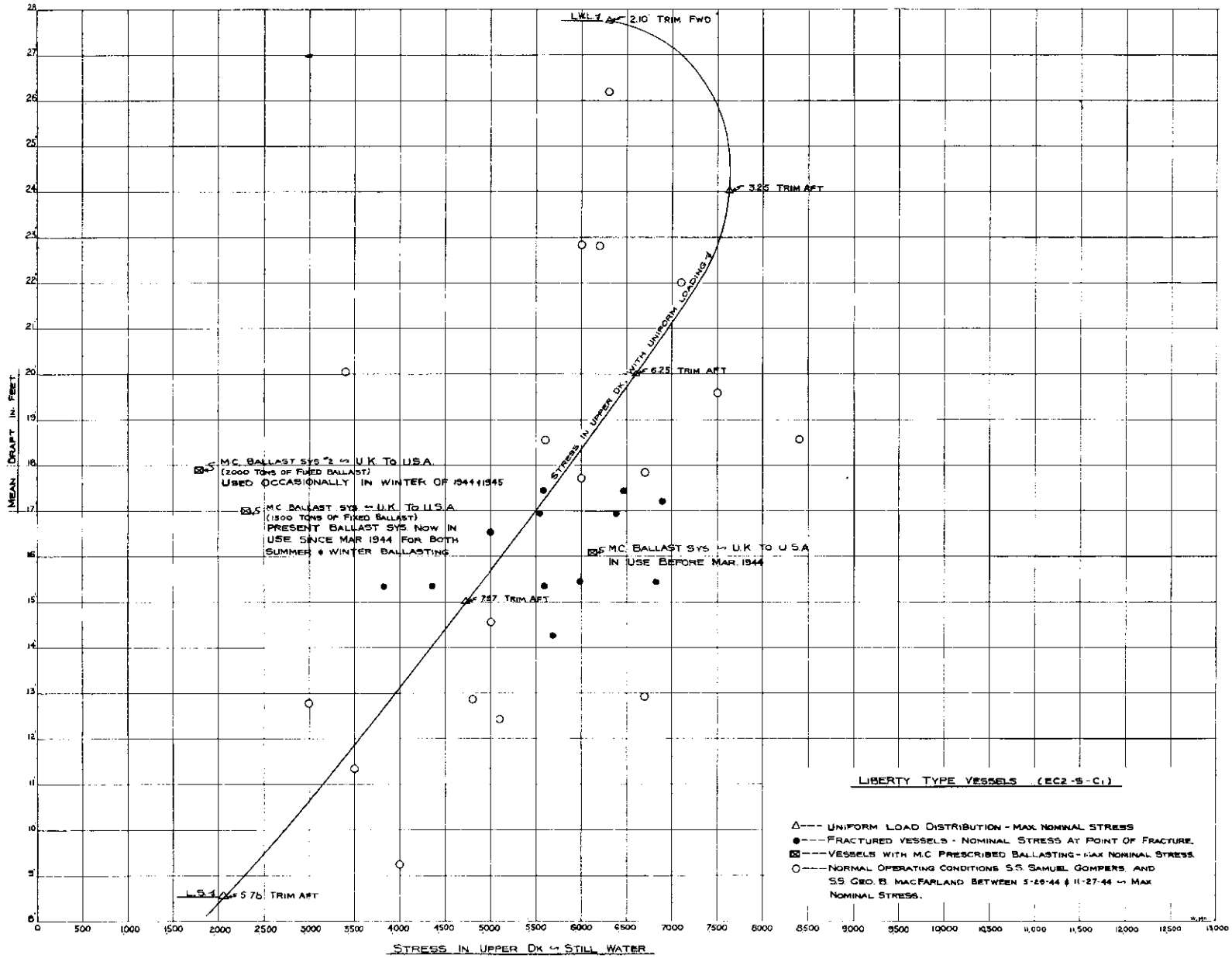

FIG. 69. STRESSES IN UPPER DECK OF LIBERTY SHIP

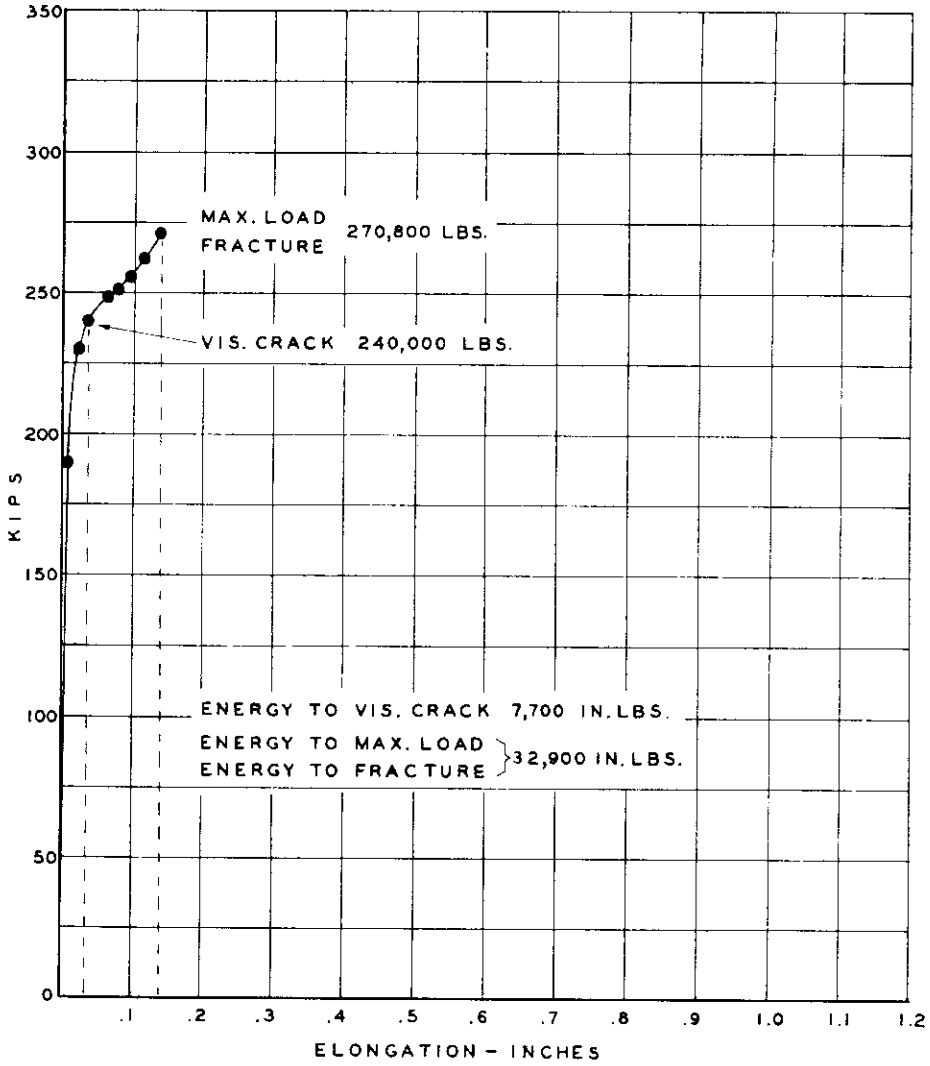

LOAD - ELONGATION CURVE
SPECIMEN BN 21-1 (1°F, 0% SHEAR)

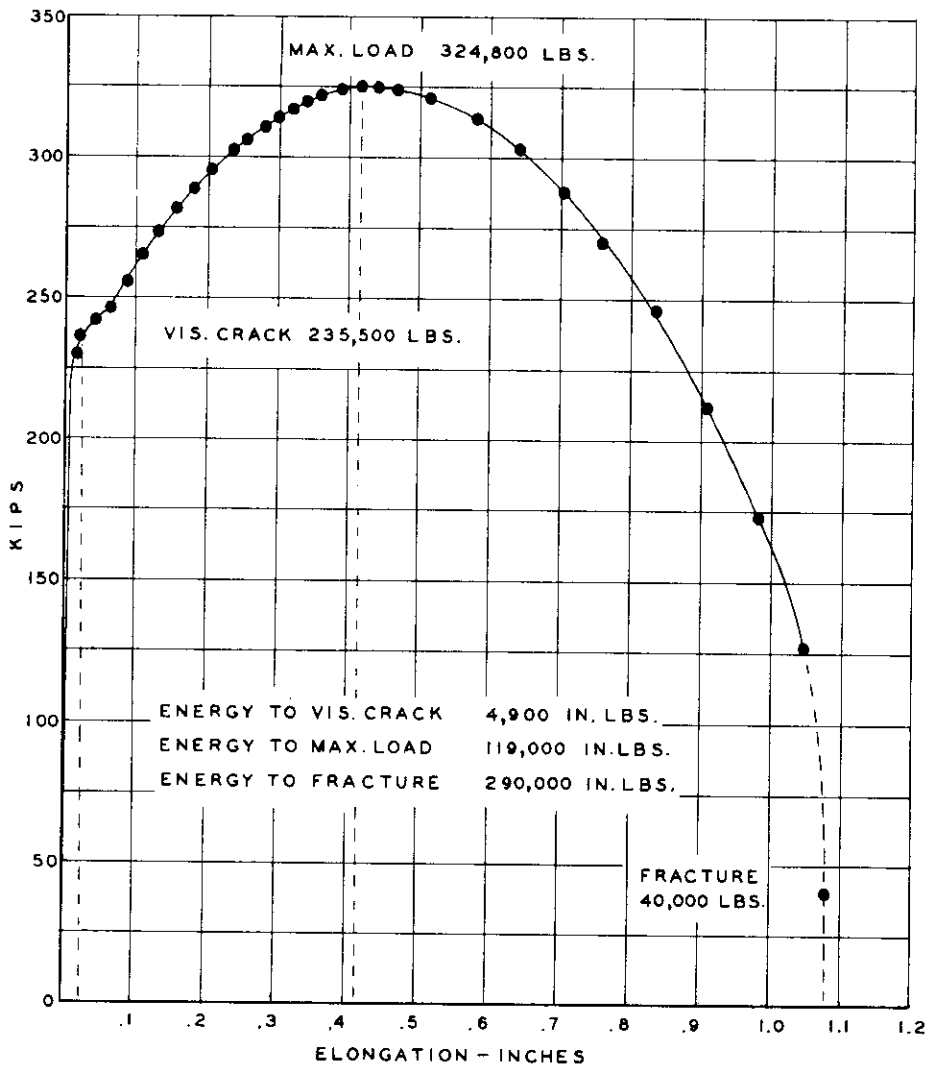

LOAD - ELONGATION CURVE
SPECIMEN BN 21-20 (30°F, 100% SHEAR)

FIG. 70. Twelve-inch wide flat plate tests. (Ref. (28))